



This is to certify that the

thesis entitled


**STRUCTURE OF A GLYCEROL ETHER LIPID AND
THE PURIFICATION AND PARTIAL CHARACTERIZATION
OF A GLYCOPROTEIN FROM
THE PLASMA MEMBRANE OF *THERMOPLASMA ACIDOPHILUM***

presented by

Li Lillian Yang

has been accepted towards fulfillment
of the requirements for

Ph. D. degree in **Biophysics**



Major professor

Date Oct. 31, 1978



OVERDUE FINES ARE 25¢ PER DAY
PER ITEM

Return to book drop to remove
this checkout from your record.

|

|

STRUCTURE OF A GLYCEROL ETHER LIPID AND
THE PURIFICATION AND PARTIAL CHARACTERIZATION OF A GLYCOPROTEIN
FROM THE PLASMA MEMBRANE OF *THERMOPLASMA ACIDOPHILUM*

By

Li Lillian Yang

A DISSERTATION

Submitted to
Michigan State University
in partial fulfillment of the requirements
for the degree of

DOCTOR OF PHILOSOPHY

Department of Biophysics

1978

ABSTRACT

STRUCTURE OF A GLYCEROL ETHER LIPID AND THE PURIFICATION AND PARTIAL CHARACTERIZATION OF A GLYCOPROTEIN FROM THE PLASMA MEMBRANE OF *THERMOPLASMA ACIDOPHILUM*

By

Li Lillian Yang

Thermoplasma acidophilum, a mycoplasma-like organism, grows optimally at pH 2 and 56°C. Since this organism does not have a cell wall, the plasma membrane directly interfaces with the harsh environment. The molecular mechanisms underlying temperature adaptation of microorganisms are not well understood although much information is available on adaptational changes in lipid side chain structures. With respect to physico-chemical parameters, such as membrane lipid fluidity and lipid phase transition temperature, the growth temperature range of a microorganism seems to depend on the ability to regulate its membrane lipid fluidity within a certain range. The first part of this dissertation is focused on answering the question of what are the key parameters of the structural and functional relationships of the lipids in the *T. acidophilum* membrane that will allow adaptation to growth at high temperature and low pH. Five spectroscopic techniques: infrared, proton magnetic resonance, gas chromatography-mass spectrometry, electron impact ionization-mass spectrometry, and carbon 13-nuclear magnetic resonance, were used to elucidate the lipid side chain structure.

The results supported the structure of two repetitively methyl branched C_{40} side chains that were ether-linked to two glycerol molecules. 80% of the lipid analyzed had the cyclopentane cyclization structure in their side chains. The branched alkyl side chains and their ether linkages with the glycerol backbone have survival value for this thermophilic and acidophilic organism. To further understand the temperature effects of *T. acidophilum*, cells were adapted to growth at 37°C. Cells grown at 37°C contained lipids with 42% more cyclopentane cyclization than the 56°C-grown cells. In 37°C-grown cells, phospholipid and serine content decreased by about 10%, carbohydrate content increased by 5%. Electron paramagnetic resonance studies demonstrated an increase in membrane lipid fluidity of 37°C-grown cells with an upper transition temperature at 35°C which was shifted down by 10°C compared with cells grown at 56°C. Membrane-bound ATPase activities also indicated similar changes upon adaptation. There is a close correlation between membrane fluidity and physiological functioning of this membrane-bound enzyme.

The second part of this dissertation is dedicated to the partial characterization of a procaryotic glycoprotein found in the *T. acidophilum* membrane. The purified membrane glycoprotein from *T. acidophilum* had an apparent molecular weight of 152,000 daltons with less than 10% carbohydrate content (w/w). The carbohydrate moiety consisted mainly of mannose residues with branched α 1-2 linkages at the non-reducing ends of the glycopeptide. The reducing end was an N-glycosidic linkage between the amino acid asparagine and N-acetylglucosamine. The glycoprotein accounted for 40% (w/w) of the total membrane proteins.

Li Lillian Yang

The nonreducing ends of the glycopeptide showed a highly branched pattern which extended like a protective coat over the entire cell surface. The hydrophobic interaction between carbohydrates and protein prevents the membrane proteins from thermal inactivation. The stereochemistry and the conformation of the carbohydrate chains in conjunction with water turgor may contribute to the rigidity of the membrane and the cation binding.

dedicated
to
all woman warriors

ACKNOWLEDGEMENTS

I wish to thank my major professor, Dr. Alfred Haug, for his guidance, encouragement and friendship during these four years of graduate study. I wish to thank my guidance committee members, especially Dr. Derek T. A. Lamport for numerous discussions and support. Special thanks are extended to Dr. Charles C. Sweeley, Dr. Sun-sang J. Sung, and their colleagues for assistance in mass spectrometry. I wish to thank Chuck Caldwell for his understanding, support and doing some of the figures.

This research was supported by the Department of Energy Contract EY-76-C-02-1338.

TABLE OF CONTENTS

	PAGE
LIST OF TABLES.....	vii
LIST OF FIGURES.....	viii
LIST OF ABBREVIATIONS.....	xi
CHAPTER 1 GENERAL INTRODUCTION.....	1
CHAPTER 2 MATERIALS AND METHODS.....	12
MATERIALS.....	12
METHODS.....	13
Growth of Cells.....	13
Membrane Preparation.....	14
Extraction of Lipids.....	14
Silicic Acid Column Chromatography.....	14
Preparative Thin-Layer Chromatography.....	14
Transmethylation of Lipids.....	15
Methanolysis.....	15
Degradation of Glycerol Ethers	
(i) Alkyl Chloride Derivatives.....	15
(ii) Alkyl Alcohol Derivatives.....	15
Determination of C-methyl Groups.....	16
Gas-Liquid Chromatography (GC) for Membrane	
Lipid Derivatives.....	16
Combined Gas Chromatography-Mass Spectrometry.....	16
Electron Impact Ionization-Mass Spectrometry.....	16
Infrared Spectroscopy.....	17
Nuclear Magnetic Resonance Spectroscopy	
(i) Proton NMR.....	17
(ii) Carbon 13-NMR.....	17
ATPase Assay.....	17
Buffer Systems for SDS Gel Electrophoresis and	
Sample Preparation.....	18
Electron Paramagnetic Resonance (EPR).....	18
Isolation and Purification of Membrane Glycoprotein	
(i) by preparative slab gel electrophoresis...	19
(ii) by phenol extraction.....	19
(iii) by Sepharose 4B Column Chromatography...	19
(iv) by Con A-Sepharose Column Chromatography.	20
Methanolysis of Carbohydrates.....	20
Permethylation for Linkage Studies.....	20

TABLE OF CONTENTS (cont'd)

	PAGE
Anhydrous Hydrogen Fluoride Deglycosylation.....	22
Amino Acid Analysis.....	22
Treatments of Glycoprotein with Glycosidases	
(i) α -mannosidase digestion.....	22
(ii) β -glucosidase digestion.....	23
(iii) β -galactosidase digestion.....	23
(iv) endo-glycosidase H digestion.....	23
Analytical Methods.....	23
CHAPTER 3 STRUCTURE OF LONG-CHAIN GLYCEROL ETHERS IN PLASMA MEMBRANE FROM <i>THERMOPLASMA ACIDOPHILUM</i> GROWN AT 56°C.....	24
Introduction.....	24
Results.....	25
Infrared Spectroscopic Studies of Compound (I).....	26
Proton NMR Studies of Compound (I).....	26
GC Studies of Alkyl Chloride and Alkyl Alcohol Deriva- tives of Side Chains.....	30
GC-MS Studies of the Alkyl Chloride Derivatives.....	35
GC-MS Studies of Alkyl Alcohol Derivatives.....	39
EI-MS Studies of Compound (I).....	52
Carbon 13-NMR Studies of Compound (I).....	54
Discussion.....	54
CHAPTER 4 CHANGES OF MEMBRANE PROPERTIES IN <i>THERMOPLASMA</i> <i>ACIDOPHILUM</i> UPON LOW TEMPERATURE (37°C) ADAPTATION.....	60
Introduction.....	60
Results.....	60
Lipids.....	60
Membrane-Bound Adenosine Triphosphotase.....	62
EPR Studies.....	64
Discussion.....	64
CHAPTER 5 PARTIAL CHARACTERIZATION OF A MEMBRANE GLYCOPROTEIN FROM <i>THERMOPLASMA ACIDOPHILUM</i>	68
Introduction.....	68
Results.....	70
Isolation and Purification of the Glycoprotein.....	70
Pronase Digestion of the Glycoprotein.....	80

TABLE OF CONTENTS (cont'd)

	PAGE
Determination of Carbohydrate Composition by Methanolysis.....	83
Amino Acid Analysis of the Glycoprotein.....	83
Glycosidic Linkage Studies of the Glycoprotein.....	83
Digestions of the Glycopeptide by Exo- and Endo- glycosidases.....	87
Permethylation Studies of the Glycopeptide.....	93
Effect of Bacitracin on Cell Growth and Glycoprotein Structure.....	95
Discussion.....	108
References.....	112

LIST OF TABLES

TABLE		PAGE
1.	Proton NMR Chemical Shifts δ (in ppm) of Glycerol Ether Downfield from TMS.....	31
2.	Carbon 13-NMR Chemical Shifts δ (in ppm) of Glycerol Ether.....	57
3.	Side Chain Comparison of 56°C- and 37°C-grown Cells as Determined by GC and GC-MS.....	62
4.	Amino Acid Composition of the Purified Membrane Glyco- protein from <i>T. acidophilum</i>	86
5.	Molar Ratios of Carbohydrate Residues from Purified Glycoprotein and after Treatments with Glycosidases.....	92
6.	Molar Ratios of Partially Methylated Alditol Acetates of Mannose, Glucose, Galactose and Glucosamine Obtained by Permethylation of the Purified Glycopeptide.....	94

LIST OF FIGURES

FIGURE		PAGE
1.	Chemical Degradation Scheme of the Glycerol Ether Lipids from the Membrane of <i>Thermoplasma acidophilum</i>	27
2.	Infrared Spectrum of Compound (I) (Figure 1).....	28
3.	Proton Magnetic Resonance Spectrum of Compound (I) (Figure 1).....	29
4.	Gas Chromatogram of Alkyl Chloride Derivative of Glycerol Ether Lipids from <i>T. acidophilum</i> Membrane.....	32
5.	Gas Chromatogram of Alkyl Alcohol Derivative of Glycerol Ether Lipids from <i>T. acidophilum</i> Membrane.....	33
6.	Mass Spectra of the High-Mass Region of GC Component 4,5 and 6 of Alkyl Chloride Derivatives.....	36
7.	Mass Spectrum of the First Component of the GC Trace of the Alkyl Alcohol Derivative of <i>T. acidophilum</i> Lipid Side Chains.....	40
8.	Assignments of the Ion Fragments of Mass Spectrum Figure 7.....	42
9.	Mass Spectrum of the Second Component of the GC Trace of the Alkyl Alcohol Derivatives of <i>T. acidophilum</i> Lipid Side Chains.....	44
10.	Assignments of the Ion Fragments of Mass Spectrum Figure 9.....	46
11.	Mass Spectrum of the Third GC Component of the Alkyl Alcohol Derivatives of the <i>T. acidophilum</i> Lipid Side Chains.....	48
12.	Assignments of the Ion Fragments of Mass Spectrum Figure 11.....	50
13.	Carbon 13-NMR Spectrum and the Assignment of the Glycerol Ether Molecule from <i>T. acidophilum</i> Membrane Lipid.....	55

FIGURE	PAGE
14. Arrhenius Plot of Membrane-Bound ATPase Activity vs Temperature for Both 56°C-Grown (-o-) and 37°C-Grown (-●-) <i>T. acidophilum</i>	63
15. Hyperfine Splitting Parameter $2T_H$ as a Function of Temperature for 56°C-Grown (-o-) and 37°C-Grown (-●-) <i>T. acidophilum</i> Membrane Labelled with ^{59}Fe	65
16. Scans of SDS Gel Electrophoresis of the Membrane Proteins from <i>T. acidophilum</i>	72
17. Elution Pattern of Membrane Glycoprotein from Con A-Sepharose Column.....	74
18. Scan of SDS Gel Electrophoresis of the Purified Glycoprotein from Con A-Sepharose Column and the Molecular Weight Determination.....	76
19. Scans of SDS Gel Electrophoresis of the Purified Glycoprotein in 9%, 7% and 5% Polyacrylamide.....	78
20. Sephadex G-100 Column Chromatography of Glycopeptides after Pronase Digestion.....	81
21. Sephadex G-75 Elution Profile of Fraction #9 from Figure 20.....	82
22. Gas-Liquid Chromatography of Trimethylsilylated Methyl Glycosides of the Purified Glycopeptide.....	84
23. Gas-Liquid Chromatography of Trimethylsilylated Methyl Glycosides of the Glycopeptide after α -mannosidase Digestion.....	88
24. Gas-Liquid Chromatography of Trimethylsilylated Methyl Glycosides of the Glycopeptide after α -mannosidase and β -glucosidase Digestions.....	90
25. Mass Spectrum of Partially Methylated Alditol Acetate Identified as 1,5-di-O-acetyl-2,3,4,6-tetra-O-methylmannitol from the Purified Glycopeptide.....	96
26. Mass Spectrum of Partially Methylated Alditol Acetate Identified as 1,2,5-tri-O-acetyl-3,4,6-tri-O-methylmannitol from the Purified Glycopeptide.....	97
27. Mass Spectrum of Partially Methylated Alditol Acetate Identified as 1,3,5,6-tetra-O-acetyl-2,4-di-O-methylmannitol from the Purified Glycopeptide.....	98

FIGURE	PAGE
28. Mass Spectrum of Partially Methylated Alditol Acetate Identified as 1,3,5-tri-O-acetyl-2,4,6-tri-O-methyl- mannitol from the Purified Glycopeptide.....	99
29. Mass Spectrum of Partially Methylated Alditol Acetate Identified as 1,5,6-tri-O-acetyl-2,3,4-tri-O-methyl- mannitol from the Purified Glycopeptide.....	100
30. Mass Spectrum of Partially Methylated Alditol Acetate Identified as 1,4,5-tri-O-acetyl-2,3,6-tri-O-methyl- glucitol from the Purified Glycopeptide.....	101
31. Mass Spectrum of Partially Methylated Alditol Acetate Identified as 1,3,5-tri-O-acetyl-2,4,6-tri-O-methyl- galactitol from the Purified Glycopeptide.....	102
32. Mass Spectrum of Partially Methylated Alditol Acetate Identified as N-acetyl-N-methyl-1,4,5-tri-O-acetyl- 3,6-di-O-methylglucosaminitol from the Purified Glycopeptide.....	103
33. Proposed Structure of the <i>Thermoplasma acidophilum</i> Membrane Glycoprotein.....	104
34. <i>T. acidophilum</i> Cell Growth Ratios in the Presence and Absence of Bacitracin.....	107

LIST OF ABBREVIATIONS

IR	Infrared
NMR	Nuclear Magnetic Resonance
PMR	Proton Magnetic Resonance
^{13}C -NMR	Carbon 13-Nuclear Magnetic Resonance
EPR	Electron Paramagnetic Resonance
GC	Gas-Liquid Chromatography
MS	Mass Spectrometry
GC-MS	Gas-Liquid Chromatography-Mass Spectrometry
EI-MS	Electron Impact Ionization-Mass Spectrometry
TLC	Thin-Layer Chromatography
Con A	Concanavalin A
SDS	Sodium Dodecyl Sulfate
PAS	Periodic Acid-Schiff
BSA	Bovine Serum Albumin
TI	Trypsin Inhibitor
EDTA	Ethylenediaminetetraacetic acid
Man	Mannose
Glc	Glucose
Gal	Galactose
GlcNAc	N-acetylglucosamine
5NS	5-nitroxylstearate
TCA	Trichloroacetic Acid

CHAPTER 1

GENERAL INTRODUCTION

The mycoplasmas are the smallest and simplest self-replicating procaryotes. The mycoplasma cell contains only the minimum set of organelles essential for cell growth and replication: a plasma membrane to separate the cytoplasm from the external environment, ribosomes to assemble the cell proteins, and a double stranded DNA molecule to provide the information for protein synthesis. Unlike all other procaryotes, mycoplasmas have no cell wall. The cell biology of these organisms is interesting not only to mycoplasmologists but also to the many workers who use mycoplasmas as simple model systems for studying general biological problems, particularly those concerning membrane structure and function.

The information explosion has been quite pronounced in mycoplasmaology, as the discoveries of insect and plant mycoplasmas and of mycoplasma viruses in the early 1970s have attracted new workers from different disciplines. Very different and phylogenetically quite remote from all the parasitic mycoplasmas are the wall-less procaryotes isolated by Darland *et al.* (1) from self-heated coal refuse piles. These organisms have adapted to a unique ecological niche--high temperature (56°C optimum) and extremely low pH (2.0 optimum)--hence the name *Thermoplasma acidophilum*. Though their lack of cell walls justifies their inclusion in the class Mycoplasma, their peculiar DNA and RNA, mobility by flagella, and minimal

nutritional requirements, set them apart from all other members of the *Mycoplasma*. Moreover, they are the only nonparasitic members in this class.

The existence of obligate, thermoacidophilic microorganisms is a relatively recent discovery. Four different types of organisms have been isolated, namely, *Thermoplasma acidophilum*, and three bacteria, *Sulfolobus acidocaldarius* (2), *Bacillus acidocaldarius* (3) and an obligately autotrophic iron and sulfur oxidizing bacterium (4) closely related to *Sulfolobus*. Since these organisms demand the extremes of a hot acid environment for growth, there is considerable interest in defining their physiological characteristics. An understanding of the anticipated unique chemical structures and biochemical properties of these organisms could find application to a better comprehension of evolutionary processes, microbial modifications of extreme environments and the mechanism of resistance of specific cells exposed to a very acid environment.

The known thermoacidophiles possess three distinct types of surface structures. The sporeforming *Bacillus acidocaldarius* has a morphologically typical gram-positive cell wall. Protection from H^+ apparently involves the cell wall and, possibly, surface sulfonolipids, but the underlying mechanism is unknown. *Sulfolobus* and its autotrophic iron and sulfur oxidizing relative (4) do not contain a typical bacterial wall. Rather, their cytoplasmic membranes are enveloped by closely packed polygonal subunits composed primarily of protein enriched with charged amino acids, such as aspartate, glutamate and lysine. These subunits apparently are not covalently bonded to the membrane or to one another but retain their integrity through hydrogen bonding. In contrast

to the peptidoglycan containing *B. acidocaldarius*, which has a typical bacillary morphology, *Sulfolobus* possesses a peculiar lobe-shaped morphology. A role for this proteinaceous coat is unknown. *Thermoplasma acidophilum* is the representative of the third type of surface structure. This organism is completely devoid of any wall, being contained by a morphologically typical unit membrane (5). *Thermoplasma* begins to leak protein and nucleic acid at pH about 4.5, while increasing pH on three other thermophilic acidophilic organisms has no effect at all. Hence the integrity of the cell may be maintained by properties of the plasma membrane. Structural and functional membrane parameters may determine the environmental limit within which *T. acidophilum* is capable to survive. Elucidation of key parameters is the primary concern of this dissertation.

Cell protein profiles indicated a high degree of homogeneity among strains of *T. acidophilum* collected at different locations, even though serological tests suggested the presence of at least five different serological groups (5,6). *Thermoplasma* appears to be coccoidal in shape and cell diameters vary between 0.5 to 1.0 micron. Some cells have one or two filamentous projections. *T. acidophilum* has a more electron dense cytoplasm than *Acholeplasma laidlawii* although the membranes have similar thickness, 80-100 Å (1,13). All the *T. acidophilum* isolates can be grown in a simple (compared to other mycoplasmas) medium consisting of inorganic ions, glucose and low concentrations of yeast extract (1).

Studies of the *T. acidophilum* genome are important because of the questionable relationship between this wall-less, free-living procaryote and the parasitic mycoplasmas. The early reports (1,5) had shown that the DNA of *T. acidophilum* resembles that of the parasitic mycoplasmas in

having a G+C content as low as 25%. Later this was proven to be incorrect. The actual G+C value is about 47% (7,8), closely resembling that of the parasitic *Acholeplasma* and *Spiroplasma* species and representing the smallest genome recorded for any nonparasitic procaryote. Another interesting feature of the *T. acidophilum* genome is its association with a histone-like protein (9). Histones, basic proteins associated with the nuclear DNA of eucaryotes, have not been found in procaryotes. The histone-like protein of *T. acidophilum* resembles eucaryotic histones in having a high basic amino acid content, but it differs in being unusually rich in amides of acidic amino acids. Recent data (10) suggest that the histone-like protein condenses the DNA into subunits that are 5 to 6 nm in diameter, each consisting of approximately 40 base pairs of DNA looped around 4 or 6 of protein molecules. Thus the nucleoprotein of *T. acidophilum* has a subunit structure similar to that of eucaryotic chromatin but of a simpler nature, as the eucaryotic subunit are larger and contain 8 histone molecules plus 130 to 140 base pairs of DNA each. By association the histone-like protein stabilizes *T. acidophilum* DNA against thermal denaturation (10). Furthermore, this association may also protect the DNA from depurination in the hot and highly acidic environment of *T. acidophilum*. Even though thermoplasmas are capable of maintaining a relatively high intracellular pH, estimated at 5.6 (11) or 6.4-6.9 (12), the rate of depurination of unprotected DNA at these pH values may be high enough to impose a severe mutational load. Searcy (9) suggested that histones may have evolved independently in eucaryotes and *T. acidophilum*. However, it is also possible that an organism related to *T. acidophilum* was the ancestor of eucaryotic cells, and in this case, histones may have first evolved to

protect its DNA from thermal denaturation or depurination. Once evolved, the histones condensed the DNA and thus were a preadaptation for the accumulation of more DNA in the eucaryotic cells. The similar properties of the *T. acidophilum* histone and histones of primitive eucaryotes, such as *Neurospora* and dinoflagellates, are consistent with this hypothesis (9).

Thermoplasma acidophilum, lacking a cell wall and intracytoplasmic membranes, has only one type of membrane, the plasma membrane. Isolation of *T. acidophilum* membranes by methods usually employed for mycoplasma have been unsuccessful (13). Low yields of lysed *Thermoplasma acidophilum* are obtained by exposing cells to osmotic shock at pH 2 or pH 7.4, or sonicating them for 30 minutes (13,14). Denaturants and detergents at high concentration (5 M urea, 1% Triton X-100, or 0.1% SDS) caused partial solubilization of cellular material, leaving intact cells or amorphous protein aggregates as determined by electron microscopy (13). High pH (9.3-10.0) has been applied to induce lysis of the osmotically resistant *T. acidophilum* (13) followed by purification via sucrose density gradient centrifugation. One criterion for purity of isolated membranes prepared by high pH lysis is the absence of cytoplasmic components. Transmission electron microscopy has shown the presence of membrane vesicles which are approximately the size of intact cells. The interior of the vesicles is free from electron dense cytoplasm(13). In contrast to membranes from pH lysis, sonically prepared membranes contain usually smaller vesicles and amorphous debris(14). The major drawback of the sonication procedure is the cytoplasmic precipitation which occurs at low pH and probably accounts for the amorphous material reported by Smith *et al.* (14). Failure to remove this cytoplasmic

material is probably due to the acidic conditions chosen (pH 5). A second criterion of membrane purity prepared by high pH lysis is the failure of contaminating cytoplasmic protein to penetrate low percentage polyacrylamide gels, even when gels were loaded with 200 micrograms of protein (13). In contrast, sonically prepared membrane, which contained amorphous material, easily penetrated native polyacrylamide gels (13). Similar gel patterns are obtained on 10% SDS polyacrylamide gels of cytoplasmic components present in the supernatant of cells sonicated at pH 6.5 (13). Third, the membrane prepared from high pH lysis is essentially devoid of DNA. The membranes contained less than 0.1% (w/w) DNA. However, membrane from high pH lysis may suffer from the deficiency that some membrane proteins or even the membranes themselves, may be solubilized at pH values higher than 10.0 (13).

The isolated *Thermoplasma* membranes resemble plasma membranes of other mycoplasma and procaryotes in gross chemical composition, being composed mainly of proteins and lipids. The protein comprises roughly three quarters of the mass of the membrane, the balance being primarily lipid. The amino acid composition of the total membrane from *T. acidophilum* has revealed no significant difference from the amino acid composition of mycoplasmal membrane proteins in general (13,14). However, the number of chargeable groups is barely half of the number found in mesophilic mycoplasmal membranes, even though the ratio of free -COOH to free -NH₂ (4:1) is identical.

The major controversy in *T. acidophilum* research lies in the lipid structure of the organism. Most researchers agree on the percentages of the lipid components to be neutral lipid: glycolipid: phospholipid = 1:1:3 (13,16). The exact chemical structures of these complex lipids

await resolution. In 1972, Langworthy *et al.* (16) reported that more than 70% of the total lipid from whole cell (virtually all mycoplasma lipids are located in the cell membrane) is a 1,2-substituted long-chain diether of glycerol. Mass spectrometry data indicate the molecular ions of the long chains are 562 and 560, accounted for by the formulas $C_{40}H_{82}$ and $C_{40}H_{80}$. Solely from the incorporation of radioactive mevalonate, they concluded that the long chains have 8 repeating units of isoprenoid. Ester linkages were not detected. After the membrane preparation by high pH lysis, membrane lipids were analyzed by Ruwart *et al.* (13). Their results agree with most of the lipid structure reported by Langworthy *et al.* (16), but disagree on the neutral lipid fraction. Ruwart *et al.* (13) found no detectable amount of cholesterol as reported by Langworthy *et al.* (16), but large amount (30%) of vitamin K₂-7. Also Ruwart *et al.* reported the presence of fatty acid esters (2.1%) in *T. acidophilum* membrane lipids by combined gas chromatography-mass spectrometry and infrared hydroxamate techniques. In 1976, de Rosa *et al.* (17) reported that the lipids are based on sn-2,3-glycerol combined as a cyclic diether with a saturated C_{40} isoprenoid residue which is either acyclic, monocyclic or bicyclic. The residues are formed from two phytanyl chains linked head to head. Recently, Langworthy (18) revised the lipid structures to be neither glycerol diethers containing two C_{40} hydrocarbon chains, nor cyclic glycerol diethers containing a single C_{40} hydrocarbon, but are diglycerol tetraethers.

Membrane lipid structure is one of the major concerns of this dissertation. Since the membrane comes in direct contact with the harsh environment (pH 2 and 56°C), the exact knowledge of the lipid structure may help to elucidate structural and functional relationships in response

to environmental stress. The glycolipids and phospholipids of this organism contain mainly glycerol ether residues rather than fatty acid ester-linked glycerides, apparently the result of adaptation to highly acidic conditions, where ester linkages are unstable. The C₄₀ long chains assume the function of thermal stability. Electron paramagnetic resonance studies by Smith *et al.* (19) indicated that *Thermoplasma* membrane is the most rigid membrane known.

Evidence for the existence of a membrane potential is available for *T. acidophilum*. The intracellular pH in this organism is estimated at between pH 5.5 and 6.9, depending on the technique used for its measurement (11,12). Since the pH of the growth medium was about 2.0, a pH gradient of 3.5 to 4.9 must exist between the outside and the inside of the cells. The finding that metabolic inhibitors and proton-conducting uncouplers did not affect this gradient led Hsung and Haug (12, 20) to conclude that it is maintained passively by a Donnan potential across the membrane, possible generated by charged intracellular macromolecules. KS¹⁴CN, known to penetrate biological membranes, accumulated in the *T. acidophilum* cells, whereas tetraethylammonium bromide, a lipophilic cation, did not, suggesting that the cells are positive on the inside, whereas their surface has a highly negative charge. Hence, some positively charged ions or macromolecules possibly including the histone-like proteins described by Searcy (9), must be present within the cells to create the Donnan potential (21). At pH 2.0, the measured membrane potential is about 120 mV, positive inside, compensating only partly for the huge pH gradient. The membrane potential decreased linearly on increasing the external pH, diminishing to less than 15 mV at pH 6.0 (20). Hsung and Haug considered whether ATP can be generated in *T. acidophilum*

crystalline phase transition to an extent dependent on the cation concentration (25). The presence of monovalent and divalent cations at the polar lipid groups of *T. acidophilum* membranes probably induces alterations of alkyl chain conformation, as indicated by the spin probes (22). Raman spectroscopic experiments on aqueous phosphatidylcholine dispersions have demonstrated that Ca^{2+} ions decrease the proportion of gauche character in the hydrocarbon chains (26). In contrast, K^+ caused no modifications.

By using electron paramagnetic resonance spectroscopy, Al^{3+} was shown to produce a dramatic decrease of membrane lipid fluidity on the microorganism at a pH higher than 2. The ability of Al^{3+} to alter lipid fluidity was enhanced with increasing pH (from 3 to 5). At pH 4, 10^{-2}M Al^{3+} increased the lower lipid phase transition by 39°C , and a detectable change was observed with AlCl_3 concentrations as low as 10^{-5}M . The ability of Al^{3+} to increase the lower lipid phase transition temperature of *T. acidophilum* is the largest of any cation/lipid interaction yet reported (23).

Thermoplasma acidophilum, a mycoplasma-like organism, grows optimally at pH 2 and 56°C . Since this organism doesn't have a cell wall, the plasma membrane directly interfaces with the harsh environment. The molecular mechanisms underlying temperature adaptation of microorganisms are not well understood although much information is available on adaptational changes in lipid side chain structures. With respect to physicochemical parameters, such as membrane lipid fluidity and lipid phase transition temperature, the growth temperature range of a microorganism seems to depend on the ability to regulate its membrane lipid fluidity within a certain range. As reviewed above, the most controversial area

of *T. acidophilum* research is concerned with the lipid structure. The first part of this dissertation (Chapters 3 and 4) is focused on answering the question of what are the key parameters of the structural and functional relationships of the lipids in the *T. acidophilum* membrane which will allow adaptation to growth at high temperature and low pH. Five spectroscopic techniques: IR, PMR, GC-MS, EI-MS and Carbon 13-NMR, were used to elucidate the lipid side chain structure. The contributions of the head groups of the lipid upon temperature adaptation were also investigated. To further understand the temperature effects of *T. acidophilum*, cells were adapted to growth at 37°C. Correlation between membrane fluidity and membrane-bound enzymes were analysed. The second part of this dissertation (Chapter 5) is dedicated to the partial characterization of a procaryotic glycoprotein found in the *T. acidophilum* membrane. The possible function of this membrane glycoprotein in protecting the organism from its harsh environment (pH 2 and 56°C) was investigated.

CHAPTER 2

MATERIALS AND METHODS

MATERIALS

The following solvents were of reagent grade: methanol, chloroform, pyridine, toluene, acetic anhydride, dichloromethane, carbon tetrachloride, benzene, acetic acid, acetone, hexanes (Mallinckrodt, St. Louis, Mo.); dimethylsulfoxide (Fisher, Fair Lawn, N.J.); acetonitrile (Aldrich, Milwaukee, Wis.). All solvents were redistilled prior to use.

Chemicals and their sources are as follows: NaH from Alfa Inorganics (Beverly, Mass.); Sephadex G-10, G-25, G-75, G-100, G-200, LH-20 and Sepharose 4B from Pharmacia (Piscataway, N.J.); silicic acid from Clarkson (Williamsport, Pa.); galactosamine hydrochloride, glucosamine hydrochloride, glucose, galactose, mannose from Pfanstiehl (Waukegan, Ill.); silica gel C TLC plates from Analtech (Newark, Del.); molecular weight calibration proteins from Boehringer-Mannheim (Indianapolis, Ind.); 3% SE-30 on Supelcoport (80-100 mesh), 3% SP-2100 on Supelcoport (80-100 mesh), 3% OV-225 on Gas Chrom Q (80-100 mesh) from Supelco (Bellefonte, Pa.); mercaptoethanol from Aldrich (Milwaukee, Wis.); Dowex 1, hexamethyldichlorosilazane, trimethylchlorosilane, glycine, bromophenol blue, fuchsin, Coomassie blue, ATP, glucose from Sigma (St. Louis, Mo.); dialysis tubings from Thomas (Philadelphia, Pa.); ninhydrin, ammonium persulfate, orcinol, ammonium molybdate from Fisher (Fair Lawn, N.J.); acrylamide, and N,N'-methylenebisacrylamide from

Canalco (Rockville, Md.); N,N,N',N'-tetramethyl-ethylenediamine and Photo-Flow 600 from Eastman Kodak (Rochester, N.Y.); silver carbonate, phenol, EDTA from Mallinckrodt (St. Louis, Mo.); ethanol amine HCl, EDTA disodium cupric salt from ICN Pharmaceuticals (Cleveland, Ohio); hydrochloric acid, sulfuric acid and iodine from Baker (Philipsburg, N. J.); Folin Ciocalteu reagent from Harleco (Phila., Pa.); HCl and BCl₃ gas from Matheson Gas (Lyndhurst, N. J.); 5-NS from Synvar (Palo Alto, Ca.); yeast extract from Difco (Detroit, Mi.); α -mannosidase, β -galactosidase, α -glucosidase, β -glucosidase, endo-glycosidase H, and endo-glycosidase D from Miles (Elkhart, Ind.); Anhydrous hydrogen fluoride reaction apparatus from Peninsula Laboratories Inc. (San Carlos, Ca.).

METHODS

Growth of Cells

Thermoplasma acidophilum was obtained from the American Type Culture Collection (ATCC 25905). The organism was grown in a medium containing 1.5 mM (NH₄)₂SO₄, 4.2 mM MgSO₄·7H₂O, 1.7 mM CaCl₂·2H₂O, 0.03% KH₂PO₄, 1% glucose, and 0.1% yeast extract (Difco Control #629756). The pH was adjusted to 2 with concentrated H₂SO₄ and the medium then autoclaved. A 10% (v/v) inoculum from a 22 hours old culture into the same medium gave the best growth. Each culture was continuously aerated for 22 hours with filtered sterilized air. Late log phase cells were harvested by centrifugation at 4200 g for 5 minutes at 4°C. Medium components were removed by multiple water washings. Cells grown at 37°C were transferred from the same culture line as 56°C-grown cells. The final inoculum for 37°C cultures was prepared from cells which had been grown for about 8 days in a culture, which, in turn, had been pre-inoculated (10%) with cells grown for about the same length of time.

Cells were adapted from 56°C to growth at 37°C for at least 30 generations.

The 37°C-grown cells were harvested as described above.

Membrane Preparation

Cells were lysed by 1 M glycine buffer, pH 9.3, 22°C, at a protein concentration higher than 10 mg/ml. Membranes were collected by centrifugation at 34,800 g for 2 hours, then layered onto a discontinuous sucrose gradient (25%/55%) pH 7.4 and centrifuged on a Beckman L2-65B Ultracentrifuge for 2 hours at 40,000 rpm with an SW 41 rotor. The membranes appeared as a single band at the interface of the two sucrose layers and were collected and freed from sucrose by washing with water.

Extraction of Lipids

Lipids were extracted from cell membrane with chloroform-methanol (2:1 v/v). Further removal of non-lipid contaminants was done by partitioning the lipid extract with 0.2 volume of salt solution (27).

Silicic Acid Column Chromatography

Silicic acid (100-200 mesh) was employed to separate the lipids. The neutral lipids were eluted with chloroform, glycolipids were obtained by elution with acetone, and phospholipids were recovered from the column by final elution with methanol (28).

Preparative Thin-Layer Chromatography (TLC)

Individual phospholipids and glycolipids were separated on silica gel G plates. Lipids were streaked onto the TLC plate with a preparative TLC sample applicator system (Applied Science Lab.). Plates were developed at room temperature with the solvent system of chloroform-methanol-water (65:45:8, v/v) for phospholipids or chloroform-methanol (9:1, v/v) for glycolipids. Lipids were visualized by iodine vapor. Spots were scraped and lipids were extracted by successive elution with chloroform-

methanol (2:1, v/v), chloroform-methanol (1:2, v/v), methanol, and finally chloroform-methanol-water (50:50:15).

Transmethylation of Lipids

Samples of lipids were hydrolyzed in 5 ml of methanol and 0.1 ml of concentrated H_2SO_4 for 24 hours at 40°C . Fatty acid methyl esters were extracted three times with equal volumes of hexane. The combined hexane phase was washed with water until neutral.

Methanolysis

Samples of lipids in 2.5% methanolic-HCl were heated at 100°C for 3 hours. The unsaponifiable material was extracted three times with equal volumes of hexane (29).

Degradation of Glycerol Ethers

(i) Alkyl Chloride Derivatives

The unsaponifiable material from methanolysis was treated with $\text{BCl}_3\text{-CHCl}_3$ (1:1 v/v) at room temperature for 24 hours. After evaporation of the $\text{BCl}_3\text{-CHCl}_3$ mixture, the sample was partitioned between hexane and water. The alkyl chloride derivative of the hexane phase was pooled and dried to constant weight under a stream of nitrogen at room temperature (29).

(ii) Alcohol Derivatives

Hydrolysis of glycerol ethers was conducted in 57% hydriodic acid (29). Samples were heated under reflux for 24 hours, cooled, and extracted three times with three volumes of hexane. Alkyl iodides contained in the hexane phase were successively washed once with 10% NaCl, saturated solution of K_2CO_3 , and finally with 50% $\text{Na}_2\text{S}_2\text{O}_3$. Alkyl iodides were converted to the acetates by refluxing with silver acetate in acetic acid for 24 hours. Alcohol derivatives were prepared from

the acetates by hydrolysis in 0.2 N NaOH at 100°C for 2 hours.

Determination of C-methyl Groups

The method of Kuhn and Roth (30) was used. Samples were sealed into an ampule with 1:4 v/v of concentrated H₂SO₄ to 2 N chromic acid and shaken for 12 hours at 135°C. After oxidation, the contents were washed over into a distillation apparatus. After adding one drop of 1% phenolphthalein solution, the distillate was quickly titrated to the first pink tinge remaining for 5 seconds.

Gas-Liquid Chromatography (GC) for Membrane Lipid Derivatives

A Hewlett-Packard gas chromatograph, Model 402, equipped with a flame ionization detector and 2 m x 2 mm glass column was used for GC analysis of the lipid derivatives. Fatty acid methyl esters were run at 170°C on 3% SP-2100. Alkyl ether derivatives were eluted isothermally on 3% SP-2100 at 325°C. Areas of peaks were determined with a Hewlett-Packard integrator, Model 3380 A.

Combined Gas Chromatography-Mass Spectrometry (GC-MS)

The LKB 9000 gas chromatograph-mass spectrometer was operated with a trap current of 60 μ A, an ion source temperature of 310°C and a molecular separator temperature of 310°C. (Dr. C. C. Sweeley, Biochemistry Department, Michigan State University) (31).

Electron Impact Ionization-Mass Spectrometry (EI-MS)

Mass spectra were obtained with a Varian MAT mass spectrometer, Model CH-5DF, with a combined electron impact/field ionization/field desorption source. The mass spectrometer was interfaced to a PDP 11/21 minicomputer (Digital Equipment Corporation) in which data collection and storage programs were functional. By direct memory access, this computer was attached to a PDP 11/40 minicomputer (Digital Equipment

Corporation) which operated in a time-shared mode employing the multi-task executive program RSX-11D. The outputs from the mass spectrometric experiments were received from the PDP 11/40 system via a Tektronix data terminal, Model 4010, and a Tektronix hard copy unit, Model 4610 (32).

Infrared Spectroscopy

Infrared spectra were recorded by a Perkin-Elmer Grating Infrared Spectrophotometer, Model 621. Attenuator speed was set at 1100, slit program at 1000 and source intensity at 0.8 A. CCl_4 was used as solvent.

Nuclear Magnetic Resonance Spectroscopy

(i) Proton NMR

Proton NMR spectrum was recorded on a Bruker WH-180 spectrometer, at 180 MHz. The sample was dissolved in CDCl_3 with tetramethylsilane as internal standard. (Chemistry Department, Michigan State University).

(ii) ^{13}C -NMR

The 15.08 MHz, proton decoupled ^{13}C -NMR spectrum was obtained using a Bruker WP-60 spectrometer, equipped with Fourier transform operation. The sample (60 mg) was dissolved in 1.5 ml of CDCl_3 and 10,000 transients accumulated at 35°C in a 10 mm tube at a sweep width of 3000 Hz, 66° pulse (12 $\mu\text{sec.}$) and 3 sec. rep. time.

ATPase Assay

The ATPase assay followed the method of Rathbun *et al.* (33). Purified membrane sample was incubated at various temperatures, ions and pH's with 0.1 M buffer and ATP as substrate. The controls had no ATP. The reaction was stopped by adding ice-cold TCA and cooled in an ice bath for 5 minutes. After centrifugation for 5 minutes at 10,000 g at 4°C , the supernatant solution is decanted into empty test tubes. An

aliquot of this supernatant solution is quickly mixed with 3 M acetate buffer and formaldehyde mixture previously pipetted in the test tube. The molybdenum blue color was developed by addition of 2% ammonium molybdate and stannous chloride. The tube contents were quickly mixed and allowed to stand at room temperature. The absorbance of each sample is measured at 735 nm 15 minutes after addition of the molybdate. The protein concentration was determined as described by Wang *et al.* (34).

Buffer Systems for SDS Gel Electrophoresis and Sample Preparation

The discontinuous SDS buffer system of Laemmli (35) was used. Separating gels, containing 3% acrylamide, were prepared from a stock solution of 30 g acrylamide and 0.8 g of N,N'-bis-methyleneacrylamide in 100 ml of water. The stacking gel which usually contained 5% acrylamide was prepared from the same stock solution. The final concentration of SDS was 0.1% in both gels and in the electrode buffer. Sample preparation was performed as described by Laemmli (35) except that samples were boiled for 2 minutes. The final membrane protein concentration in the sample was 2 mg/ml. After addition of glycerol and bromophenol blue, samples were layered onto the gels (10 cm) and run at 5 mA/tube for 3½ hours. Proteins were stained with Coomassie brilliant blue (36). Carbohydrates were stained as described by Fairbanks *et al.* (37). Stained gels were scanned spectrophotometrically with a Gilford linear transport system, Model 2520, at 550 nm for Coomassie blue stain, and at 540 nm for carbohydrate stain.

Electron Paramagnetic Resonance (EPR)

The nitroxide stearate spin label, 5NS, was used for the EPR studies of membranes. Aliquots from a stock solution of spin label in hexane

were measured into small glass test tubes; hexane was removed by evaporation. Membrane vesicles were suspended in water at pH 6. The suspension was added to the spin label. The mixture was then sonicated for 10 minutes. The membrane protein concentration of the membrane vesicles ranged from 20 mg/ml to 30 mg/ml. The spin label concentration was approximately 0.1% of the lipid weight of the vesicles. All EPR experiments were carried out with a Varian spectrometer, Model E-112, with an attached Variable Temperature Controller (VTC) unit. Temperature calibrations were obtained by comparing VTC settings and a Bailey thermocouple measuring the temperature of the sample located in the microwave cavity.

Isolation and Purification of Membrane Glycoprotein

(i) by preparative slab gel electrophoresis

Buffer system of Laemmli (35) was used to run slab gels. The Bio-Rad slab gel apparatus was operated at 30 mA with a slab thickness of 3 mm. After electrophoresis, three strips of gels were cut vertically and stained with PAS and Coomassie blue. The gel was reconstructed after staining and glycoprotein bands were cut, and eluted with buffer. SDS was removed by dialysis.

(ii) by phenol extraction

Membrane was extracted with 50% phenol solution at 70°C for 15 minutes. Material at the interface was collected and dialysed.

(iii) by Sepharose 4B Column Chromatography

Membrane was solubilized by 1% SDS and loaded onto a 90 x 1.5 cm (i.d.) Sepharose 4B column. Fractions of 3 ml were collected and assayed for protein and carbohydrate.

(iv) by Con A-Sepharose Column Chromatography

Glycoprotein isolated by the above three methods can be further purified by Con A-Sepharose column. Glycoprotein was loaded on the column and eluted first with a solution of 0.5% Triton X-100, 50 mM Tris, pH 8.0, 0.5 M NaCl, and then with 0.5% Triton X-100, 50 mM Tris, pH 8.0, 0.2 M α -methylmannoside. Triton X-100 was removed by dialysis.

Methanolysis of Carbohydrates

Methanolysis of glycoprotein to study the carbohydrate-portion was performed by the method of Chambers and Clamp (38). Samples were hydrolysed in 1.5 N methanolic-HCl in sealed teflon-lined vials at 95°C for 90 minutes with mannitol as internal standard. Silver carbonate was added until the solution is neutral. Acetic anhydride was added to re-N-acetylate the aminosugars for at least 6 hours at room temperature. The sample was then centrifuged and the supernatant fraction removed. The residue was washed four times with dry methanol. The pooled supernatant fraction was dried under nitrogen at room temperature and derivatized with pyridine/hexamethyldichlorosilazane/trimethylchlorosilane (5:1:1, v/v). Trimethylsilylated methyl glycosides were analysed on a Perkin-Elmer gas-liquid chromatograph, Model 910, with a 12 ft 3% SP-2100 on Supelcoport (80-100 mesh) column with initial hold of 4 minutes at 120°C, then programmed at 0.5°C/min to 185°C, and held at 185°C for 20 minutes.

Permethylation for Linkage Studies

Permethylation of carbohydrates was performed by the method of Hakomori (39). All the permethylation operations were done under dry nitrogen. Hexane was dried by refluxing with BaO (20 g/liter) for 2 hours, redistilled and stored over molecular sieves. All the other

solvents used were redistilled. A sample of NaH (0.9 g of 57% oil emulsion) was washed 7 times with 15 ml aliquots of dried redistilled hexane. Dry redistilled dimethylsulfoxide (10 ml) was added and allowed to react at 65-70°C until bubbling of hydrogen ceased (approximately 90 minutes). The dimethylsulfinyl ion solution (0.5 ml) was added to samples (0.5 mg) dissolved in 0.5 ml dimethylsulfoxide and allowed to react for 30 minutes with periodic sonications. Redistilled iodomethane (2 ml) was then slowly added and allowed to stand for 2 hours at room temperature. The solutions were then dissolved in 5 ml of chloroform and washed twice with 5 ml water, once with 5 ml 20% Na₂S₂O₃ and thrice with water. The samples were dried under nitrogen with the aid of absolute alcohol and hydrolysed in 0.5 ml 0.5 N H₂SO₄ in 95% acetic acid for 24 hours at 85°C. Water was then added and allowed to react for an additional 5 hours at 85°C. A small column with 2 ml of Dowex 1 x 8, acetate form (50-100 mesh) was used to adsorb the sulfate. The column was washed with 2-3 ml of acetic acid. The hydrolysate was evaporated to dryness under nitrogen and reduced with 0.5 ml of NaBH₄ (10 mg/ml) for 2 hours. Reduction was terminated with the addition of several drops of glacial acetic acid. The solution was dried under nitrogen. Borate was removed as its methyl ester by 1-2 drops of acetic acid and 2 ml methanol, heating in a boiling water bath for 5 minutes, and evaporating under nitrogen. The esterification procedure was repeated three more times. The dried sample was acetylated in 0.5-1.0 ml acetic anhydride for 60-90 minutes at 100°C. After drying under nitrogen with the aid of toluene, dissolved in 2 ml of CH₂Cl₂, washed three times with 1-2 ml water and drying under nitrogen again, the partially methylated alditol acetates were ready for analyses by GC or GC-MS. Column packings used for these

analyses were 3% OV-210 on Gas Chrom Q (80-100 mesh) or 3% OV-225 on Gas Chrom Q (80-100 mesh). The mass spectra were interpreted according to Björndal *et al.* (40).

Anhydrous Hydrogen Fluoride Deglycosylation

Reaction vessel containing freeze-dried sample was cooled in liquid nitrogen bath. 10 ml of HF was distilled over from the reservoir. Allow the reaction vessel to warm up to room temperature. At the end of the reaction, evacuate the reaction vessel via a calcium oxide trap. To ensure complete removal of HF, the line was evacuated for an additional hour after removal of visible HF. The sample was then taken up in water and passed through an Amicon ultrafiltration cell to separate the carbohydrate and the protein (106).

Amino Acid Analysis

5.7 N HCl was added to the purified glycoprotein. Hydrolysis was complete after 18 hours at 110°C. The suspension was taken to dryness under nitrogen and resuspended in 0.01 N HCl. Amino acid analysis was performed on a single column accelerated flow Technicon system modified by Dr. D.T.A. Lamport, Plant Research Laboratory, Michigan State University.

Treatments of Glycoprotein with Glycosidases

(i) α -mannosidase digestion

Reaction mixtures containing approximately 5 mg of purified glycoprotein in 1 ml of 0.1 M citrate buffer, pH 4.5, were incubated at 37°C with 2 to 3 units of α -mannosidase. Incubation was continued until no additional release of mannose was observed. The reaction was terminated by introducing 2 ml of 0.2 M borate buffer, pH 9.8. The reaction mixtures were then passed through an ultrafiltration cell to separate the

free carbohydrates from the rest of the glycoproteins.

(ii) β -glucosidase digestion

The same procedure for α -mannosidase was used for β -glucosidase.

(iii) β -galactosidase digestion

The same procedure for α -mannosidase was used only the buffer was different. β -galactosidase has an optimum pH at 7.0.

(iv) endo-glycosidase H digestion

Glycopeptide in 1 ml of 0.1 M acetate buffer, pH 5.0 was incubated with 1 unit of endo-glycosidase H for 16 hours at 37°C. The reaction was stopped by heating for 1 minute in a boiling water bath and the reaction mixture was ultrafiltrated. Endo-glycosidase H from *Streptomyces griseus* hydrolyzes the β -di-N-acetylchitobiose structure in asparagine-linked sugar chains of glycopeptides.

Analytical Methods

Phosphorus was determined by the method of Fiske and SubbaRow (41). Total nitrogen content was measured according to the method of Lang (42). Glycerol was determined colorimetrically after periodate oxidation (43). Carbohydrate was estimated by the anthrone procedure (44). Choline content was determined by the method of Wells *et al.* (45). Serine and ethanolamine was estimated by the method of Dittmer *et al.* (46).

CHAPTER 3
STRUCTURE OF LONG-CHAIN GLYCEROL ETHERS
IN PLASMA MEMBRANE FROM *THERMOPLASMA ACIDOPHILUM* GROWN AT 56°C

Introduction

Microorganisms have a great capacity to adapt to a wide range of environmental temperatures. The molecular mechanisms underlying temperature adaptation are not well understood although much information is available on adaptational changes in fatty acid composition (47,48). Since temperature has a crucial influence on the structure and function of biological membranes (49,50), it is a reasonable working hypothesis that physico-biochemical membrane properties are fundamental to the ability of microorganisms to exist in thermal habitats. Generally thermophilic microorganisms contain a higher amount of saturated and branched-chain fatty acids (51,52). With respect to physico-chemical parameters, such as membrane lipid fluidity and lipid phase transition temperatures (53,54), the growth temperature range of a microorganism seems to depend on the ability to regulate its membrane lipid fluidity within a certain range (55,56).

An attractive system for investigating mechanisms of temperature adaptation is *Thermoplasma acidophilum* which grows optimally at pH 2 and 56°C (1). The temperature extremes at which this cell can grow and reproduce are 37°C and 65°C (57). Since its plasma membrane directly interfaces with the harsh environment, structural and functional membrane

parameters may determine the environmental limits within which the cell is capable to survive.

Electron paramagnetic resonance experiments using spin labels demonstrated that the lipid regions of *Thermoplasma acidophilum* may be best described as highly rigid (19), even more rigid than those reported for the halophilic *Halobacterium cutirubrum* (58). To understand the high rigidity of the lipid matrix, the structural determination of membrane lipids is important. After we had embarked in this investigation, four different structures have been proposed (13, 16-18); therefore, a further objective of this study is directed to resolve this discrepancy.

Results

Lipids from *T. acidophilum* membranes accounted for 25% of the membrane dry weight. The relative quantities of neutral lipid: glycolipids: phospholipids were 1:1:3 (w/w). On TLC plates the glycolipids could be separated into 8 bands, where 70% (w/w) were monoglycosylated. The carbohydrate content was 88% glucose and 11.5% mannose. On the other hand, phospholipids could be separated into 9 bands where one band accounted for 60% (w/w) of the total membrane lipids. Previously reported experiments showed that these two lipid classes comprise 83% (w/w) of the total lipids (13). After recovery from the TLC plates, material from each individual glyco- or phospholipids band was trans-methylated. Approximately 0.3% (by weight) of fatty acids were found in either type of lipid class, which agreed with previously reported results (13). As determined by gas-liquid chromatography, the chain lengths of the fatty acids varied from C₁₆ to C₂₀. Since ester-linked fatty acids are acid-labile, this finding is consistent with the

ability of growth at pH 2 of *T. acidophilum*.

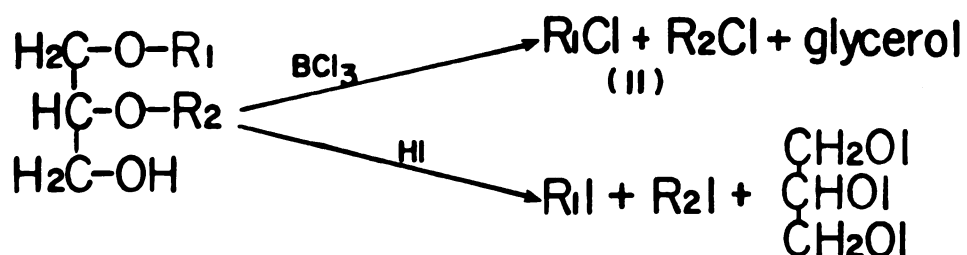
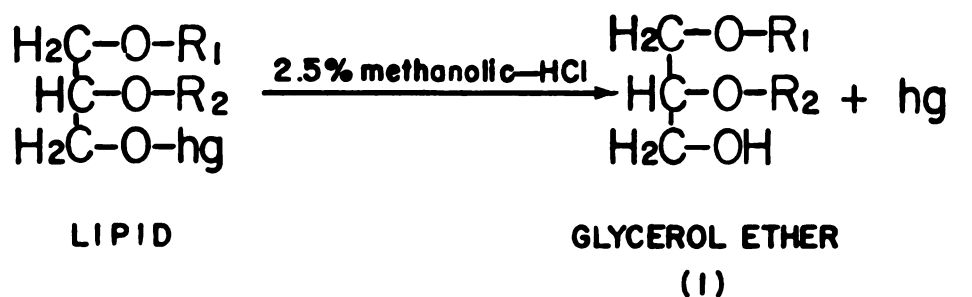
The unsaponifiable material from transmethylation was treated with 2.5% methanolic-HCl at 100°C for 3 hours (glycolipids) or 5 hours (phospholipids). Methanolysis reaction will cleave the head group of the lipids, and leave the glycerol backbone intact (Figure 1). The unsaponifiable material (I) (Figure 1) was extracted three times with equal volumes of hexane. The hexane phase was pooled and dried under nitrogen. Thin-layer chromatogram of compound (I) developed in the solvent system chloroform/diethyl ether 9/1 (v/v) showed a single band regardless of the origin of the lipid class or band. The dried material (I) was taken up in CCl₄ for infrared measurements, in CDCl₃ for NMR studies, or in hexane for direct probe mass spectrometry studies.

Infrared Spectroscopic Studies of Compound (I)

Infrared spectrum of compound (I) (Figure 1) is illustrated in Figure 2. The unsaponifiable material (I) gave OH absorption at 3590-3620 cm⁻¹, alkyl stretching at 2850-2960 cm⁻¹, C-H bending at 1455 and 1370 cm⁻¹, ether C-O-C stretching at 1110 cm⁻¹, and primary hydroxyl C-O at 1040 cm⁻¹. The absorptions of C=C, C=C-H, C=O and COOH were absent. These absorptions indicated that the side chains were linked to the glycerol backbone by ether linkages, and there were no ester or double bonds in compound (I), hence the name glycerol ether. Bands at 840-890 cm⁻¹ provided evidence for the possible existence of cyclo-alkane ring. This was further supported by the presence of a -CH₂- scissoring vibration at 1455 cm⁻¹ which occurred in cyclopentane and cyclohexane derivatives.

Proton-NMR Studies of Compound (I)

The proton magnetic resonance spectrum obtained for the glycerol ether is illustrated in Figure 3. The assignment of chemical shifts



hg = head group

Figure 1. Chemical Degradation Scheme of the Glycerol Ether Lipids from the Membrane of *Thermoplasma acidophilum*.

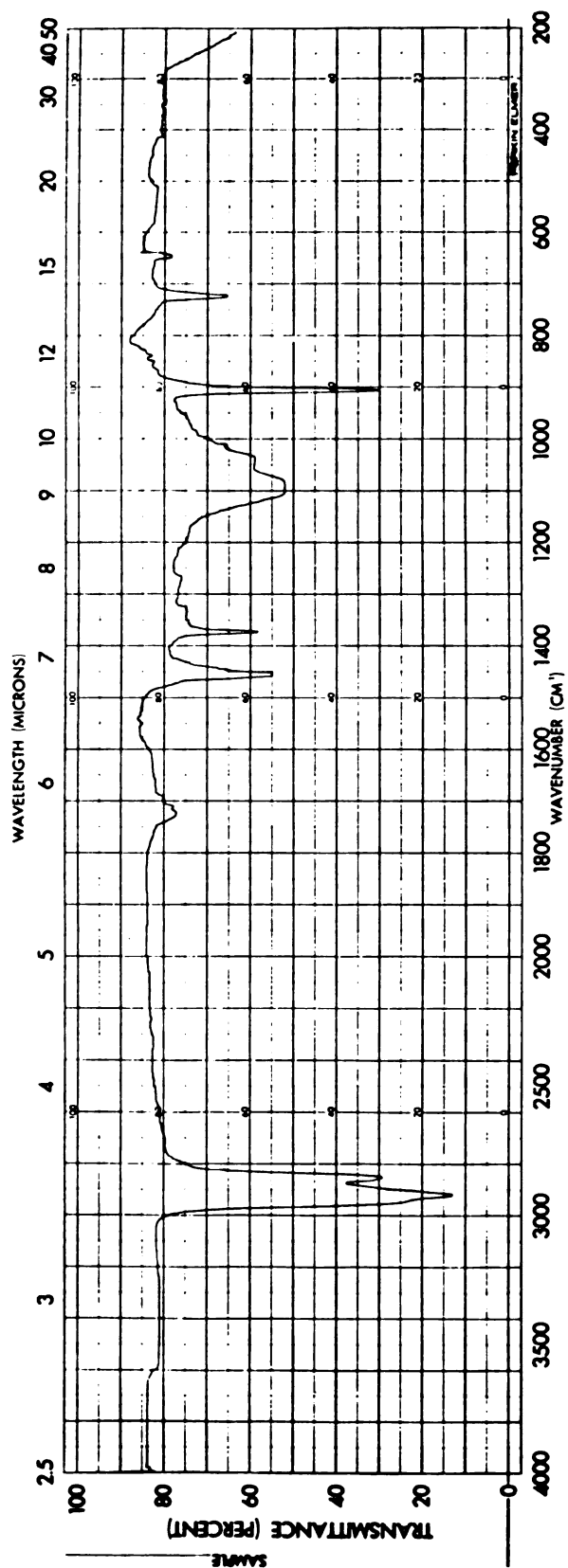


Figure 2. Infrared Spectrum of Compound (I) (Figure 1).

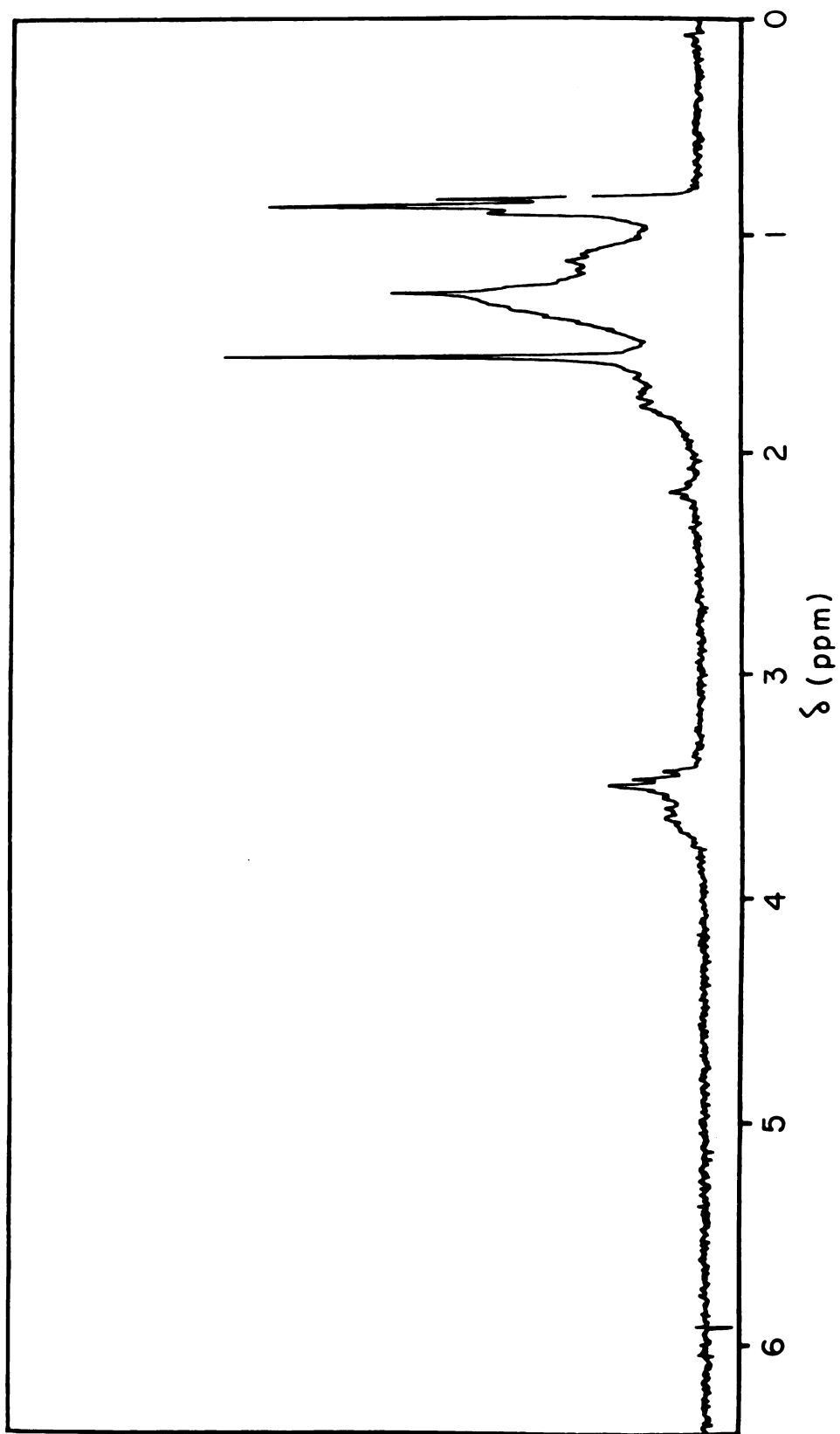


Figure 3. Proton Magnetic Resonance Spectrum of Compound (I) (Figure 1).

of proton signals of glycerol ether is summarized in Table 1. The PMR spectrum showed a triplet at δ 0.83, 0.86 and 0.89, assigned to the methyl groups $-\text{CH}_3$. The resolved signals, those at δ 1.25 were assigned to the interior methylene groups, $\text{CH}_2-\text{CH}_2-\text{CH}_2$, those at δ 1.55 were assigned to the ring methylene groups, those at δ 1.72 were assigned to the interior methine groups, CH , those at δ 2.15 were assigned to the primary hydroxyl, $-\text{OH}$, and those at δ 3.50, 3.63 were assigned to $\text{H}-\text{C}-\text{O}-\text{CH}_2$ and $-\text{CH}_2-\text{OH}$ respectively. There were no $\text{C}=\text{C}-\text{H}$, or $-\text{COOH}$ absorption, which was consistent with the infrared spectrum. Both the PMR and IR spectra supported the structure of the unsaponifiable material (I) to be an ether-linked lipid with methyl branching and the possible existence of cyclo-alkane ring in the side chains. No double bond was detectable in either spectrum.

GC Studies of Alkyl Chloride and Alkyl Alcohol Derivatives of Side Chains

To further study the detailed structure of the side chains, (I) was either reacted with $\text{BCl}_3/\text{CHCl}_3$ to their alkyl chloride derivatives (II) (Figure 1), or reduced to their alkyl alcohol derivatives (III)(Figure 1). Both derivatives did not elute on the gas chromatograph, equipped with a 6 ft 3% SP-2100 column, until 325°C . A rough estimate from the retention times indicated that the side chain should consist of more than 35 carbon atoms. Since high molecular standard for GC analyses was unavailable, combined GC-MS was used to determine the molecular weights and the structures of the lipid side chains.

The alkyl chloride derivatives gave 7 GC peaks where peaks #3-6 accounted for 90% of the lipids analyzed (Figure 4). However, the alkyl alcohol derivatives showed 3 GC peaks with the ratio #1/#2/#3 = 20/45/30 (Figure 5). At first these differences were rather confusing. The discrepancy was resolved when the GC-MS and EI-MS spectra were analysed.

Table 1. Proton NMR Chemical Shifts δ (in ppm) of Glycerol Ether
Downfield from TMS.

δ (ppm)	Assignment
0.83, 0.86, 0.89	-CH ₃
1.10	-CH ₃ next to ring
1.25	-CH ₂ -CH ₂ -CH ₂ -
1.55	-CH ₂ in ring
1.72	-CH
2.15	-OH
3.50	H-C-O-CH ₂ -
3.63	-CH ₂ -OH

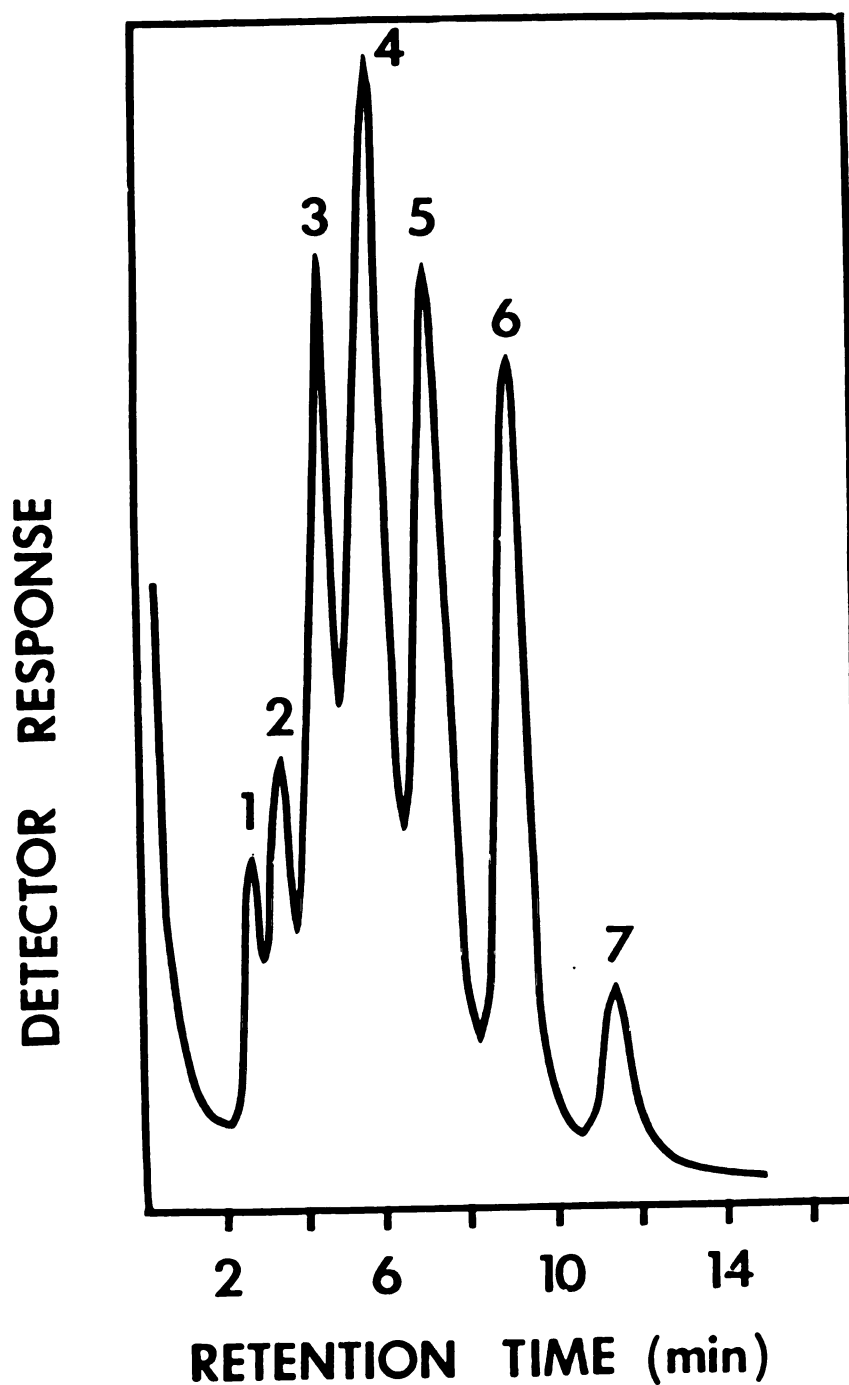


Figure 4. Gas Chromatogram of Alkyl Chloride Derivative of Glycerol Ether Lipids from *T. acidophilum* Membrane. GC analyses were performed on a 6 ft 3% SP-2100 column, operated isothermally at 325°C, with helium as carrier gas.

Figure 5. Gas Chromatogram of Alkyl Alcohol Derivative of Glycerol Ether Lipids from *T. acidophilum* Membrane.

The gas chromatograph was operated as described in Methods.

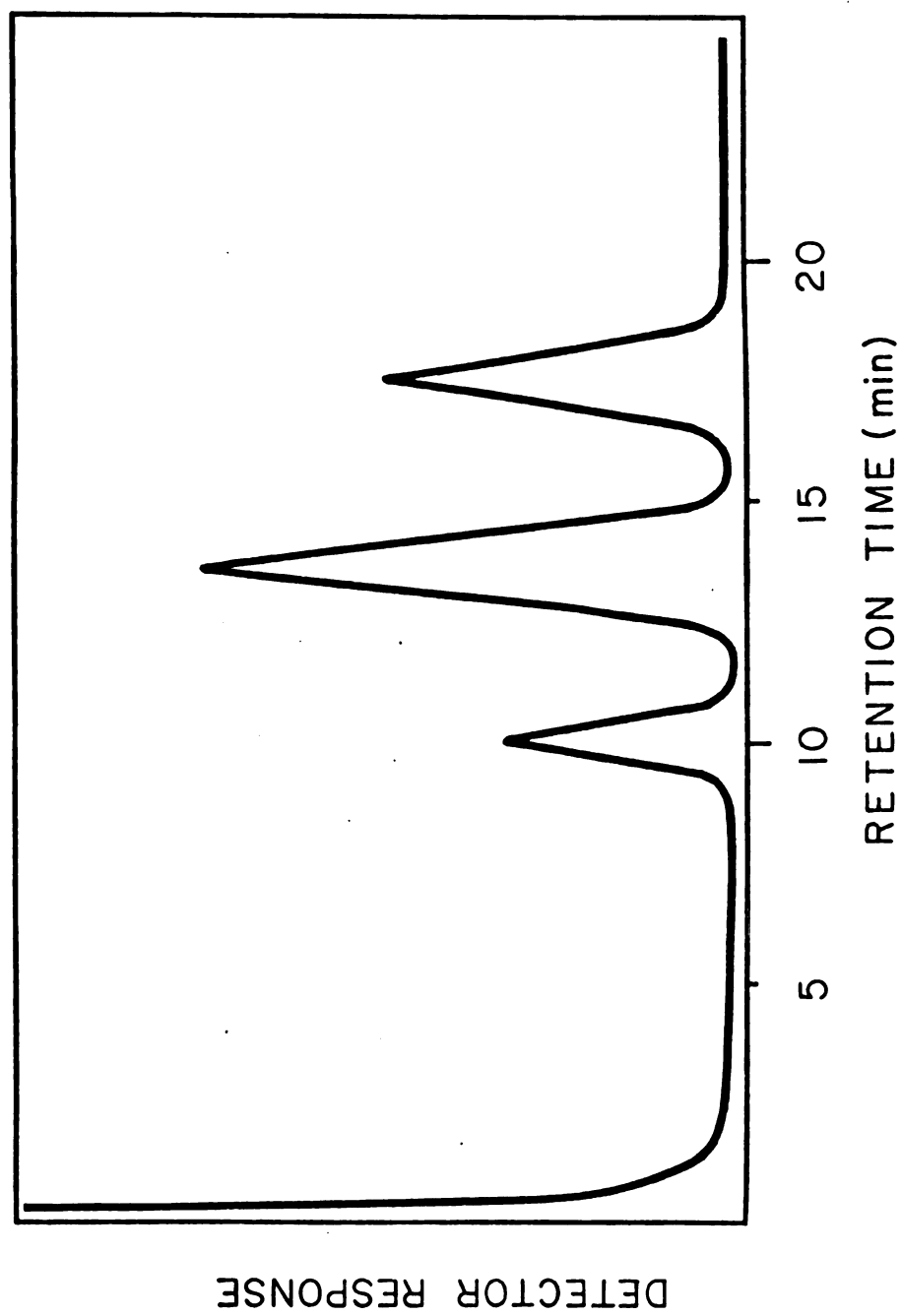


Figure 5.

Organic halides in general, particularly di-halides, undergo several on-column reactions, including rearrangement, loss of one or more molecules of HCl, or $H \rightleftharpoons Cl$ exchange with the liquid phase, even on non-polar phases in glass columns. This is particularly true at high temperatures ($>250^{\circ}C$). For alkyl derivatives of (I), because of the chain length, column temperature was set at $325^{\circ}C$. Some of the GC peaks were generated by de-chlorinated products of the alkyl chloride derivatives. For alkyl alcohol, the column temperature was also set at $325^{\circ}C$, however, alkyl alcohol was TMS-derivatized which is not known to undergo any rearrangement or exchange reactions.

GC-MS Studies of the Alkyl Chloride Derivatives

The GC-MS data of the alkyl chloride derivative will be discussed first. Peak #4, which accounted for 28% of the side chains (Figure 4), generated a very similar fragmentation pattern as that of peak #6 (18%). GC component #4 gave a molecular ion at m/e 592 with the molecular formula $C_{40}H_{77}Cl$, whereas peak #6 gave a molecular ion at m/e 628 with the molecular formula of $C_{40}H_{78}Cl_2$ (Figure 6). Peak #3 apparently corresponded to a mixture of $C_{40}H_{78}$ and $C_{40}H_{79}Cl$. Peak #5 and peak #7 also generated similar fragmentation patterns. Since alkyl chloride derivatives were thermally unstable as discussed above, peaks 3, 4 and 5, which were identified as monochloride derivatives, might be a result of on-column conversion of dichloride derivatives: peaks 6 and 7. The sum of the peak percentages that contributed to the formulae $C_{40}H_{80}Cl_2$, $C_{40}H_{78}Cl_2$ and $C_{40}H_{76}Cl_2$ were 18%, 46% and 32% respectively. These values are in good agreement with that of the alkyl alcohol derivatives (Figure 5).

Although the alkyl chloride derivatives looked confusing, they provided valuable information concerning the structures of the side chains. In the mass chromatograms, pronounced peaks appeared in the

Figure 6. Mass Spectra of the High-Mass Region of GC Component 4,5 and 6 of Alkyl Chloride Derivatives. Combined gas chromatography-mass spectrometry was carried out as described in Methods. M represents the molecular ion.

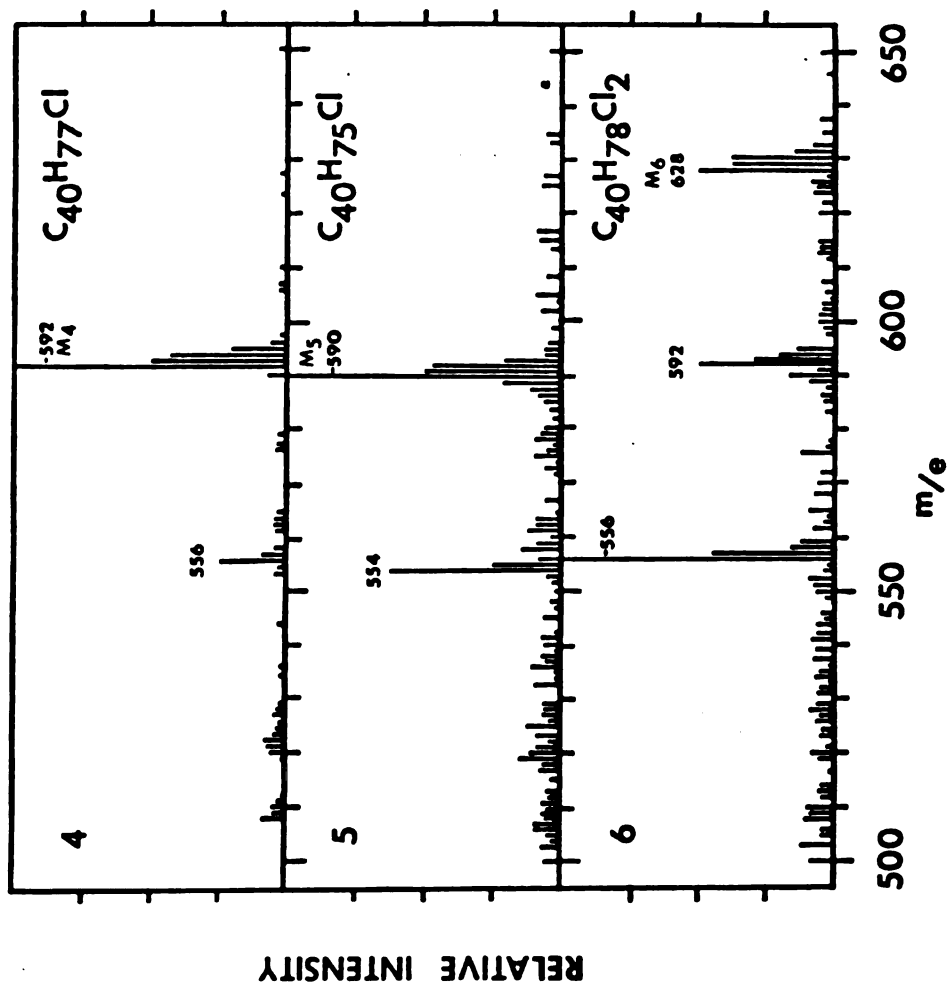


Figure 6.

low-mass region which were characteristic for hydrocarbon-type ion fragments. The relative intensities of these ions decreased as m/e increased. The base peaks were either at m/e 55 or at m/e 57. Ion fragments which contained chlorine could be identified from the isotopic clusters of the mass spectrum (59), because monochlorinated ions are characterized by relative intensity ratios of $P_{m+1}/P_m = 0.5$ and $P_{m+2}/P_m = 0.42$, where P is the relative intensity. In the case of dichlorinated ions, the relative intensity ratio is $P_{m+2}/P_m = 0.7$. In the absence of chlorine, the ion fragment has a relative intensity ratio of $P_{m+2}/P_m = 0.1$ (60) (Figure 6). The mass spectra from each GC component revealed the presence of methyl branches in the alkyl chloride chains. It is possible to deduce the position of methyl branching by searching for relatively high peaks, so-called α -eliminations. In the absence of branches, the relative intensities decrease exponentially as m/e increases. As independent evidence, the Kuhn and Roth (30) reaction was used to determine the number of methyl branchings of the side chains. Application of the sulfuric acid-chromic acid mixture cleaved the methyl branches to give acetic acid. After separating acetic acid from sulfuric and chromic acid by distillation, acetic acid was quantitated by titration. The results derived from the Kuhn and Roth reaction showed an average of seven methyl branches in the alkyl chloride side chains.

From the GC-MS data of alkyl chloride derivatives of compound (I), it was concluded: (i) each side chain has 40 carbon atoms; (ii) from the molecular ions and the isotope patterns, that the side chains have two functional groups per chains, hence gave the dichlorinated derivatives; (iii) because of the lack of absorption characteristic of double bonds, as evidenced by PMR and IR data, the molecular formulae of $C_{40}H_{78}Cl_2$

and $C_{40}H_{76}Cl_2$ indicated certain cyclic structures in the chains; (iv) there existed evidence of methyl branchings in the chains; (v) alkyl chloride derivatives were thermally unstable.

GC-MS Studies of Alkyl Alcohol Derivatives

The detailed GC-MS analysis was carried out on the alkyl alcohol derivatives of compound (I). Alkyl alcohols were derivatized with pyridine/hexamethyldichlorosilazane/trimethylchlorosilane 10/5/2. Figure 5 shows the gas chromatogram of the derivatives. The corresponding mass spectra are shown in Figures 7, 9 and 11. Figure 7 shows the first component of the GC trace (Figure 5) which accounted for 20% of the side chains. The molecular ion was identified at m/e 738. After losing one methyl group from the TMS, ion fragments were seen at m/e 723. Pronounced peaks were seen at m/e 708, 634 and 559 by losing one or both TMS (Figure 8). The next prominent peak was at m/e 354, which was exactly half of m/e 708. This was a strong indication of a symmetric molecule. This was further supported by the fragment m/e 280, which was half of m/e 559+ H^+ . The fragmentations after m/e 280 differed either by 42, 28 or 14 mass units (m/e 253, 239, 225, 211, 169 and 143). This suggested repetitive branching patterns. The major difference between the mass spectra of GC component 2 (also 3) and GC component 1 was the pronounced peak at m/e 165 and m/e 253. The fragment m/e 165 was completely absent in component 1, and fragment m/e 253 was not an outstanding peak compared to peaks close by. The mass spectra 2 and 3 (Figure 9 and 11) looked rather similar, only spectrum 2 showed mixed character of components 1 and 3. Component 3 which accounted for 32% of the total side chains had a symmetric mass fragmentation pattern (Figure 11). The molecular ion was identified at m/e 734. Further fragments were seen at m/e 719, 705, 646, 631 and 557

Figure 7. Mass Spectrum of the First Component of the GC Trace of the Alkyl Alcohol Derivatives of *T. acidophilum* Lipid Side Chains.
The LKB 9000 gas chromatograph-mass spectrometer was operated as described in Methods.

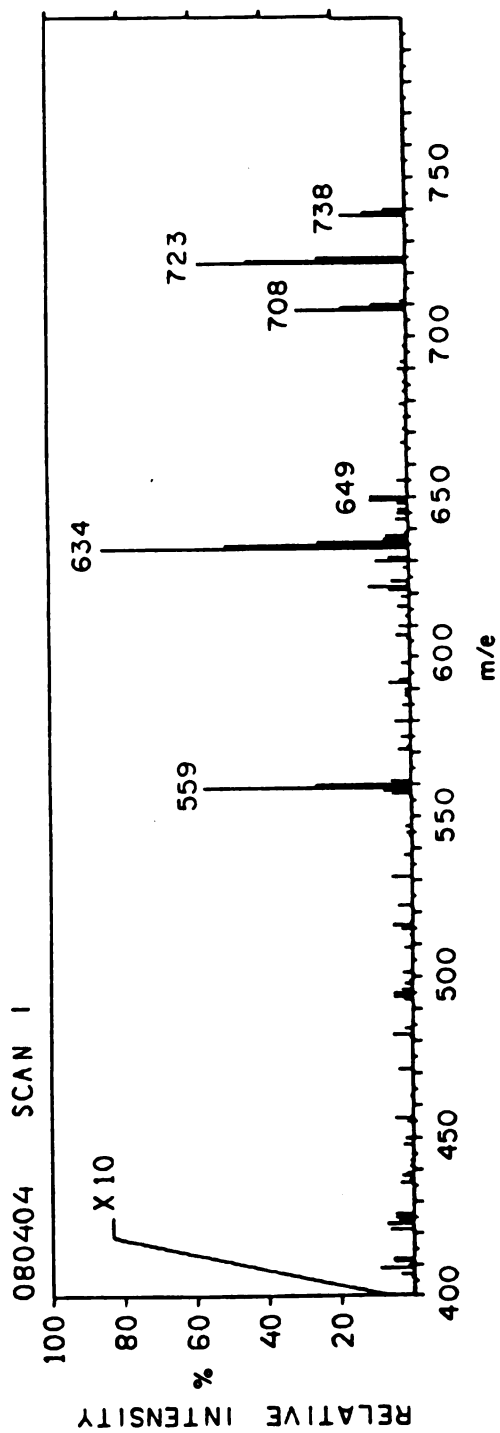
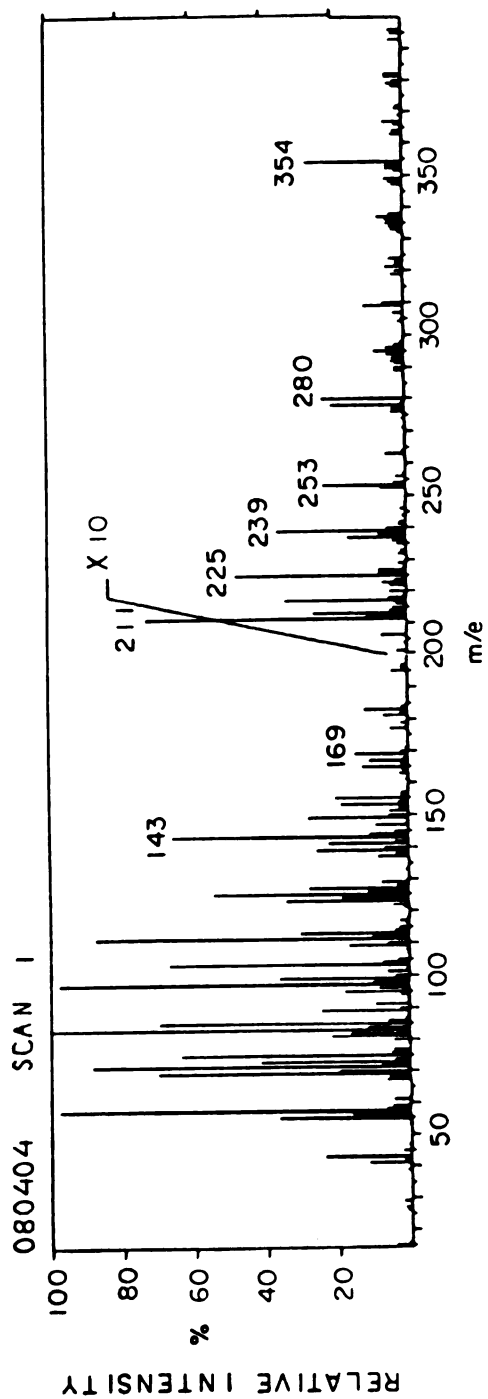


Figure 7.

Figure 8. Assignments of the Ion Fragments of Mass Spectrum Figure 7.

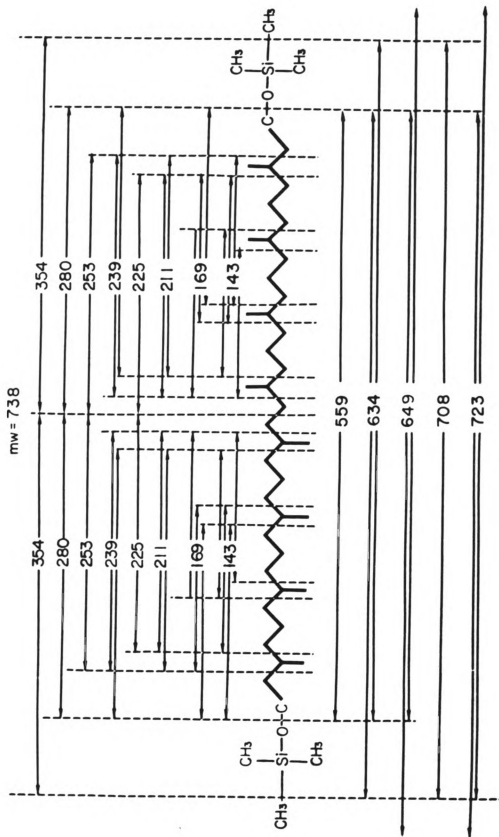


Figure 8.

Figure 9. Mass Spectrum of the Second Component of the GC Trace of the Alkyl Alcohol Derivatives of *T. acidophilum* Lipid Side Chains.

The LKB 9000 gas chromatograph-mass spectrometer was operated as described in Methods.

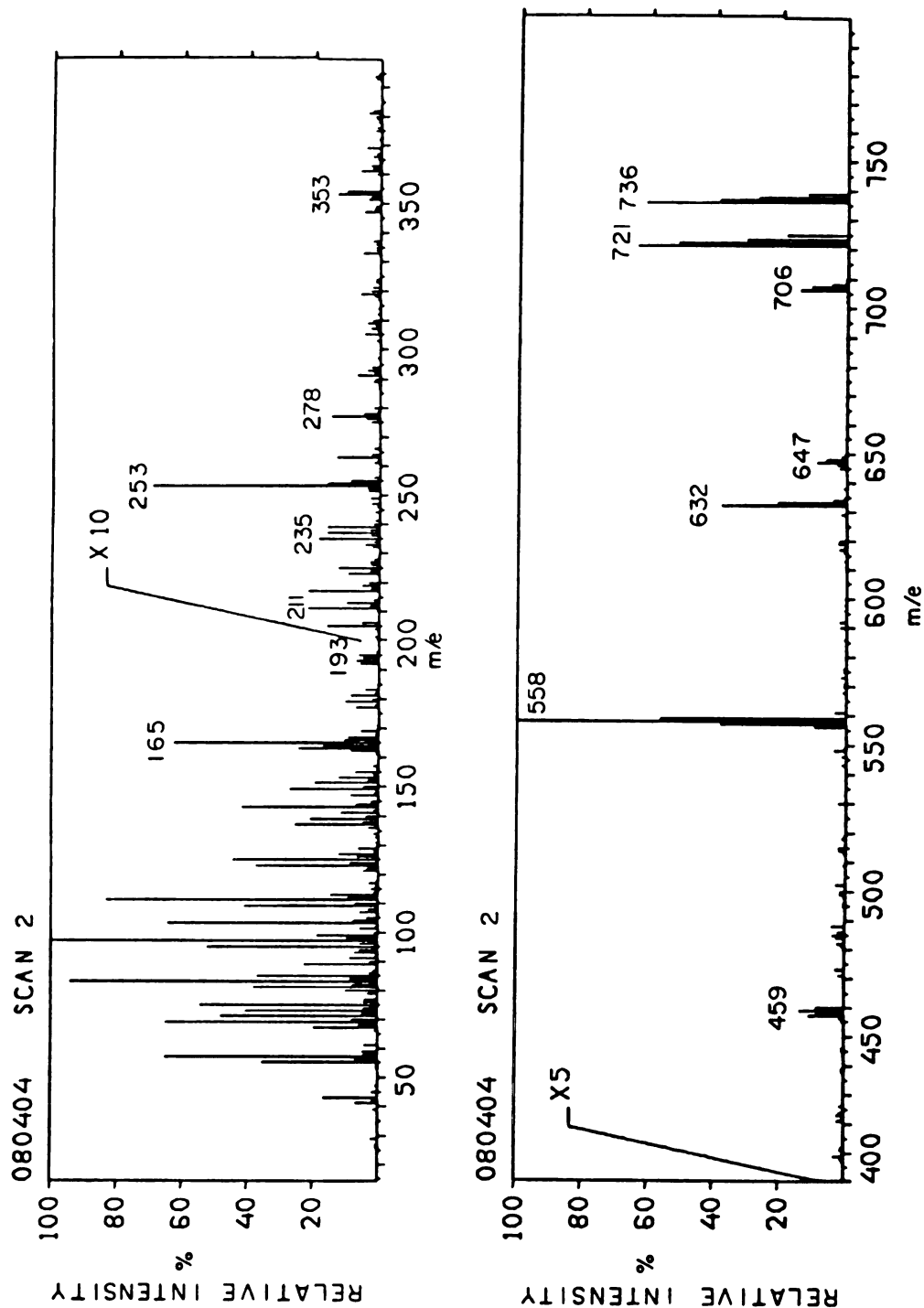


Figure 9.

Figure 10. Assignments of the Ion Fragments of Mass Spectrum Figure 9.

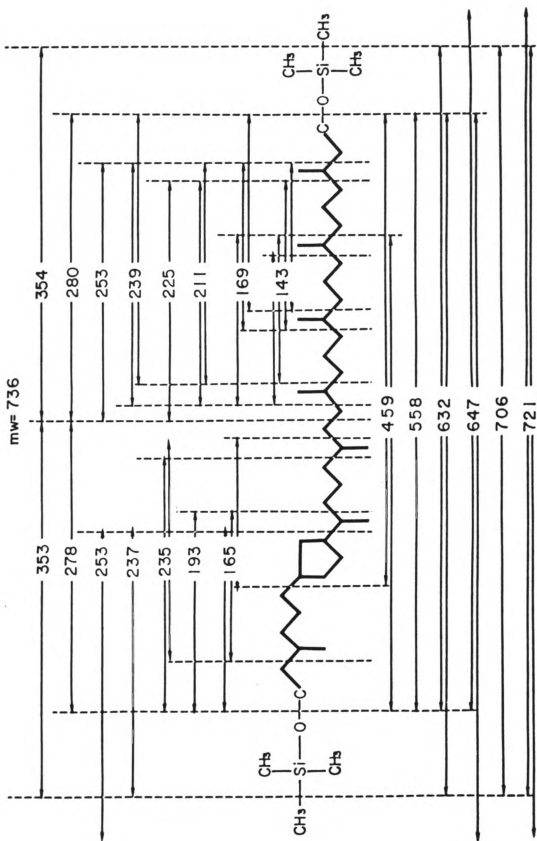


Figure 10.

Figure 11. Mass Spectrum of the Third GC Component of the Alkyl Alcohol Derivatives of the *T. acidophilum* Lipid Side Chains.
The LKB 9000 gas chromatograph-mass spectrometer was operated as described in Methods.

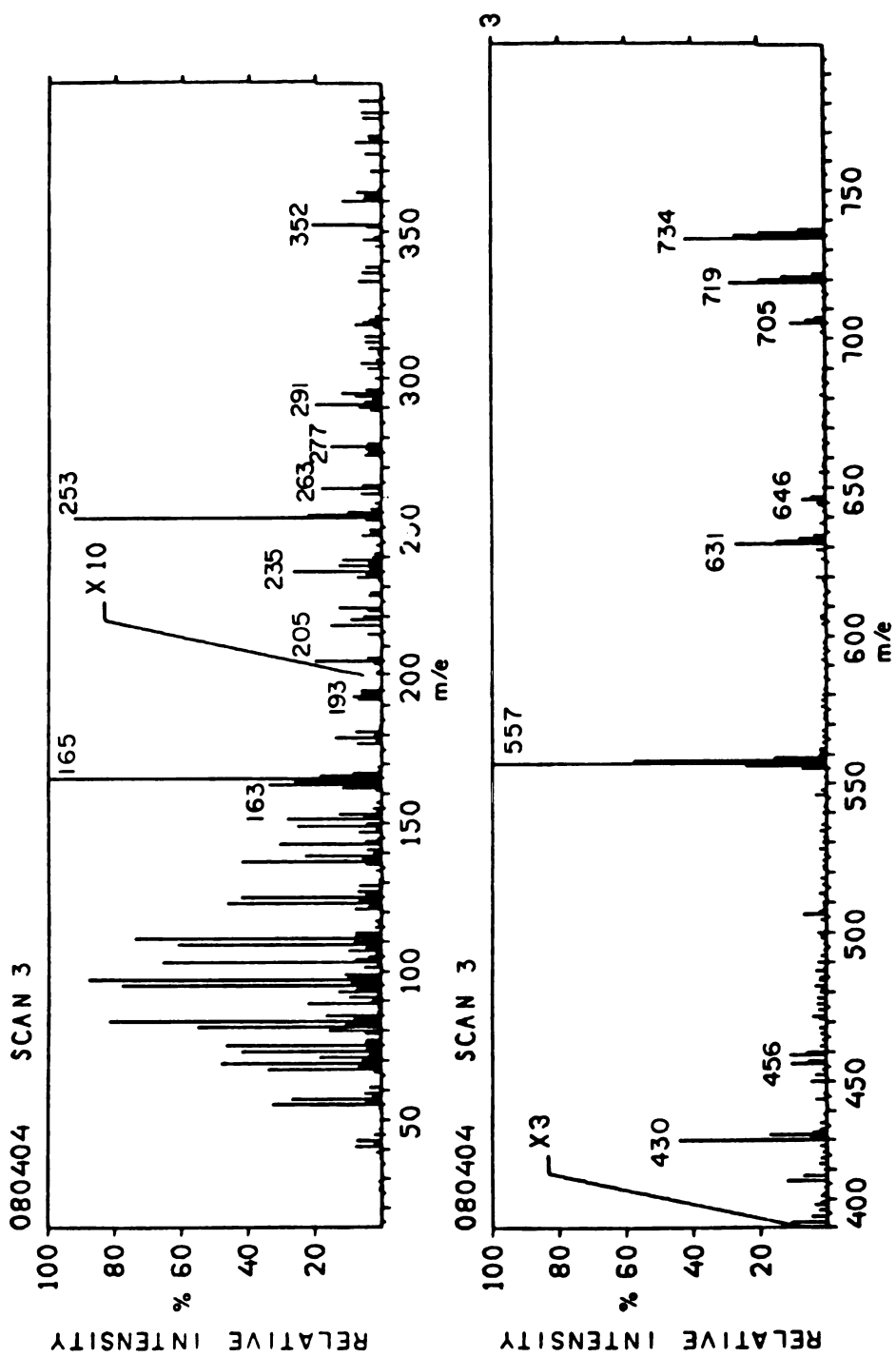


Figure 11.

Figure 12. Assignments of the Ion Fragments of Mass Spectrum Figure 11.

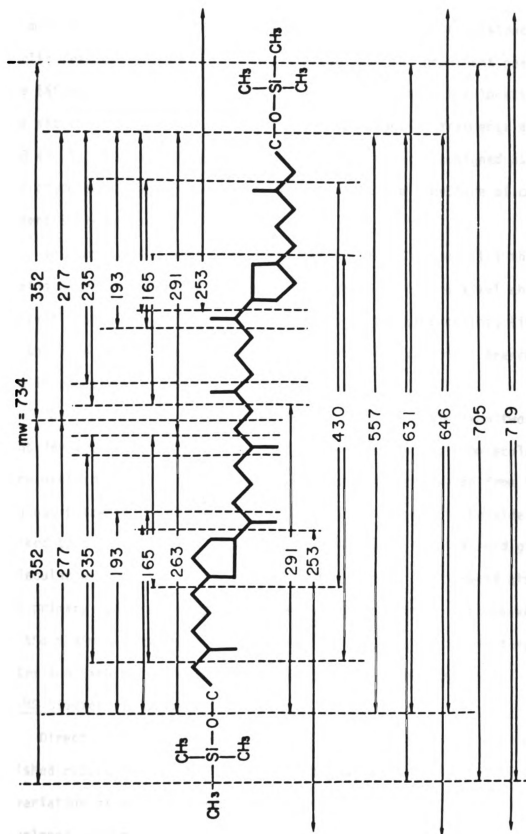


Figure 12.

by losing one or two methyl or TMS groups (Figure 12). Again, fragments at m/e 352 and 277 suggested a symmetric structure. The existence of a cyclic fragment at carbon #12 was inferred from the prominent peaks at m/e 165 and 253 (Figure 12). The conclusion regarding the location and the size of the ring was supported by the presence of fragments at m/e 430 and 193. Fragments of component 2 were similarly assigned as those for components 1 and 3. The mass spectrum and the structure of component 2 are shown in Figures 9 and 10.

In summary: (i) each side chain has 40 carbon atoms; (ii) the side chains have two functional groups, in agreement with the alkyl chloride derivatives; (iii) high degree of symmetry in the side chains; (iv) 75% of the side chains have cyclo-alkane structures; (v) methyl branchings are in repetitive patterns.

The finding of two functional groups per side chain from two different derivatives suggested that more studies on the whole molecule of (I) were necessary. Solely the glycerol molecule was recovered from the aqueous phase in the $\text{BCl}_3/\text{CHCl}_3$ 1/1 reactions. Were all the side chains linked to two glycerol molecules with ether bonds? This should give a molecular weight of 1300 for acyclic side chains. This should also give two primary hydroxyl groups per molecule. Material (I) was non-volatile at the maximum temperature of any GC column. Direct probe mass spectrometry and Carbon 13-NMR were employed to answer these questions.

EI-MS Studies of Compound (I)

Direct probe field desorption mass spectrometry has a well-established record for the analysis of solid samples with little volatility. A variation of the techniques generally used in its analysis has been developed, using a combined electron impact/field ionization/field

desorption source on a Varian MAT CH-5 mass spectrometer. In this procedure, the activated field desorption emitter with sorbed sample is heated in the normal manner, but without the high voltage that is usually applied to the extraction plate during field desorption analysis. Instead, the sample is evaporated from the emitter and ionized by an electron beam. The resulting ions are accelerated and focused into the mass spectrometer for analysis. In this mode, the field desorption emitter is acting as a direct probe sample injector and the resulting mass spectra show characteristic electron impact fragmentation patterns. Since material (I) seemed to be rather unusual, this method was employed to provide additional information about the molecular ion of the entire glycerol ether. An important consideration in the usage of EI-MS was to find appropriate compound(s) for calibration, especially after m/e 1000. For our purpose, a mixture of perfluoroalkane, triazine and tris-(heptafluoropropyl)-s-triazine was used as reference compound which has fragments at m/e 866, 910, 966, 1016, 1065, 1128, 1165, 1200, 1309 and 1329. Mass spectrum of (I) showed two major peak regions, viz., one region from m/e 555 to 740, the second one from m/e 1200 to 1305. Fragments from the first region represented ions from individual side chains (m/e 556, 558, 560), side chains with oxygen (m/e 572, 574 and 576), side chains with methoxy (m/e 585, 587 and 589), side chains with mono-methyl methoxy (m/e 599, 601 and 603), side chains with di-methyl methoxy (m/e 614, 616 and 618), side chains with one glycerol (m/e 646, 648 and 650) and side chains with two glycerols (m/e 736, 738 and 740). Molecular ions were identified at m/e 1300-1304 which have the formula $M+2H$, where M 's represent the molecular weights. Fragments in the region of m/e 1284-1289 were contributed by $M+2H-H_2O$, fragments in

the region of m/e 1269-1275 were derived from $M+2H-CH_2OH$, fragments in the region of m/e 1230-1239 resulted from $M+2H-2(CH_2OH)$. The fragmentation patterns in this second region supported the presence of two glycerols per molecule and two hydroxy groups per molecule. The calibration was off by 2 mass units for (I); nevertheless, for the purpose of verifying the number of glycerols and hydroxyls per molecule the results are still conclusive.

Carbon 13-NMR Studies of Compound (I)

Figure 13 shows the carbon 13-NMR spectrum of (I). The chemical shifts and their assignments are listed in Table 2. The assignments are based on chemical shift rules (62), comparisons with appropriate model compounds (63) and observed multiplicities. The ^{13}C -NMR spectrum of (I) showed 23 resolved signals, because many of the 86 carbon atoms were effectively equivalent. The chemical shifts are also consistent with the symmetric structure supported by GC-MS data. The important assignments at carbon 11, 14 and 18 were consistent with chemical shift rules: $-\gamma + \delta$, ϵ and $\delta + \epsilon$ methyl shielding effects compared to carbon 9 and 13. The assignments of the carbons in the ring and near the ring were determined by comparison with model compounds and calculations according to chemical shift rules. The chemical shifts also favored the 1,3-trans configuration of the cyclopentane ring, but the mutual stereochemistry of the two rings remained unknown.

Discussion

The plasma membrane of *T. acidophilum* contained 75% (w/w) proteins and 25% (w/w) lipids. In this study, the structure of membrane phospholipids and glycolipids, which comprised approximately 80% of the total membrane lipids was examined.

Figure 13. Carbon 13-NMR Spectrum and the Assignment of the Glycerol Ether Molecule from *T. acidophilum* Membrane Lipid.

Carbon 13-NMR spectrometry was performed as described in Methods.

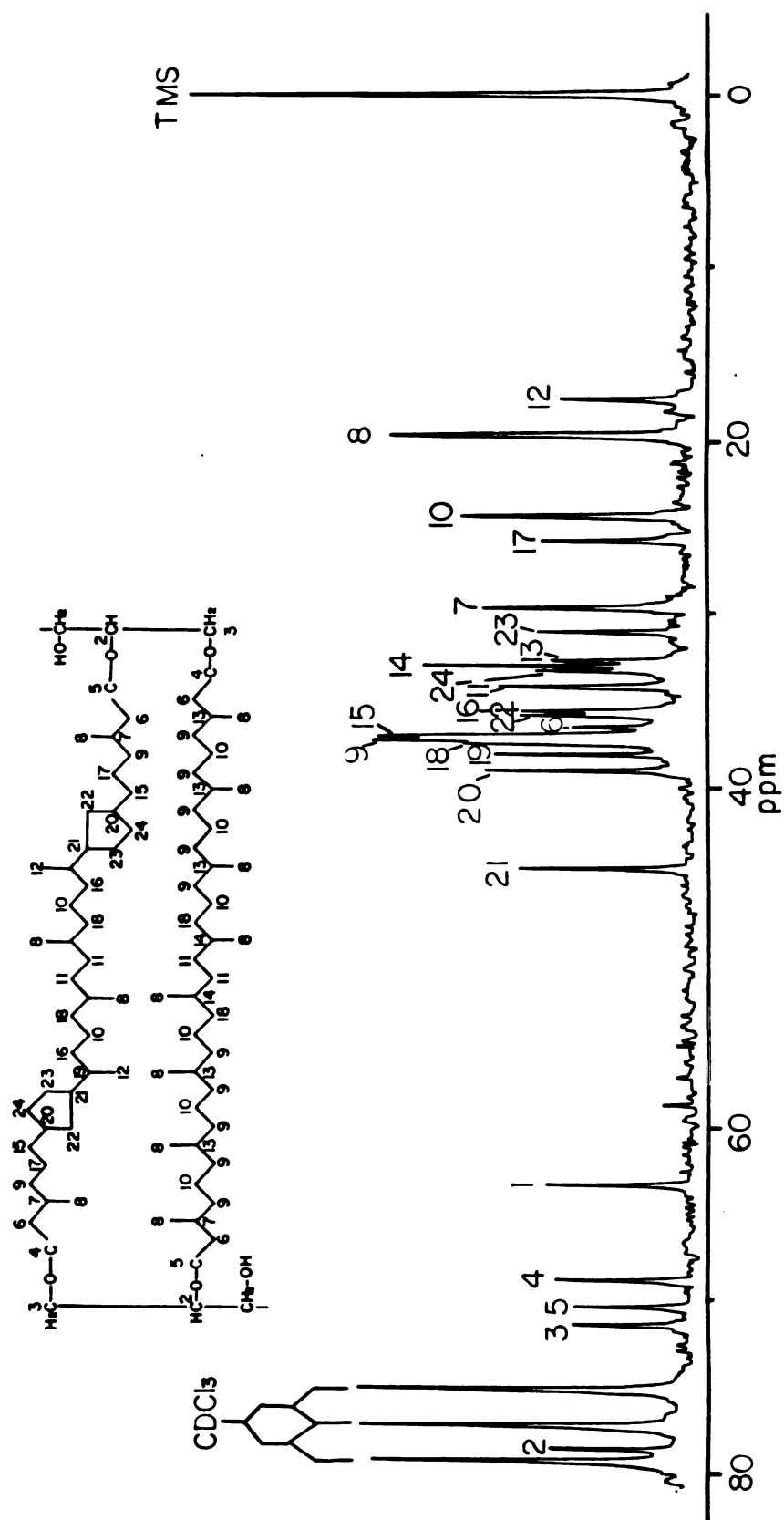


Figure 13.

Table 2. Carbon 13-NMR Chemical Shifts δ (ppm)* of Glycerol Ether

Carbon #	δ (ppm)
1	63.105
2	78.468
3	71.176
4	68.648
5	70.155
6	36.657
7	29.802
8	19.835
9	37.435
10	24.454
11	34.275
12	17.745
13	32.816
14	33.108
15	37.192
16	35.734
17	25.913
18	37.600
19	38.213
20	39.137
21	44.825
22	35.977
23	31.212
24	33.400

* down field from TMS.

Five independent spectroscopic techniques: IR, PMR, ^{13}C -NMR, GC-MS and EI-MS were used to determine the structure of the glycerol backbone and their side chains. The results supported the structure of two repetitively methyl branched C_{40} side chains that were ether-linked to two glycerol molecules. 20% of the side chains were acyclic, 45% of the side chains were monocyclic (cyclopentane), and the rest of the side chains were bi-cyclic. The length of an individual side chain is about 50 Å, taking into account the methyl branches and the known bond length of carbon-carbon bonds. The polar head groups are about 10 Å wide on each side of the membrane. This comes to 10-15 Å short of the observed membrane thickness (80-85 Å) (1). The study of membrane glycoproteins in Chapter 6 of this dissertation will resolve part of the discrepancy.

The ether linkages assured the stability of the molecule exposed to the acidic environments (pH 2), whereas the long side chains (C_{40}), which are double the chain length of most membrane fatty acid, assured the thermal stability. The structure of two side chains linked to two glycerol molecules contributed to the extremely rigid membrane as reported by spin labelling studies (19).

A previous report (13) showed that 35% of the neutral lipid of *T. acidophilum* was vitamin K_2 -7. There are 7 isoprenes linked to each other in vitamin K_2 -7. This is very similar to the side chains of phospho- and glycolipids. The occurrence of high levels (85%) of similar alkyl side chains conveys an appreciable degree of cooperativity among the chains. This idea is consistent with findings from electron paramagnetic resonance experiments where sharp lipid phase transitions had been detected (19). The cooperative motions should be also enhanced

by the interchain steric effects due to the methyl groups along the alkyl chains. The steric interactions favor the trans configuration (64). The presence of methyl groups lowers the melting point of the alkyl side chains. In other words, since methyl groups enhance the membrane lipid fluidity, the temperature region over which *T. acidophilum* can grow is extended. In fact, evidence has been presented (19) that the upper lipid phase transition temperature at 42°C correlates roughly with the low-temperature limit for growth (1). The branched alkyl side chains and their ether linkage therefore have survival value for this thermophilic, acidophilic cell.

This study provides evidence that the glycerol ethers represent an important membrane parameter which contributes to the cell's ability to grow at high temperature and low pH.

CHAPTER 4
CHANGES OF MEMBRANE PROPERTIES IN
THERMOPLASMA ACIDOPHILUM UPON LOW TEMPERATURE (37°C) ADAPTATION

Introduction

Biological membranes are widely believed to exist as a liquid-crystalline lipid bilayer in which protein structural units are embedded (65). There exists evidence that the degree of fluidity of the lipid bilayer must be maintained within rather narrow limits so that optimal protein interaction will ensure proper membrane function (66,67). Environmental factors can markedly influence membrane fluidity, where cell temperature fluctuations induce profound changes in membrane physical properties, such as permeability properties of the cellular membrane (68), activity of certain membrane-bound enzymes (69,70) and transport systems (71-73). However, many cells can adapt to a change in growth temperature by altering their lipid composition in such a way as to maintain membrane fluidity at a functional level (74-77).

Thermoplasma acidophilum, a mycoplasma-like organism, grows optimally at 56°C and pH 2 (1). The low temperature extreme at which it can grow is 37°C (57). The intracellular pH was close to neutrality (12). To further understand the structural and functional alterations in membranes in response to temperature stress, *T. acidophilum*, originally grown at 56°C, was adapted to growth at 37°C. After isolation of plasma membranes from both 56°C- and 37°C-grown cells, the lipid structures were

investigated by GC-MS, membrane lipid fluidity by EPR. The correlation between membrane-bound ATPase activity and membrane fluidity was analysed.

Results

Lipids

Membrane lipids from both 56°C- and 37°C-grown cells accounted for 25% of the membrane dry weight. The relative quantities of neutral lipid: glycolipid: phospholipid were 1:1:3 (w/w) for 56°C-grown cells, but 1:1:2 (w/w) for cells grown at 37°C. The distribution of lipid moieties of 56°C-grown cells was reported previously (13). Besides a 10% decrease in phosphate content, the carbohydrate content increased by 5% in 37°C-grown cells; choline and ethanolamine contents were unchanged, but the serine content was decreased by 12% compared to that of 56°C. For both kinds of cells, glyco- and phospholipid band patterns on TLC plates were rather similar. After recovery from TLC plates, material from each individual glyco- and phospholipids was transmethylated. Approximately 0.3% (w/w) of the side chains, i.e., fatty acids, were released from the lipid analyzed for 56°C-grown cells compared to 2% of fatty acids released from 37°C-grown cells. As determined by gas chromatography, the chain lengths of the fatty acids varied from C₁₆ to C₂₀. The majority of the side chains, however, were linked to glycerol by ether linkages. After methanolysis, the unsaponifiable material ran on TLC plates as single bands. The unsaponifiable material was further degraded to ROH (Figure 1). GC data showed that side chains isolated from cells grown at the two growth temperatures differed only in terms of their quantitative distributions (Table 3). This was also supported by GC-MS data.

Table 3. Side Chain Comparison of 56°C- and 37°C-Grown Cells as Determined by GC and GC-MS.

	peak #1 $C_{40}H_{80}O_2(TMS)_2$	peak #2 $C_{40}H_{78}O_2(TMS)_2$	peak #3 $C_{40}H_{76}O_2(TMS)_2$
56°C cell	20%	45%	32%
37°C cell	17%	11%	70%

Membrane-Bound Adenosine Triphosphatase

Both 56°C- and 37°C-grown *T. acidophilum* showed ATPase activity localized in the cell membrane. Optimum pH for ATPase activity was 6.8 for 56°C grown cells, but was 9.0 for 37°C-grown cells. Magnesium was found to be essential for ATPase activity of the membrane. Ca^{2+} seemed to inhibit ATPase activity. The monovalent cations, sodium and potassium, had no stimulatory effect on the ATPase activity, neither did the combination of these two monovalent cations.

For both kinds of cells, ATPase activity was assayed from 5°C to 55°C (Figure 14). The K_M values stayed rather constant with various concentrations of protein. The changes in activities were solely due to the changes of V_{max} . The activities were expressed as μ moles of inorganic phosphate released per milligrams of membrane protein per 30 minutes. Arrhenius plots (Figure 14) revealed discontinuities in slope at 15°C and 42.5°C for 56°C-grown cells and at 14°C and 35°C for 37°C-grown cells. From the slopes of the Arrhenius plots, the apparent activation energies were calculated by the Arrhenius equation. For cells grown at 56°C, the activation energy was 5.2 kcal/mole for temperatures above 42.5°C, 12.6 kcal/mole for temperatures between 15°C and

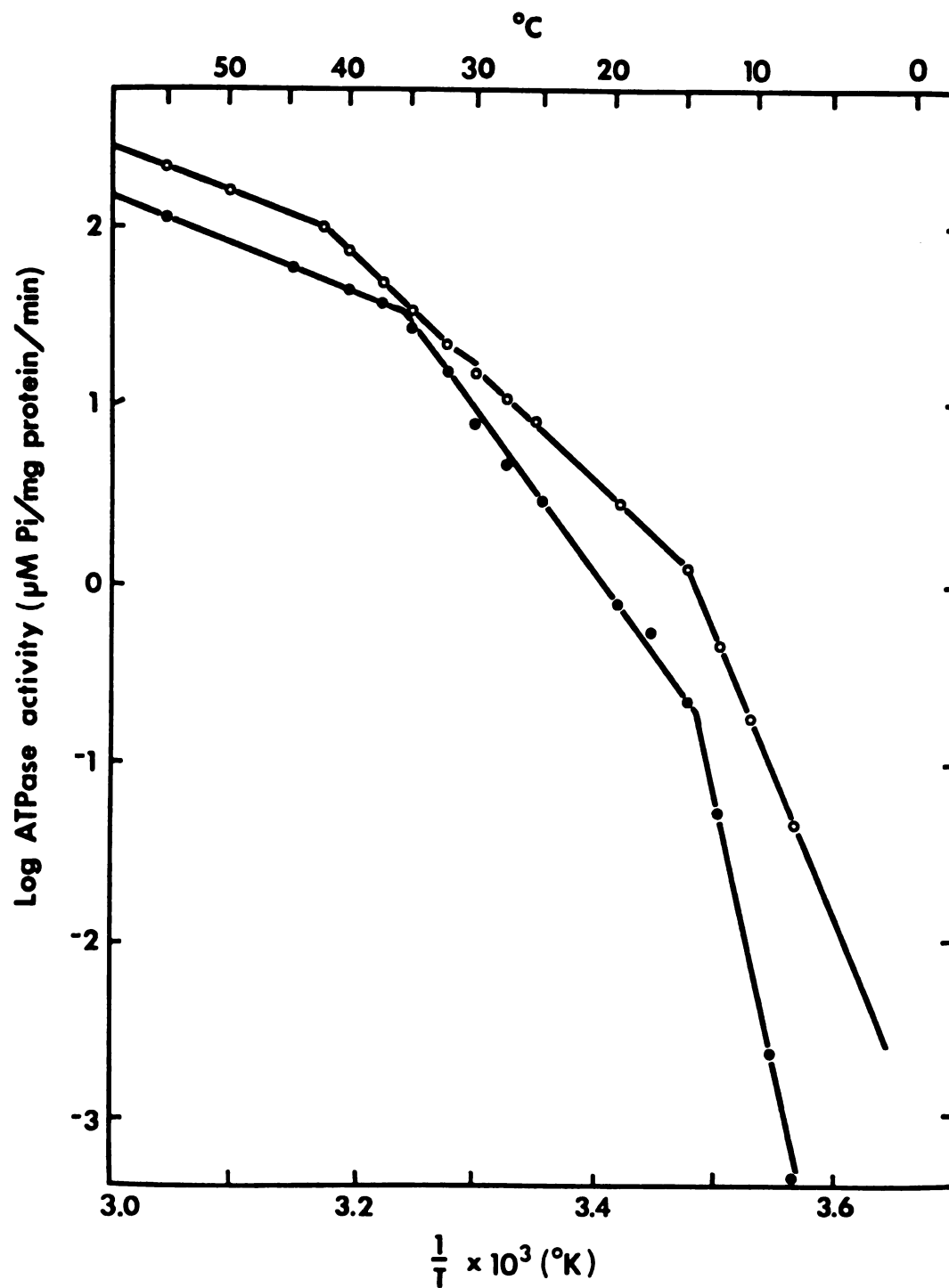


Figure 14. Arrhenius Plot of Membrane-Bound ATPase Activity vs Temperature for Both 56°C-Grown (-o-) and 37°C-Grown (-●-) *T. acidophilum*.

42.5°C, and 31.8 kcal/mole for temperatures below 15°C. For 37°C-grown cells, the activation energies are 5.5 kcal/mole above 35°C (which is practically identical to that of cells grown at 56°C), 18 kcal/mole between 14°C and 35°C, and 58.4 kcal/mole below 14°C.

EPR Studies

The temperature dependence of *T. acidophilum* membrane fluidity is illustrated in Figure 15. The hyperfine splitting parameter $2T_1$ is related to the rotational mobility of the spin label and therefore reports the local fluidity of membrane lipids. When the membranes were labelled with 5NS, lipid phase transitions were observed at 15°C and 45°C for 56°C-grown cells and at 16°C and 35°C for 37°C-grown cells. Thus, these physically determined transitions temperatures are virtually identical with those obtained biochemically from ATPase measurements.

Discussion

Similar to other microorganisms (78-79), there appears to exist a causal relationship between the physical state of membrane lipids and the range within which *T. acidophilum* is able to grow. The physical state is partially determined by the type of lipids which constitute the membrane lipid matrix. Compared to cells grown at 56°C, cells grown at 37°C contain lipids with 42% more cyclization; the phospholipid content decreased by 10%, the serine content of the phospholipid head groups diminished by 12%. On the other hand, the carbohydrate content of membrane lipid from cells grown at 37°C increased by 5% compared to that from 56°C-grown cells.

As determined by EPR experiments, the membrane lipid fluidity in cells grown at 37°C is generally higher than in 56°C cells. The upper

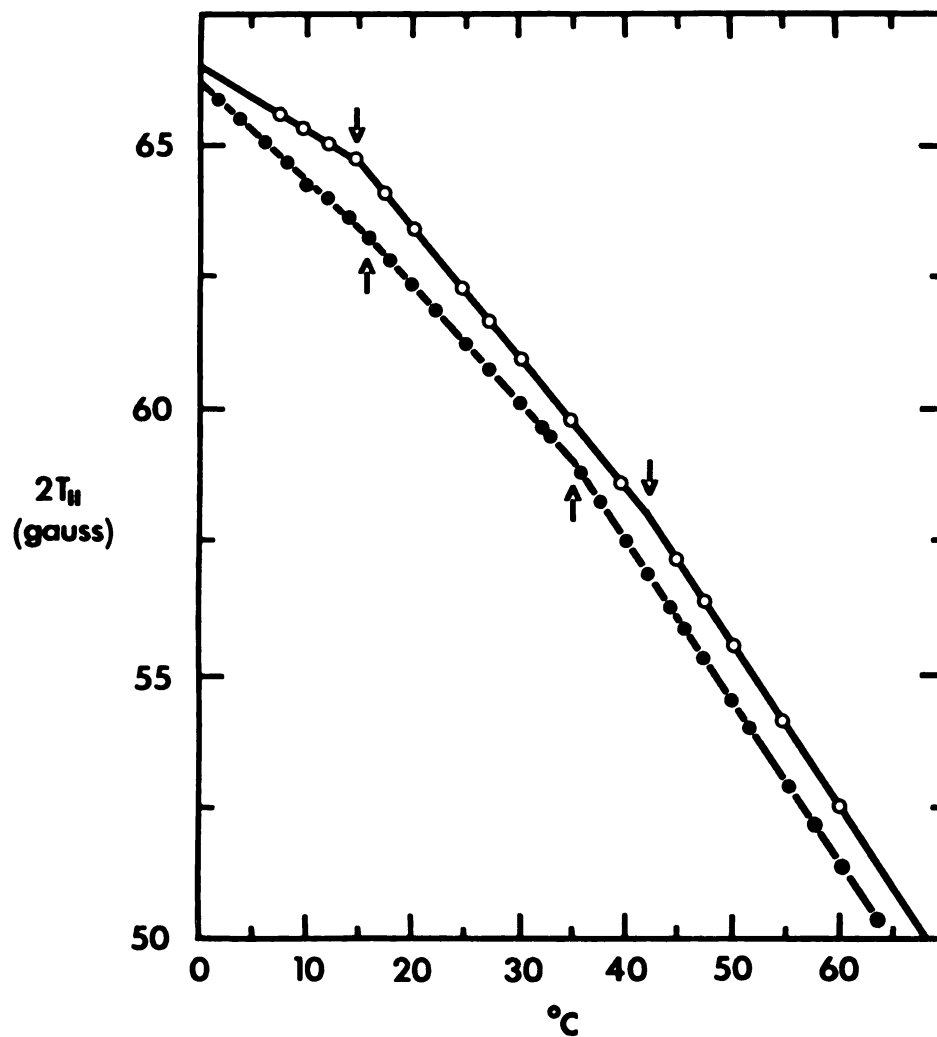


Figure 15. Hyperfine Splitting Parameter $2T_H$ as a Function of Temperature for 56°C-grown (-o-) and 37°C-grown (-●-) *T. acidophilum* Membrane Labelled with 5NS (Methods).

lipid phase transition temperature is shifted downwards by about 10°C in cells grown at 37°C. This latter shift extends the fluid region of membrane lipid in *T. acidophilum* grown at 37°C and the organisms' growth temperature falls within the fluid lipid regime. The lower lipid phase transition temperature (around 15°C) seems to be unaffected by adaptation.

Membrane-bound ATPase activities showed pronounced changes upon adaptation. The correlation between enzymatic activity and lipid state is indicative of the role of membrane fluidity in modulating the function of the ATPase (Figures 14 and 15).

The membrane lipid fluidity depends on the extent of length of the alkyl side chains and also on the phospholipid head groups, as evidenced by physico-chemical studies with artificial membranes (80,81). As already mentioned, cells grown at 37°C contain less phosphatidylserine. If these molecules were located at the outer layer of the membrane, and thus face the nutrient medium of pH 2, then its carboxyl groups will be protonated because the pK value lies around 3. On the other hand, if the molecules face the cytoplasmic side, then the head group will carry a negative charge, because the intracellular pH of *T. acidophilum* is about neutral (12). In erythrocytes phospholipids are asymmetrically distributed across the membrane; phosphatidylserine and phosphatidylethanolamine are mainly located at the inner membrane leaflet (82). Let us therefore assume that a certain fraction of phosphatidylserine molecules reside at the cytoplasmic face of the *T. acidophilum* membrane, then, as a consequence of the adaptation process occurring in cells grown at 37°C, a decrease in serine content and/or changes in its distribution might enhance membrane lipid fluidity

with a downward shift of the phase transition temperature (81).

When *T. acidophilum* is adapted to growth at 37°C, membrane-bound ATPase functions properly as long as the membrane remains in the fluid lipid state. The precise nature of the role of the lipid environment in regulating the activity of *Thermoplasma*'s membrane-bound ATPase has yet to be determined. In the thermophilic *B. stearrowthermophilus*, physical properties of ATPase have been investigated (83). It was suggested that this enzyme undergoes conformational changes at the lipid phase transition temperature, and that a more active enzymatic species exists above the transition temperature where the membrane is in the fluid state.

CHAPTER 5

Partial Characterization of a Membrane Glycoprotein from

Thermoplasma acidophilum

Introduction

One of the major modifications that a protein may undergo after synthesis of its peptide chains is the attachment of sugar residues. A large number of proteins of diverse origin and biological function are known to contain such covalently linked carbohydrates and are called glycoproteins. Numerous studies (84,85) have been made to understand the structural chemistry of glycoproteins, as well as the enzymatic machinery involved in the biosynthesis and degradation of these carbohydrate-containing molecules. More recently, attention has been focused on a clarification of the biological role which the carbohydrate may play in fulfilling the diverse functions of glycoproteins and in regulating their intracellular migration and export.

Glycoproteins are widely distributed in eucaryotes, occurring not only in vertebrate and invertebrate animals, but also in plants and unicellular organisms. It is already clear that a considerable portion of the polymerized carbohydrate of higher animals is covalently conjugated to protein, and it is quite likely that a similar situation may prevail in the sugar polymers of less evolved animals, as well as in plants. While attention was directed initially to the isolation and characterization of the numerous glycoproteins present in body fluids, such as plasma, saliva,

and gastrointestinal secretions, and to those which can be readily extracted in soluble form from various glandular and supportive tissues, increasing emphasis is being currently focused on the study of the insoluble glycoproteins which are components of complex structures, such as plasma membranes, basement membranes, and plant cell walls (84).

The known or presumed functions of glycoproteins are diverse, spanning a wide range of vital biological activities, participating in transport, blood clotting, antibody activity, thyroid-stimulation and storage. The protective and lubricating roles of the glycoproteins from epithelial secretions as well as their structural support to multicellular organisms are also known. The glycoprotein components of the cellular plasma membranes appear to participate in a multitude of biological functions. Plasma membranes, which separate the cell from its external environment, appear to play a crucial role in active transport of molecules, serve as receptors for viruses, hormones, and antibodies, and take part in intercellular recognition and adhesion. While the physiological function of many glycoproteins seems to be well established, the role which the carbohydrate plays in helping these proteins carry out their activities is in many cases much less clear (86).

Glycoproteins, though quite common in eucaryotes, are rare in prokaryotes (87,88), and the search for glycoproteins in mycoplasma membranes is still in its initial stage. The only membrane glycoprotein of mycoplasma reported in literature was that of *M. pneumoniae* (89). The periodic acid-Schiff positive band of the SDS polyacrylamide gel was extracted by lithium diiodosalicylate from the membrane. The isolated glycoprotein consisted of 80-90% amino acids (with the unusual composition of 50 mol% glycine and 20 mol% histidine) and about 7% carbohydrates (mainly glucose, galactose, and glucosamine). The possibility that this glycoprotein may

be identical with the binding site involved in *H. pneumoniae* attachment to cell surfaces is under investigation. The only other procaryotic glycoprotein was found in the cell envelope of *Halobacterium salinarium* (88,90). The intact glycoprotein has a single N-linked heterosaccharide, 22-24 O-linked disaccharides and 12 to 14 O-linked trisaccharides per molecule. The glycoprotein has a 33 mol% excess of acidic over basic amino acid residues. Growth of *H. salinarium* in the presence of bacitracin, an inhibitor of glycoprotein synthesis, or the removal of the glycopeptide with proteolytic enzymes causes morphological alteration of the cells. This suggests that the glycoprotein forms a rigid matrix at the cell surface and is responsible for maintenance of the characteristic rod shape of *H. salinarium* (91).

Thermoplasma acidophilum, a mycoplasma, grows optimally at pH 2 and 56°C. The organism is totally deprived of a cell wall, only its plasma membrane encounters the harsh environment. Since very little research has been carried out on procaryotic glycoproteins, the existence of glycoproteins in the *Thermoplasma* membrane initiated the studies reported in this Chapter. The primary concern was to elucidate the structural and functional relationships of the glycoprotein. The results of the studies will also give us a better comprehension of the mechanism of resistance of the cells that are exposed to environmental stress.

Results

Isolation and Purification of the Glycoprotein

200 µg of purified membrane protein was treated with 4% SDS, 10% 2-mercapto-ethanol in 0.125 M Tris buffer, pH 6.8, for 2 minutes at 100°C. The samples were then loaded onto a series of 10 cm long gels. The discontinuous sodium dodecyl sulfate buffer system of Laemmli (35) was used.

Separating gels usually contained 8% acrylamide and the stacking gels contained 5% acrylamide. Both the buffer and the gels contained 0.1% SDS (Methods). The gels were run at 5 mA per tubes for 3½ hours. After marking the tracking dye front, one set of duplicate gels was stained with Coomassie blue for proteins, the other set with periodic acid-Schiff (PAS) for carbohydrates. Membrane proteins showed 21-22 protein bands (Figure 16). Two bands which have the apparent molecular weights of 180,000 and 152,000 daltons were PAS positive (Figure 16).

Several methods were used to isolate the glycoproteins. The three most satisfactory ones are listed in the Materials and Methods section. Using slab gel electrophoresis, the quantities of the isolated glycoproteins are rather small. Since 1 mg of membrane proteins could be maximally loaded onto a slab to get good resolution, the glycoproteins recovered from the gel eluent were in the range of 200 µg. This was a rather small quantity for structural analysis. Phenol extraction was preferred for the first step in glycoprotein isolation. Glycoproteins were recovered at the interphase between water and phenol. After dialysis to remove phenol, the glycoproteins were solubilized in 1% SDS, then loaded onto a 90 by 1.5 cm (i.d.) Sepharose 4B column to separate glycoproteins. Further purification can be achieved by application to a Con A-Sepharose column (Figure 17). A *Thermoplasma* glycoprotein (molecular weight 152,000 daltons) was isolated and purified by the procedure listed above (Figure 18). The purified glycoprotein was homogeneous as determined by gel electrophoresis in three different concentrations of acrylamide (5%, 7%, and 9%) (Figure 19).

Since many glycoproteins stain very poorly with Coomassie blue, it will be inaccurate to estimate the glycoprotein content in the membrane

Figure 16. Scans of SDS Gel Electrophoresis of the Membrane Proteins from *T. acidophilum*.

**A: Membrane proteins were stained with Coomassie blue.
The gel was scanned at 550 nm.**

B: Membrane proteins were stained with periodic acid-Schiff. The gel was scanned at 540 nm.

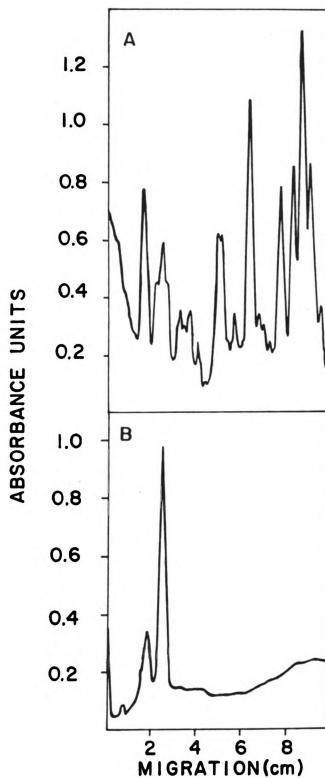


Figure 16.

Figure 17. Elution Pattern of Membrane Glycoprotein from Con A-Sepharose Column.

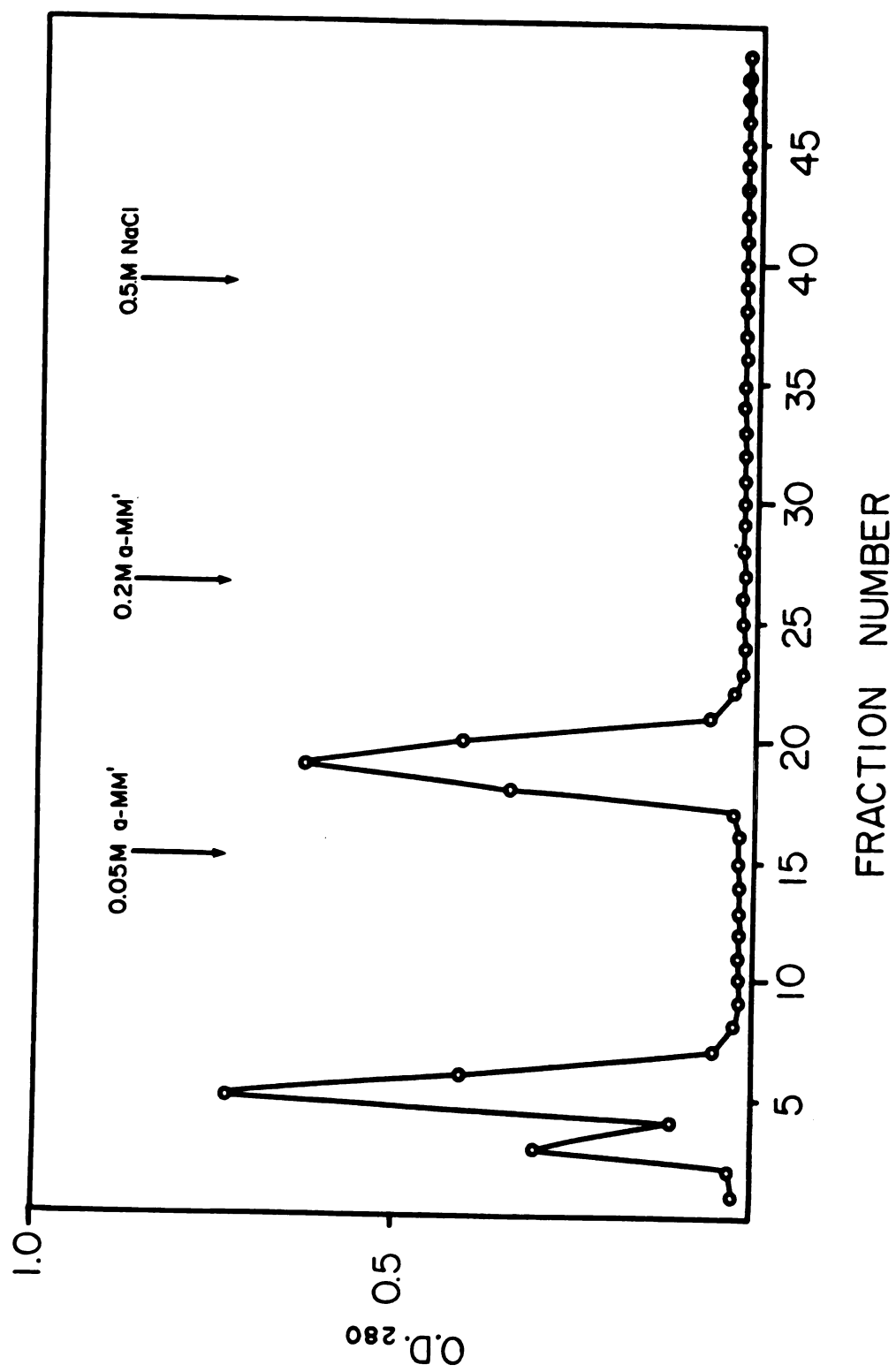


Figure 17.

Figure 18. Scan of SDS Gel Electrophoresis of the Purified Glycoprotein from Con A-Sepharose Column and the Molecular Weight Determination.

Molecular weight standards are:

β' -subunit of RNA-polymerase from *E. coli* (165,000 daltons)

β -subunit of RNA-polymerase from *E. coli* (155,000 daltons)

bovine serum albumin (BSA) (68,000 daltons)

α -subunit of RNA-polymerase from *E. coli* (39,000 daltons)

trypsin inhibitor (TI) (21,500 daltons).

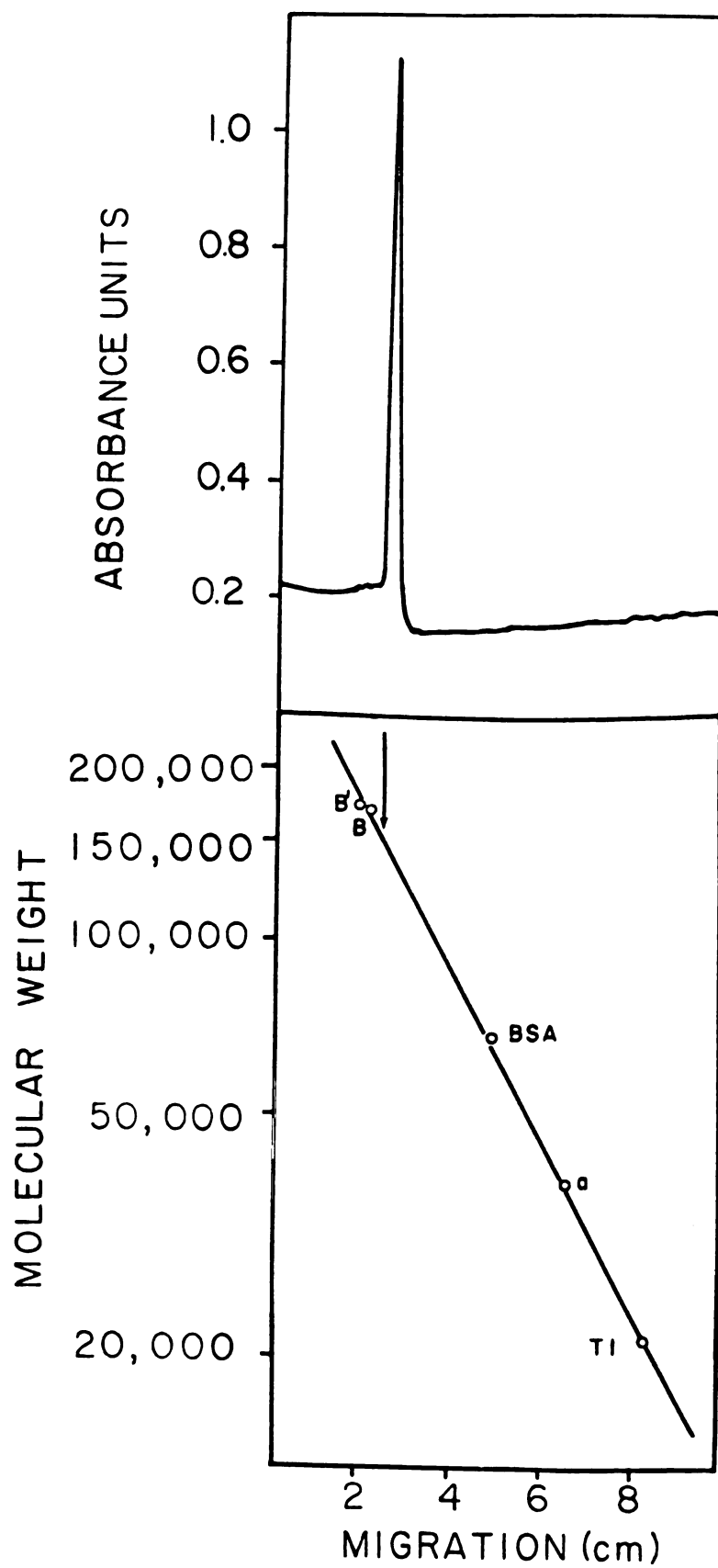


Figure 18.

Figure 19. Scans of SDS Gel Electrophoresis of the Purified Glycoprotein in 9%, 7% and 5% Polyacrylamide.

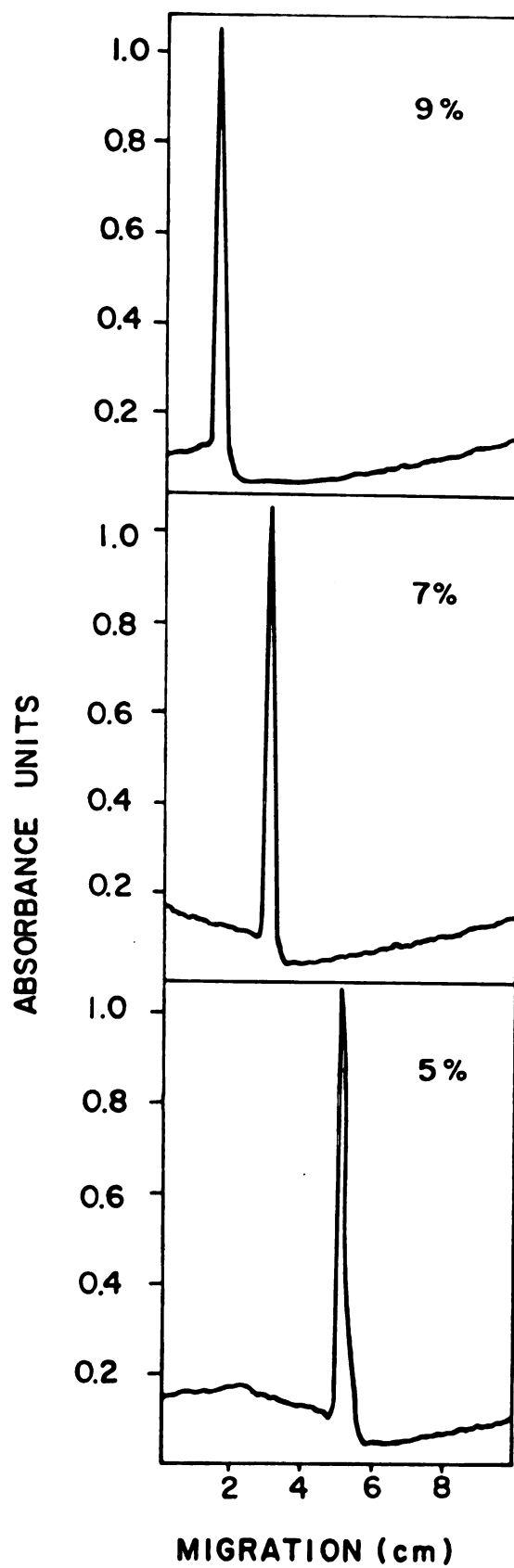


Figure 19.

by staining intensity. Membrane proteins and isolated glycoproteins were determined by the method of Wang and Smith (34) with Triton X-100. The two membrane glycoproteins accounted for approximately 40% of the total membrane proteins. Since the major membrane glycoprotein has a molecular weight of 152,000 daltons, the following analysis deals with this glycoprotein.

Pronase Digestion of the Glycoprotein

Proteolytic digestion of this purified glycoprotein was performed with pronase (Calbiochem) in 0.01 M Tris buffer, pH 7.8, at an enzyme-to-protein ratio of 1:10. Mixtures were incubated at 37°C for 48 hours with 0.02% sodium azide added to prevent bacterial growth. After digestion, the sample was loaded onto a 90 by 1.5 cm (i.d.) Sephadex G-100 column. Figure 20 shows the elution curves. The first small anthrone positive peak may result from incomplete digestion of the glycoprotein. The major anthrone positive fraction was then loaded onto a 90 by 1.5 cm (i.d.) Sephadex G-75 column to give further purification of the glycopeptides (Figure 21). The estimated molecular weight of the glycopeptide was close to 14,000 daltons by gel filtration. Gel electrophoresis of the purified glycopeptides showed a single band with an apparent molecular weight of 15,000 daltons. Molecular weight estimations by gel electrophoresis of highly glycosylated protein are known to give anomalously high values. 15,000 daltons should be considered as the upper limit for the true molecular weight of the glycopeptides. Therefore, the carbohydrate content of the isolated glycoprotein amounts to 8-10%. One interesting remark: pronase digestion of the 180,000 daltons glycoprotein seemed to give rather similar glycopeptides, including sugar composition and their respective percentages.

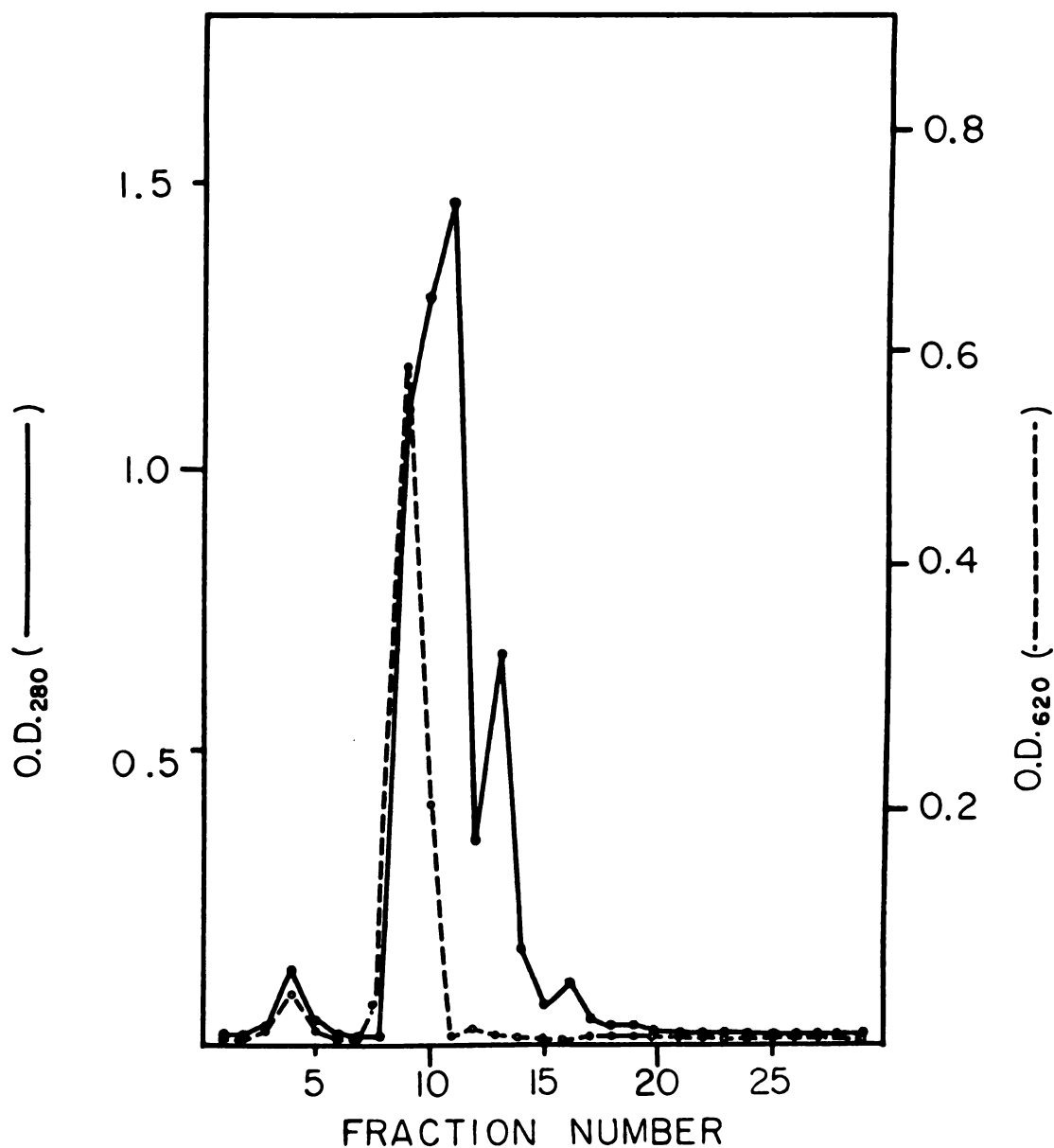


Figure 20. Sephadex G-100 Column Chromatography of Glycopeptides after Pronase Digestion.

Chromatography was performed with a 90 x 1.5 cm i.d. column. Fractions of 7 ml were collected. Each fraction was assayed for protein (O.D. 280) and carbohydrate (O.D. 620).

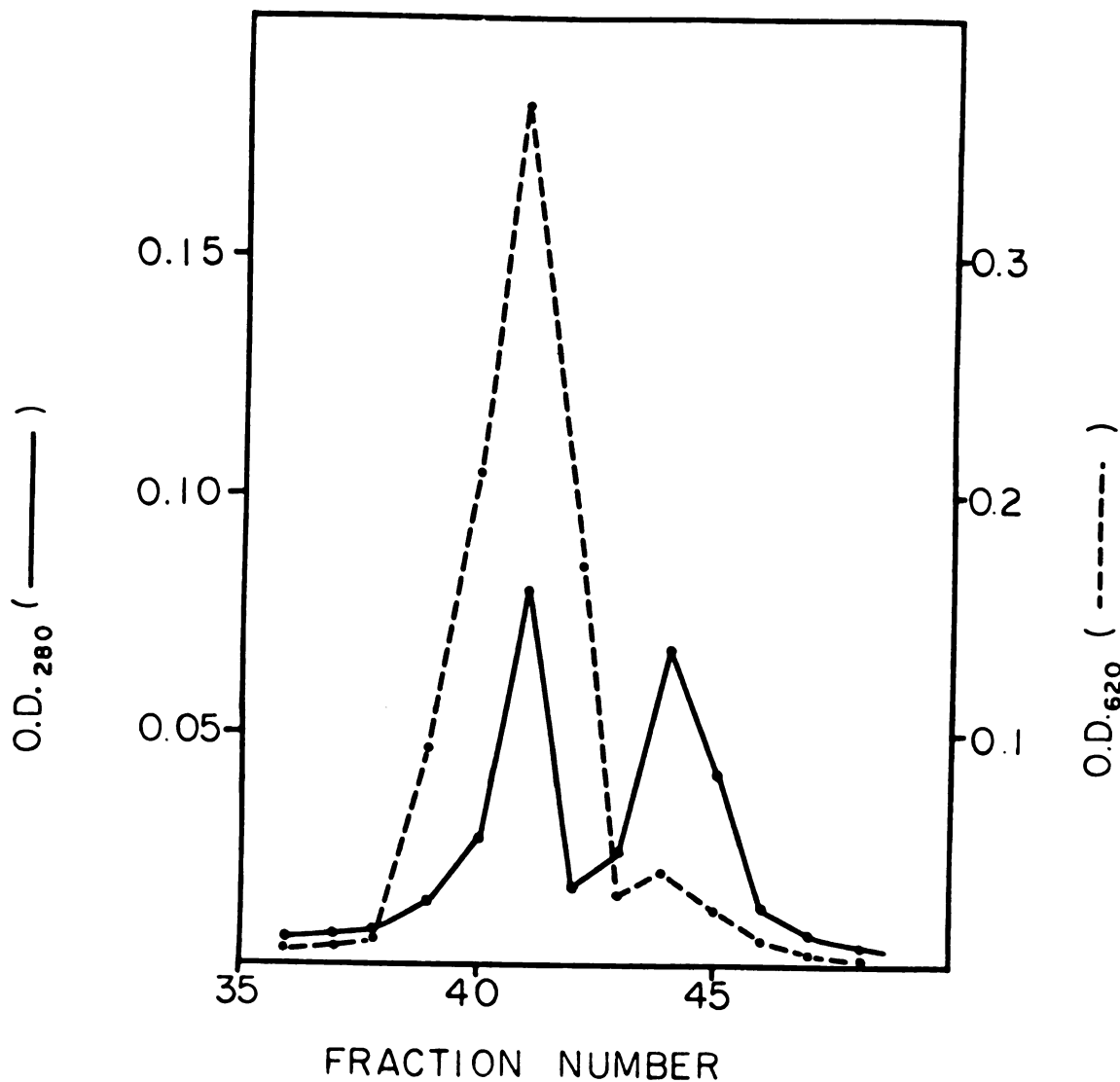


Figure 21. Sephadex G-75 Elution Profile of Fraction #9 from Figure 20.

Chromatography was performed with a 90 x 1.5 cm i.d. column. Fractions of 3 ml were collected. Each fraction was assayed for protein (O.D. 280) and carbohydrate (O.D. 620).

Determination of Carbohydrate Composition by Methanolysis

Methanolysis of glycoprotein to study the carbohydrate-portion was performed by the method of Chambers and Clamp (38). The trimethylsilyl derivatized methyl glycosides were run on a 12 ft, 3% SP-2100 column with a Perkin-Elmer gas chromatograph as described in Methods. Gas chromatographic analysis showed that the carbohydrate portion of the glycoprotein consisted mainly of mannose, glucose and galactose (molar ratio 20/2/1) and a trace amount of glucosamine (Figure 22). This finding was consistent with the Con A binding ability of the isolated glycoprotein (92).

Amino Acid Analysis of the Glycoprotein

The amino acid composition of the glycoprotein is listed in Table 4. Hydrophobic amino acids comprised 62 mol% of the protein portion, while acidic amino acids were 9 mol% more than the basic amino acids.

Glycosidic Linkage Studies of the Glycoprotein

An important aspect in the study of a glycoprotein concerns the characterization of the bonds which link its carbohydrate units to the peptide. All bonds involve C-1 of the most internal sugar residue of the carbohydrate unit and a functional group on an amino acid in the peptide chain. Generally linkages can be categorized into two groups: (1) the glycosyl amine bond which always involves N-acetylglucosamine and the amide group of asparagine; and (2) the alkali-labile O-glycosidic bond to serine or threonine which may involve N-acetylgalactosamine, galactose, xylose, or mannose as the sugar component (84). Since the purified *Thermoplasma* glycoprotein resisted alkaline hydrolysis, this suggested that the carbohydrates were N-glycosidically linked to the peptide.

Exposure of glycoproteins to anhydrous hydrogen fluoride cleaves all the linkages of neutral and acidic sugars while leaving peptide bonds

Figure 22. Gas-Liquid Chromatography of Trimethylsilylated Methyl Glycosides of the Purified Glycopeptide.

Analysis was performed on a 12 ft 3% SP-2100 column (80-100 mesh, on Supelco port). Mannitol was used as internal standard (I.S.).

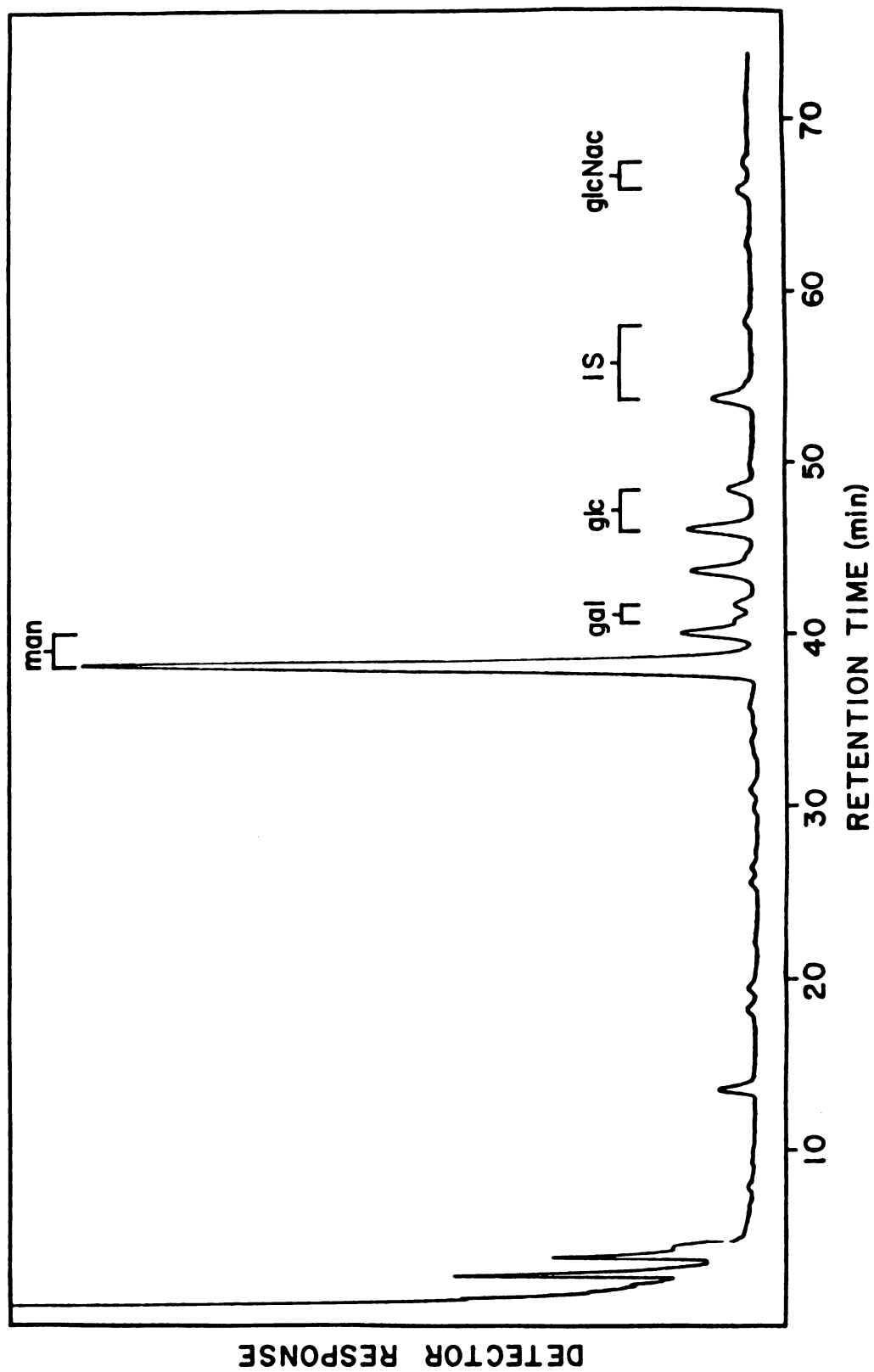


Figure 22.

Table 4. Amino Acid Composition of the Purified Membrane Glycoprotein from *T. acidophilum*

	mol %
Lysine	4.3
Histidine	1.4
Arginine	3.9
Aspartic Acid	11.2
Threonine	8.2
Serine	10.3
Glutamic Acid	7.5
Proline	1.1
Glycine	9.6
Alanine	8.1
Valine	7.5
Methionine	0.5
Isoleucine	5.8
Leucine	8.3
Tyrosine	7.2
Phenylalanine	5.0

and glycopeptide linkages of amino sugars intact. Following HF treatment, the protein portion was separated from the carbohydrate moiety by dialysis. Methanolysis was carried out on the protein portion. Glucosamine was the only sugar detected.

To further understand the structure of the carbohydrate portion of the glycoprotein, series of glycosidase degradations and permethylation studies were performed.

Digestions of the Glycopeptide by Exo- and Endo-glycosidases

The purified glycoprotein was first incubated with α -mannosidase. This enzyme was selected since the glycoprotein can be purified by Con A-affinity column. Also from the carbohydrate content (Figure 22), mannose accounted for 85%. After 72 hours of incubation (Methods), 70% of the mannose was released. Further digestion with α -mannosidase in the presence of SDS (1%) for another 48 hours did not remove any more mannose (Figure 23). The glycopeptide recovered from α -mannosidase digestion was further treated with β -glucosidase and α -mannosidase. This reaction enabled the release of 70% of the glucose and 90% of the mannose residues (Figure 24). Further digestion with β -galactosidase, β -glucosidase and α -mannosidase resulted in virtually total removal of the galactose and glucose residues (Table 5). From the experiments on exo-glycosidase digestions, it was concluded that the carbohydrate portion of the glycoprotein had a long chain of α -mannose (55-56 residues) at its non-reducing end, followed by a portion of β -glucose (5-6 residues) and α -mannose (15-16 residues), then the β -galactose (3-4 residues), β -glucose (2-3 residues) and α -mannose (5-6 residues). After the exo-glycosidases digestion, the glycopeptide was treated with endo-glycosidase H. The ability of this enzyme to remove the rest of the carbohydrates indicated

Figure 23. Gas-Liquid Chromatography of Trimethylsilylated Methyl Glycosides of the Glycopeptide after α -mannosidase Digestion.

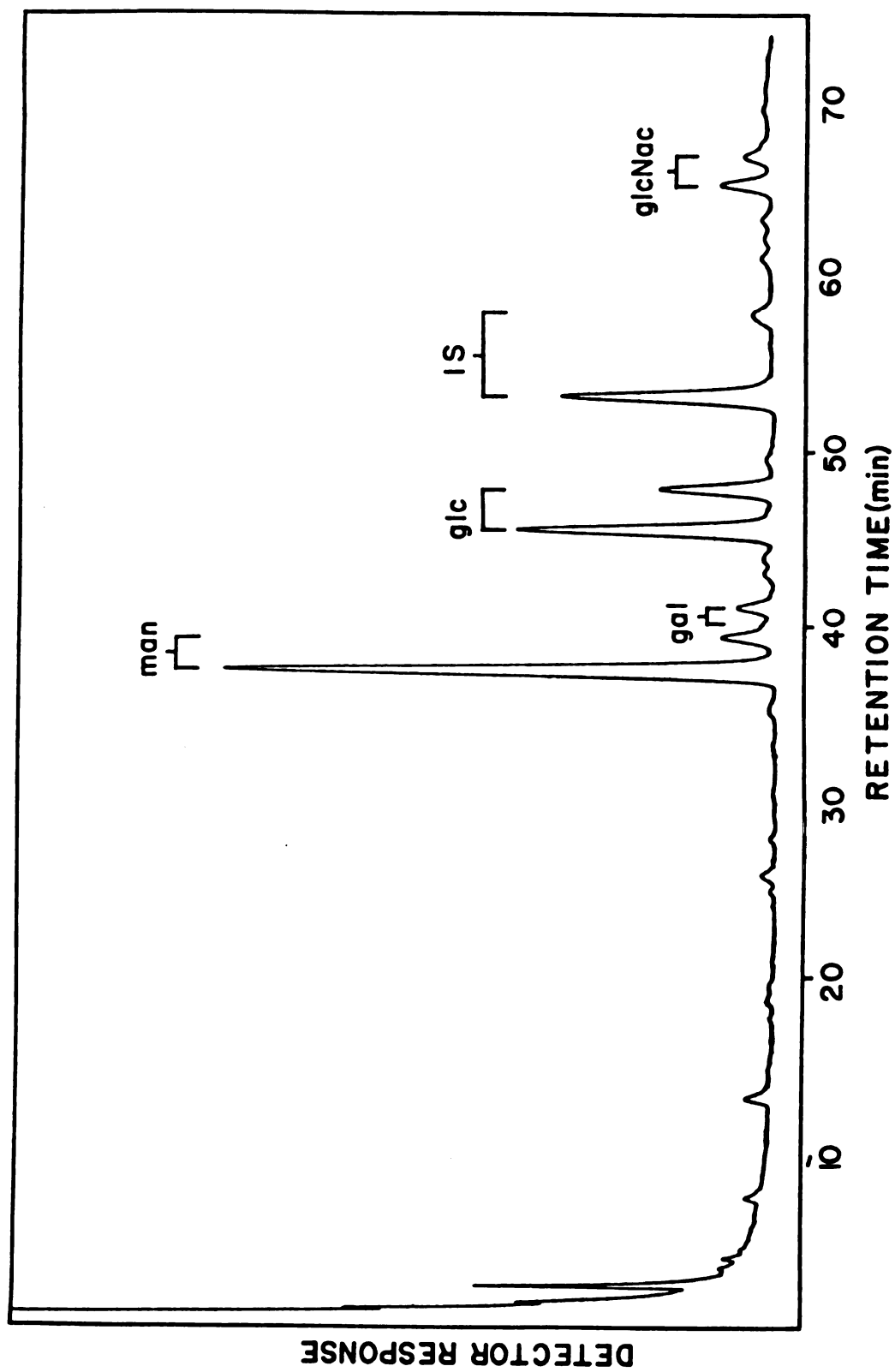


Figure 23.

Figure 24. Gas-Liquid Chromatography of Trimethylsilylated Methyl Glycosides of the Glycopeptide after α -mannosidase and β -glucosidase Digestions.

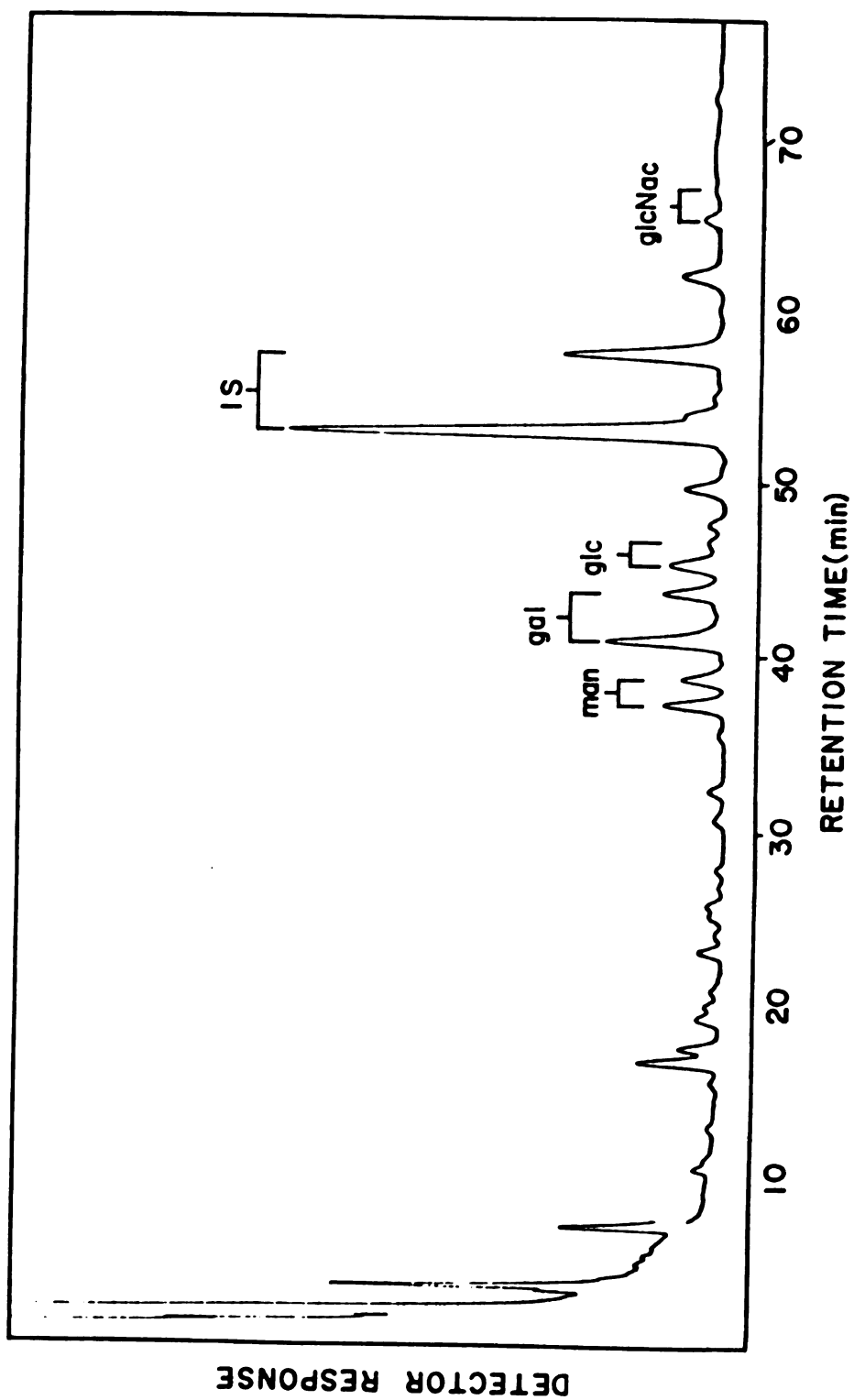


Figure 24.

Table 5. Molar Ratios* of Carbohydrate Residues from Purified Glycoprotein and after Treatments with Glycosidases

	Glycoprotein	after α -mannosidase digestion	after α -mannosidase β -glucosidase digestions	after α -mannosidase β -glucosidase β -galactosidase digestions
mannose	40.1	11.8	3.9	0.9
glucose	3.9	3.9	1.5	trace
galactose	1.9	1.9	1.9	trace
glucosamine	1.0	1.0	1.0	1.0

* calculated by setting the value for glucosamine as 1.0

that the reducing end comprised two glucosamine residues (chitobiose), β -linked, followed by mannose (1-2 residues)(94). The inability of removing the last trace (1-2 residues) of mannose with α -mannosidase suggested that at least one of the mannose residues was β -linked.

Permethylation Studies of the Glycopeptide

To determine the linkages, the glycopeptides were subjected to permethylation (39). Partially methylated alditol acetates were analyzed by combined gas chromatography-mass spectroscopy and the data were interpreted according to Björndal et al. (40). The identification of the partially methylated derivatives of mannose, glucose, galactose and glucosamine was established both by their retention times in the gas-liquid chromatograms and by mass spectrometry by their fragmentation patterns, and were further compared with known reference standards. Primary fragments are formed by fission between carbon atoms in the chain. Fission between a methoxylated and an acetoxyated carbon atom is preferred over fission between two acetoxyated carbon atoms. When a molecule contains two adjacent methoxylated carbon atoms, fission between those two atoms is preferred over fission between one of these and an acetoxyated carbon atom. Both fragments from this fission are detected as positive ions. Secondary fragments are formed from the primary ones by single or consecutive loss of acetic acid (m/e 60), methanol (m/e 32), ketene (m/e 42), and formaldehyde (m/e 30). Permethylation and mass spectral analysis of the glycopeptides after acid hydrolysis, borohydride reduction, and acetylation gave evidence for the presence of 2,3,4,6-tetra-0-methylmannitol, 3,4,6-tri-0-methylmannitol, 2,4,6-tri-0-methylmannitol, 2,3,4-tri-0-methylmannitol, 2,4-di-0-methylmannitol, 2,3,6-tri-0-methylglucitol, 2,4,6-tri-0-methylgalactitol and 3,6-di-0-methylglucosaminitol (Table 6). The presence of 2,3,4,6-tetra-0-methylmannitol

Table 6. Molar Ratios* of Partially Methylated Alditol Acetates of Mannose, Glucose, Galactose and Glucosamine Obtained by Permethylation of the Purified Glycopeptide

2,3,4,6-tetra-0-methylmannitol	4.1 (8.2)
3,4,6-tri-0-methylmannitol	18.4 (36.8)
2,4,6-tri-0-methylmannitol	6.1 (12.2)
2,3,4-tri-0-methylmannitol	5.1 (10.2)
2,4-di-0-methylmannitol	3.5 (7.0)
2,3,6-tri-0-methylglucitol	3.1 (6.2)
2,4,6-tri-0-methylgalactitol	1.5 (3.0)
3,6-di-0-methylglucosaminitol	1.0 (2.0)

*Molar ratios were calculated using 3,6-di-0-methylglucosaminitol as 1.0. The values in parentheses were calculated as mol carbohydrate/glycoprotein.

(Figure 25) as the only tetra-methylated carbohydrate, indicated that mannose residues were the nonreducing ends. The presence of an abundant amount of 3,4,6-tri-O-methylmannitols (Figure 26, 1,2-substituted) was consistent with the ability of the glycoprotein to bind Con A. The presence of 2,4-di-O-methylmannitol (Figure 27, 1,3,6-substituted) was indicative of a branched glycopeptide. From the molar ratios (Table 6), it was obvious that the glycopeptide branched at 7 locations. 2,4,6-tri-O-methylmannitol (Figure 28, 1,3-substituted) and 2,3,4-tri-O-methylmannitol (Figure 29, 1,6-substituted) seemed to have about equal amounts. After α -mannosidase digestion, the 2,4-di-O-methylmannitol and 3,4,6-tri-O-methylmannitol derivatives were drastically reduced. This indicated that the branching was mainly at the outer mannose residues which amounted to 70% (Table 5) and which were linked predominantly via α 1 \rightarrow 2 linkages. The middle inner core of the glycopeptides consisted of 1,4-substituted glucose (Figure 30), 1,3-substituted galactose (Figure 31), 1,2-, 1,3-, and 1,6-substituted mannose. The innermost of the glycopeptide was 1,4-substituted glucosamine residues (Figure 32). The inability to remove the last trace of mannose with α -mannosidase (Table 5), suggested that there probably existed one mannose residue which was β -linked to the distal N-acetylglucosamine residue (Figure 33).

Effect of Bacitracin on Cell Growth and Glycoprotein Structure

Thermoplasma acidophilum, a mycoplasma-like organism, grows optimally at 56°C and pH 2. The existence of the membrane glycoprotein leads to the following studies on the structural and functional relationship of this procaryotic glycopeptide. The protective and lubricating roles of the glycoproteins from epithelial secretions are well known. Do the membrane glycoproteins found in *Thermoplasma acidophilum* have the similar

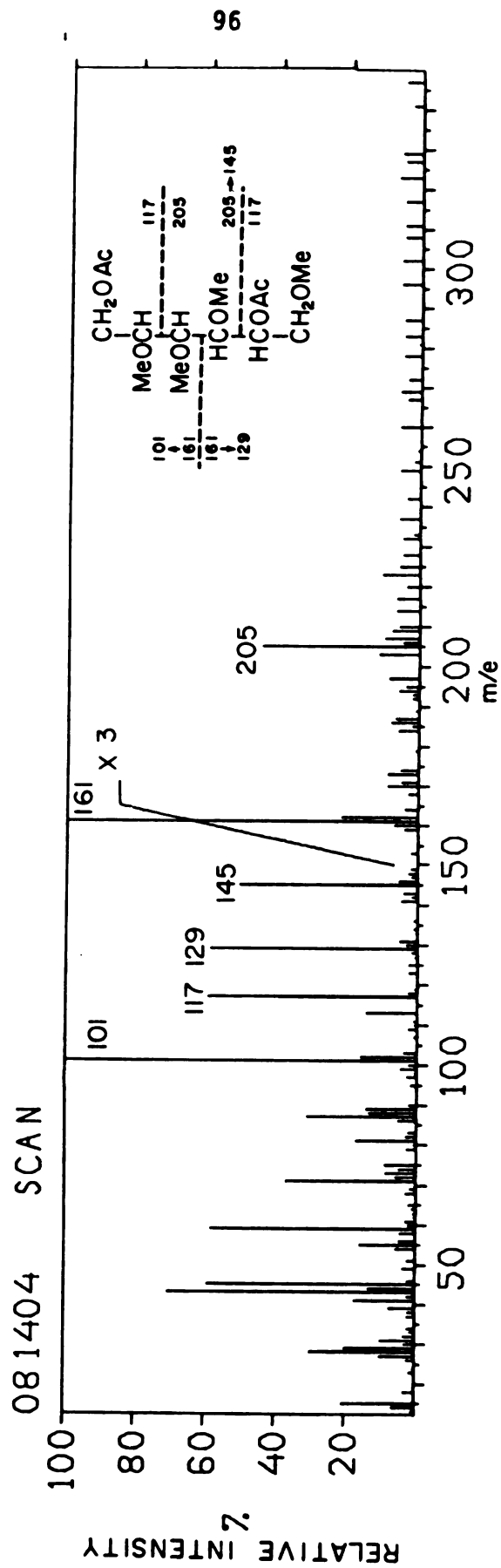


Figure 25. Mass Spectrum of Partially Methylated Alditol Acetate Identified as 1,5-di-O-acetyl-2,3,4,6-tetra-O-methylmannitol from the Purified Glycopeptide.

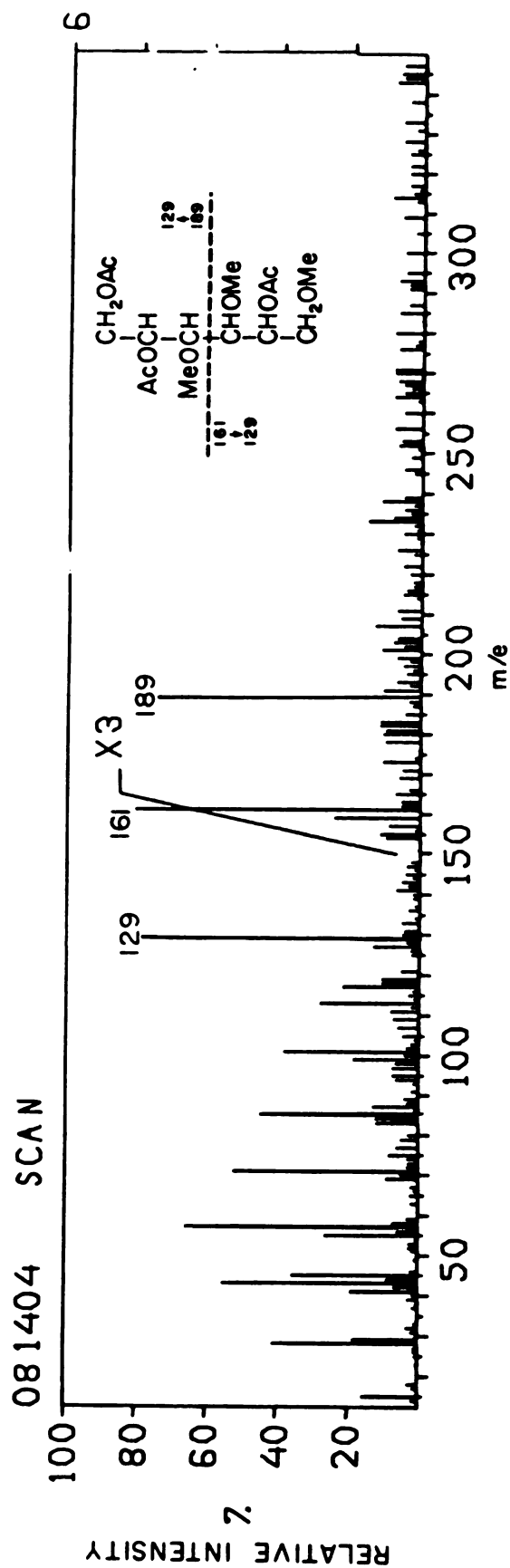


Figure 26. Mass Spectrum of Partially Methylated Alditol Acetate Identified as 1,2,5-tri-O-acetyl-3,4,6-tri-O-methylmannitol from the Purified Glycopeptide.

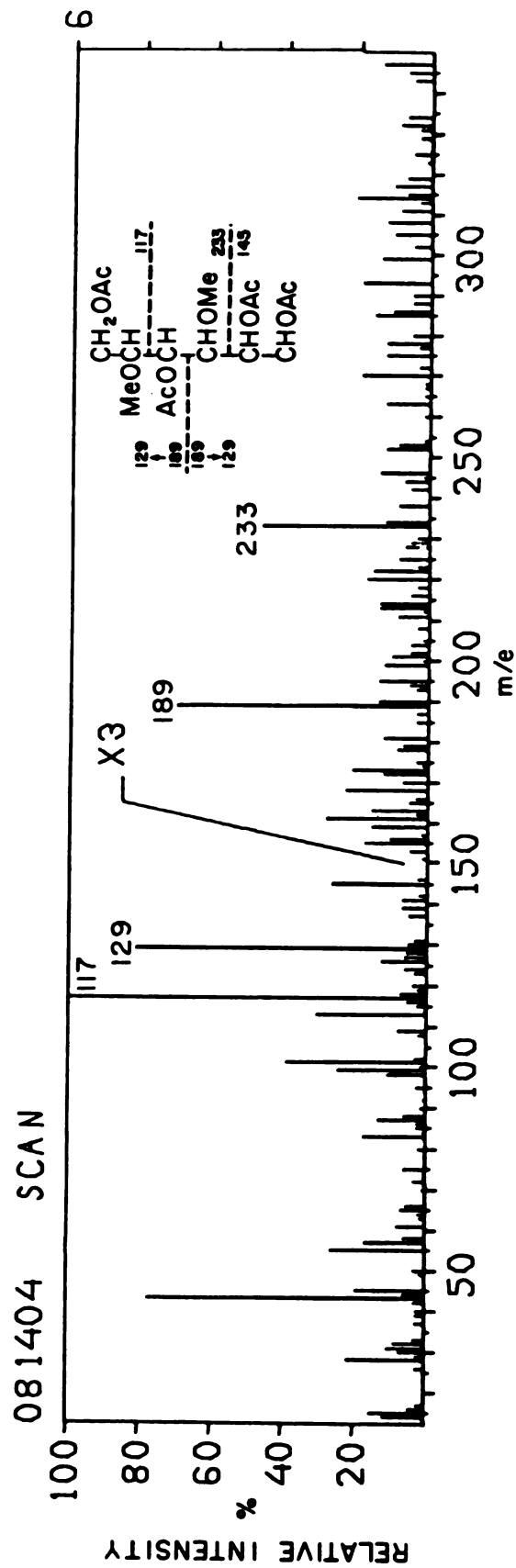


Figure 27. Mass Spectrum of Partially Methylated Alditol Acetate Identified as 1,3,5,6-tetra-O-acetyl-2,4-di-O-methylmannitol from the Purified Glycopeptide.

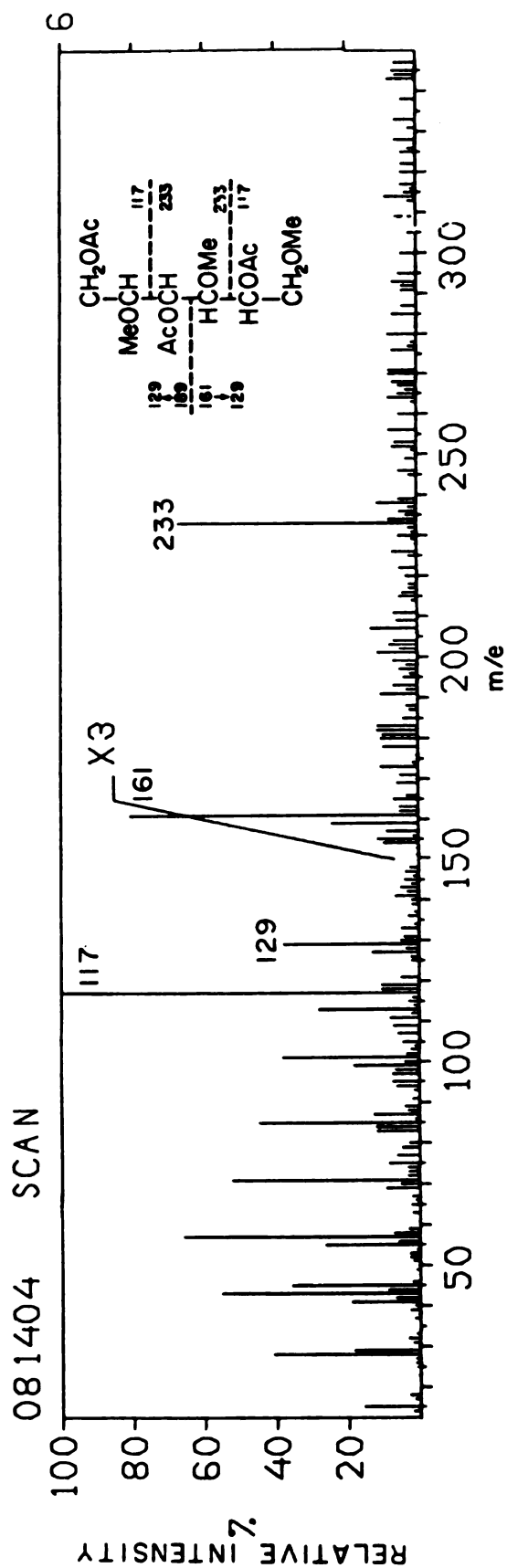


Figure 28. Mass Spectrum of Partially Methylated Alditol Acetate Identified as 1,3,5-tri-O-acetyl-2,4,6-tri-O-methylmannitol from the Purified Glycopeptide.

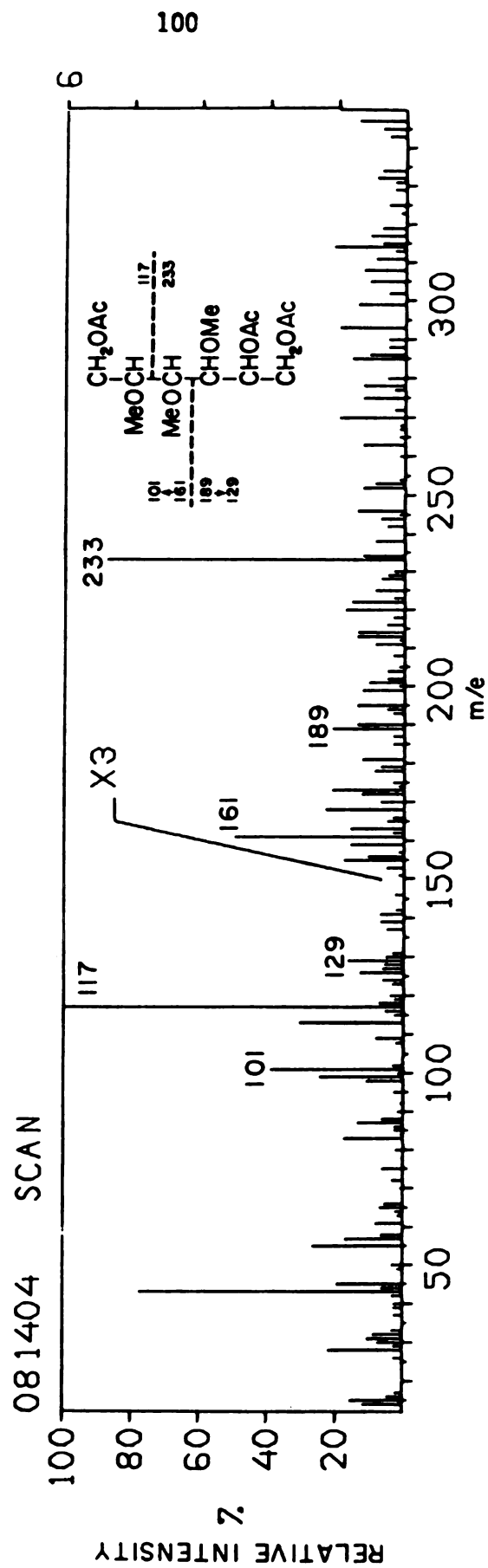


Figure 29. Mass Spectrum of Partially Methylated Alditol Acetate Identified as 1,5,6-tri-O-acetyl-2,3,4-tri-O-methylmannitol from the Purified Glycopeptide.

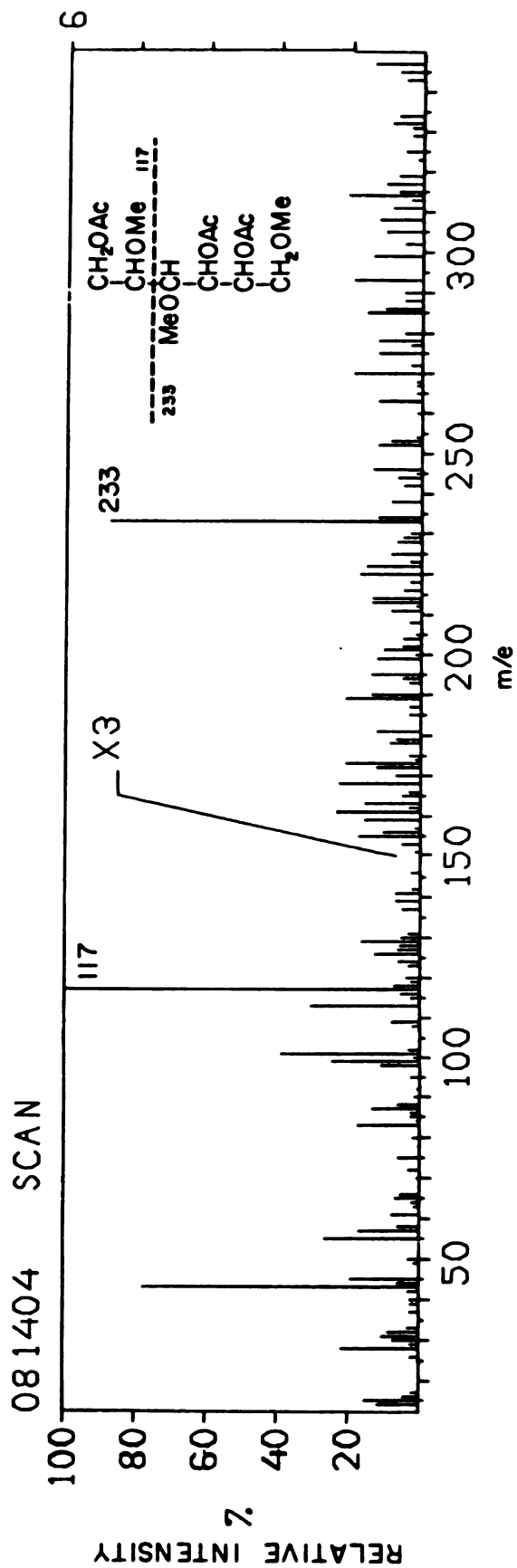


Figure 30. Mass Spectrum of Partially Methylated Alditol Acetate Identified as 1,4,5-tri-O-acetyl-2,3,6-tri-O-methylglucitol from the Purified Glycopeptide.

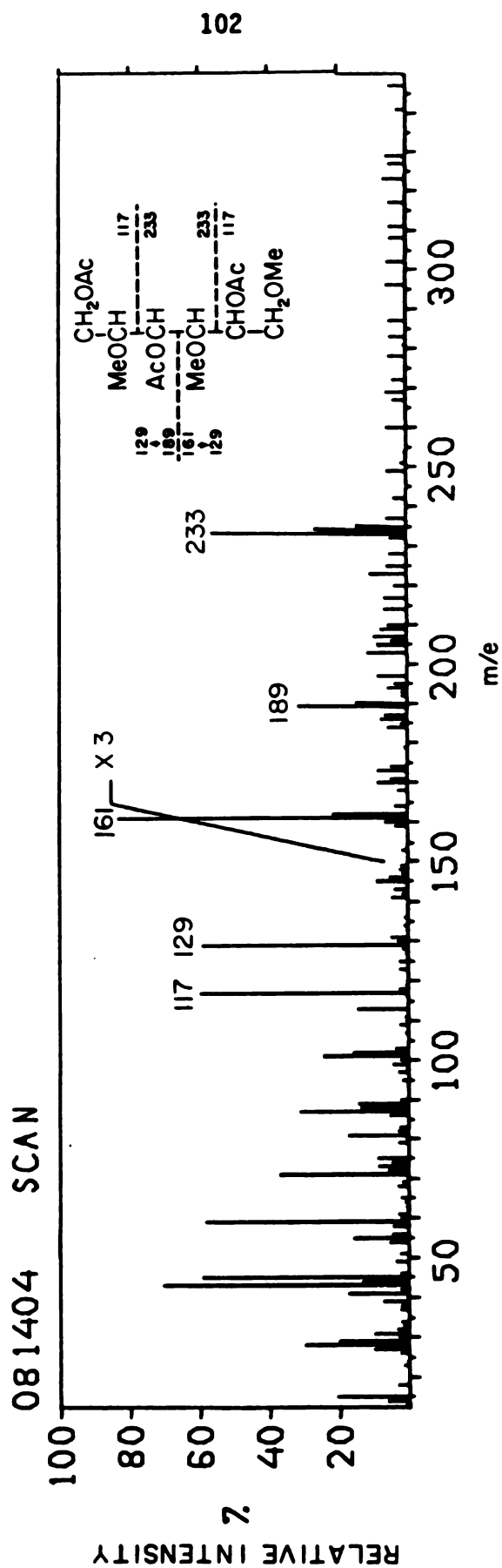


Figure 31. Mass Spectrum of Partially Methylated Alditol Acetate Identified as 1,3,5-tri-O-acetyl-2,4,6-tri-O-methylgalactitol from the Purified Glycopeptide.

Figure 32. Mass Spectrum of Partially Methylated Alditol Acetate Identified as N-acetyl-N-methyl-1,4,5-tri-O-acetyl-3,6-di-O-methylglucosaminitol from the Purified Glycopeptide.

Figure 33. Proposed Structure of the *Thermoplasma acidophilum* Membrane Glycoprotein.

a+b+c+d+e+f+g+h+i+j+m+n+k = 45 residues

q+r+t = 20 residues

p = 5 residues

s = 3 residues

The sequence of the residues in segment I and II is not certain.

function as the epithelial secretions? That is: do the glycoproteins found in *Thermoplasma acidophilum* act like a protective coat against the harsh environments (pH 2 and 56°C)?

Removal of surface glycopeptide by proteolytic enzymes was unsuccessful, since no enzyme retained activity at the growth conditions (56°C and pH 2) of *Thermoplasma*. Therefore, bacitracin was used. Bacitracin is an antibiotic that blocks peptidoglycan synthesis in normal bacteria by complexing with the lipid pyrophosphate released after transfer of the lipid-linked subunit to the growing peptidoglycan chain (95), thus making the carrier lipid unavailable for formation and transfer of additional subunits.

For three different pH values, cell growth ratios of *T. acidophilum* in the presence and absence of bacitracin are shown in Figure 34. The growth of cells at pH 2 and 3 was not influenced by addition of bacitracin, the % control values stayed pretty much around 100%. However, the growth of cells at pH 4 increased by 150% over the control (without bacitracin) within 3 hours after addition of the antibiotic. The SDS polyacrylamide gel electrophoresis pattern of the membrane proteins, isolated from both the control and the bacitracin treated cells, showed no difference for cells grown at pH 2 or pH 3. For cells grown at pH 4, the glycoprotein was found to have a higher mobility on SDS gels than that of control cells, and the carbohydrate content was reduced.

Bacitracin is a cyclic peptide with a molecular weight of 1500 daltons. At pH 2 and 3, bacitracin is positively charged, while at pH 4, it is less positively charged because the pK's of aspartic acid and glutamic acid lie around 4. The internal pH of the *Thermoplasma* is close to neutral; at pH 2, there exists a 290 mV pH gradient. Under this condition, it is

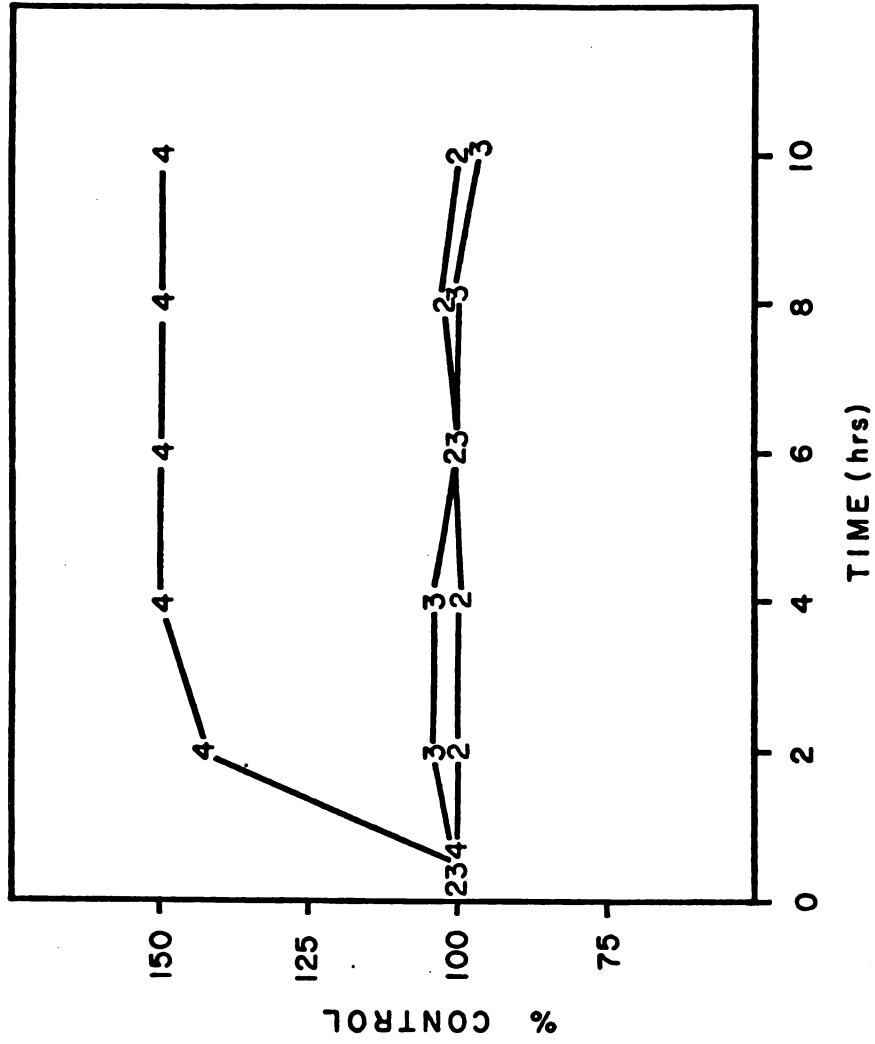


Figure 34. *T. acidophilum* Cell Growth Ratios in the Presence and Absence of Bacitracin.

very difficult for bacitracin to enter the cells at pH 2 and 3. This is consistent with above findings where no effect on growth and glycosylation of glycoprotein was observed after addition of bacitracin at pH 2 and 3. At pH 4, the pH gradient is much reduced and the bacitracin molecule is less positively charged. The evidence of the antibiotic activity was expressed in both the growth rate and the change in glycosylation of the membrane glycoprotein.

On the basis of the above information, it was concluded that glycosylation of the protein may be one of the factors for the cell's survival ability at acidic environment.

Discussion

The purified membrane glycoprotein from *T. acidophilum* had an apparent molecular weight of 152,000 daltons with less than 10% carbohydrate content (w/w). The carbohydrate moiety consisted mainly of mannose residues with branched α 1 \rightarrow 2 linkages at the nonreducing ends of the glycopeptide. The reducing end was an N-glycosidic linkage between the amino acid asparagine and N-acetylglucosamine. At least one mannose residue was not α -linked. The glycoprotein accounted for 40% (w/w) of the total membrane proteins. The nonreducing ends of the glycopeptide showed a highly branched pattern (Figure 33) which extended like a protective coat over the entire cell surface. This was supported by EM studies on *T. acidophilum* membranes labelled with Con A (96). The carbohydrate coat might also account for the 10 Å difference between the lipid model and the actual membrane thickness as discussed in Chapter 3.

Structural glycoproteins at the cell surface of eucaryotes have been implicated in a number of processes involving the interaction of molecules with plasma membranes, or of one cell with another. Such processes

include cell recognition, cell adhesion, contact inhibition, and growth regulation (97). The protective and lubricating roles of the glycoproteins from epithelial secretions are also well known (98,99). The results of the bacitracin experiments indicate that there appears to exist a correlation of growth at increasing pH values and the reduced amount of carbohydrates found in the membrane glycoprotein. Consequently glycosylation of certain membrane proteins may contribute to the survival ability of *T. acidophilum* at extreme acidic environments.

The amino acid composition of the glycoprotein showed 62 mol% hydrophobic residues, while the acidic amino acid content contributed 9 mol% more than that of the basic amino acids. The amount of chargeable groups (at most 28 mol%) may be diminished further at the low optimal pH value because of the protonation of free carboxyl groups which predominate over the number of free amino groups. A high degree of hydrophobicity is of survival value since it possesses advantages for thermophily as well as acidophily. Hydrophobic interactions have a maximum stability around 60°C (15), which is very close to the optimum growth temperature of *T. acidophilum*.

The native structure of proteins is stabilized by a combination of hydrogen bonding, electrostatic and hydrophobic interactions (100). The driving force for hydrophobic interactions involves a rearrangement of water molecules which surround hydrophobic groups into a more ordered three-dimensional hydrogen bonded structure than that of bulk water. Thus, the effect of carbohydrates on protein depends on how sugars affect the structure of water (101). As a contribution to keep cells dispersed in the aqueous environment, the carbohydrate coat generates a hydrophobic meshlike surface where water molecules are immobilized. Moreover, the

resulting water turgor stabilizes the limiting plasma membranes.

It has been known for years that sugars may protect proteins against loss of solubility during drying and may inhibit heat coagulation (102). Differential scanning calorimetry studies (103) indicated that thermal protein stabilization by carbohydrates may result from an increase in temperature of denaturation. The increase can be as large as 20°C (103).

From the view point of stereochemistry and interactions of carbohydrate chains, the outer mannose-rich portion of the glycoprotein from *T. acidophilum* membrane can be categorized as the periodic type, while the inner core of the glycoprotein can be categorized as the aperiodic type (104). In the periodic type structures, regular sequences of sugar residues have the same glycosidic configurations and are linked through the same positions in each repeating unit. The chains may exist either in ordered or disordered conformations, depending on the balance between conformational entropy and any possibilities for cooperative stabilization under the particular conditions. If the conformation is ordered, the regular periodic sequence will generate a regular periodic conformation such as a helix or a ribbon (105). The cooperative interactions between these repetitive carbohydrate units within the same glycopeptide molecule or between adjacent glycopeptides will provide additional factors in the rigidity of the membrane. The aperiodic type carbohydrate chains are characterized by short chain lengths and irregular sequences of sugar units, linkage positions and sometimes configurations. As a result, it is geometrically and/or energetically impossible for these molecules to form extended helices or ribbons. There is a growing appreciation that the aperiodic type carbohydrate chains are likely to have important biological functions that depend on their shape and interactions with proteins,

and perhaps with cations (105). The effect of variable ionic strength of the suspending medium (Ca^{2+} and Al^{3+}) on membrane stability of *T. acidophilum* has been demonstrated by Weller and Haug (22) and Vierstra and Haug (23). The cation binding ability of the carbohydrate portion of the glycoprotein may also contribute to the effect of Ca^{2+} and Al^{3+} observed by spin label experiments.

Constructing Pauling-Corey space-filling models of the carbohydrate portion of the *Thermoplasma* glycoprotein, one easily visualizes the extreme flexibility of the 1,6-linkages in the carbohydrate sections. Furthermore, sugar conformations may be visualized capable of generating polysaccharide surfaces which are virtually hydrophobic. The mutual hydroxyl orientations play obviously a considerable role. The array of hydroxyl groups participates in the formation of hydrogen bonds with water. It appears worth while to mention that rather limited information is available regarding structural and thermodynamic properties of 1,2-linked polysaccharides (105).

In conclusion, the existence of a mannose-rich glycoprotein in the wall-less *T. acidophilum* provides presumably a protective coat towards the harsh environment. The hydrophobic interaction between carbohydrates and protein prevents the membrane proteins from thermal inactivation. The stereochemistry and the conformation of the carbohydrate chains in conjunction with water turgor may contribute to the rigidity of the membrane and the cation binding.

REFERENCES

REFERENCES

1. Darland, G., Brock, T., Samsonoff, W., and Conti, S. F. (1970), *Science* 170, 1416
2. Brock, T. D., Brock, K. M., Belly, R. T., and Weiss, R. L. (1972), *Arch. Mikrobiol.* 84, 54
3. Darland, G., and Brock, T. D. (1971), *J. Gen. Microbiol* 67, 9
4. Brierley, C. L., and Brierley, J. A. (1973), *Canad. J. Microbiol.* 19, 183
5. Belly, R. T., Bohlool, B. B., and Brock, T. D. (1973), *Ann. N. Y. Acad. Sci.* 225, 94
6. Bohlool, B. B., and Brock, T. D. (1974), *Appl. Microbiol.* 28, 11
7. Christiansen, C., Freundt, E. A., and Black, F. T. (1975), *Int. J. Syst. Bacteriol.* 25, 99
8. Searcy, D. G., and Doyle, E. K. (1975), *Int. J. Syst. Bacteriol.* 25, 286
9. Searcy, D. G. (1975), *Biochim. Biophys. Acta* 395, 535
10. Searcy, D. G., Stein, D. B., and Green, G. R. (1978), *BioSystems*, in press
11. Searcy, D. G. (1976), *Biochim. Biophys. Acta* 451, 278
12. Hsung, J. C., and Haug, A. (1975), *Biochim. Biophys. Acta* 389, 477
13. Ruwart, M. J., and Haug, A. (1975), *Biochemistry* 14, 860
14. Smith, P. F., Langworthy, T. A., Mayberry, W. R., and Hougland, A. E. (1973), *J. Bacteriol.* 116, 1019
15. Scheraga, H. (1963), *Proteins I*, p. 47
16. Langworthy, T. A., Smith, P. F., and Mayberry, W. R. (1972) *J. Bacteriol.* 112, 1193
17. de Rosa, M., Gambacorta, A., and Bu'Lock, J. D. (1976), *Phytochemistry* 15, 143

18. Langworthy, T. A. (1977), *Biochim. Biophys. Acta* 487, 37
19. Smith, G. G., Ruwart, M. J., and Haug, A. (1974), *FEBS Lett.* 45, 96
20. Hsung, J. C., and Haug, A. (1977), *FEBS Lett.* 73, 47
21. Hsung, J. C., and Haug, A. (1977), *Biochim. Biophys. Acta* 461, 124
22. Weller, H. G. Jr., and Haug, A. (1977), *J. Gen. Microbiol.* 99, 379
23. Vierstra, R., and Haug, A. (1978), *Biochem. Biophys. Res. Comm.*, 84, 138
24. Träuble, H., and Eibl, H. (1975), in *Functional Linkage in Biomolecular Systems*, Schmitt, E. O., Schneider, D. M., and Crothers, D. M., Eds., Raven Press, N. Y., N.Y., pp. 59-101
25. Jacobson, K., and Papahadjopoulos, D. (1975), *Biochemistry* 14, 152
26. Lis, L. J., Kauffman, J. W., and Shriver, D. F. (1975), *Biochim. Biophys. Acta* 406, 453
27. Radin, N. S. (1969), *Methods Enzymol.* 14, 245
28. Rouser, G., Kritchevsky, G., and Yamamoto, A. (1967), in *Lipid Chromatographic Analysis*, Vol. 1, Marinetti, G. V., Ed., N. Y., N. Y., Marcel Dekker, Inc., p. 99
29. Kates, M., Yengoyan, L. S., and Sastry, P. S. (1965), *Biochim. Biophys. Acta* 98, 252
30. Kuhn, K., and Roth, H. (1933), *Ber.* 66, 1274
31. Soltmann, B., Swelley, C. C., and Holland, J. F. (1977), *Anal. Chem.* 49, 1164
32. Young, N. D., Holland, J. F., Gerber, J. N., and Sweeley, C. C. (1975), *Anal. Chem.* 47, 2373
33. Rathbun, W. B., and Betlach, M. V. (1969), *Anal. Biochem.* 24, 436
34. Wang, C.-S., and Smith, R. L. (1975), *Anal. Biochem.* 63, 414
35. Laemmli, U. K. (1970), *Nature* 227, 680
36. Weber, K., and Osborn, M. (1969), *J. Biol. Chem.* 244, 4406
37. Fairbanks, G., Steck, T. L., and Wallach, D. F. H. (1971), *Biochemistry* 10, 2602
38. Chambers, R. E., and Clamp, J. R. (1971), *Biochem. J.* 125, 1009
39. Hakomori, S.-I. (1964), *J. Biochem. (Tokyo)* 55, 205

40. Björndal, H., Hellerqvist, C. G., Lindberg, B., and Svensson, S. (1970), *Angew. Chem. Internat. Ed.* 8, 610
41. Fiske, C. H., and SubbaRow, Y. (1925), *J. Biol. Chem.* 66, 375
42. Lang, C. A. (1958), *Anal. Chem.* 30, 1692
43. Wells, M. A., and Dittmer, J. C. (1965), *Biochemistry* 4, 2459
44. Roe, J. H. (1955), *J. Biol. Chem.* 212, 335
45. Wells, M. A., and Dittmer, J. C. (1965), *J. Chromatog.* 18, 503
46. Dittmer, J. C., and Wells, M. A. (1969), *Methods Enzymol.* 14, 502
47. Rattray, J., Schibeci, M. A., and Kidby, D. K. (1975), *Bacteriol. Rev.* 39, 197
48. Fulco, A. J. (1974), *Ann. Rev. Biochem.* 43, 215
49. Singer, S. J., (1971), in *Structure and Function of Biological Membranes*, Rothfield, L. I., Ed., N.Y., N.Y., Academic Press, p. 145
50. Singer, S. J. (1974), *Ann. Rev. Biochem.* 43, 215
51. Ambron, R. T., and Pieringer, R. A. (1973), in *Form and Function of Phospholipids*, Anwell, G. B., Hawthorne, J. N., and Dawson, R. M. C., Eds., Amsterdam, The Netherlands, Elsevier Scientific Publ. Co. p. 289
52. Daron, H. H. (1973), *J. Bacteriol.* 116, 1096
53. Mehlhorn, R. J., and Keith, A. D. (1972), in *Membrane Molecular Biology*, Fox, C. F., and Keith, A. D., Eds., Stamford, Conn., Sinauer Assoc. Inc., p. 192
54. Chapman, D., (1975), in *Biomembranes*, Vol. 7, Eisenberg, H., Katchalski-Katzier, E., and Manson, L. A., Eds., N.Y., N.Y., Plenum Press, p. 1
55. Melchior, D. L., and Steim, J. M. (1976), *Ann. Rev. Biophys. Bioengin.* 5, 205
56. Huang, L., and Haug, A. (1974), *Biochim. Biophys. Acta* 352, 361
57. Weller, H. G. Jr., and Haug, A. (1976), *Biophys. J.* 16, 102a
58. Esser, A. F., and Lanyi, J. K. (1973), *Biochemistry* 12, 1933
59. McLafferty, F. W., (1966), *Interpretation of Mass Spectra*, W. A. Benjamin, Inc., N. Y., N. Y.

60. Beynon, J. H., and Williams, A. E. (1963), Mass and Abundance Tables for Use in Mass Spectrometry, Amsterdam, The Netherlands, Elsevier Publ. Co.
61. Schulten, H.-R., and Beckey, H. D. (1975), Angew. Chem. Ed. Engl. 14, 403
62. Stothers, J. B. (1972), Carbon-13 NMR Spectroscopy, Academic Press, N. Y., N. Y.
63. Johnson, L. F., and Jankowsky, W. C. (1972), Carbon-13 NMR Spectra, Wiley-Interscience Publ., N. Y., N. Y.
64. Planchy, W. Z., Lanyi, J. K., and Kates, M. (1974), Biochemistry 13, 4906
65. Singer, S. J., and Nicolson, G. L. (1972), Science 175, 720
66. Chapman, D. (1975), Quarterly Rev. Biophys. 8, 185
67. Lee, A. G. (1977), Biochim. Biophys. Acta 472, 237
68. McElhaney, R. N., DeGier, J., and Van der Neut-Kok, E. C. M. (1973), Biochim. Biophys. Acta 298, 500
69. De Kruffyff, B., Van Dijk, P. W. M., Goldbach, R. W., Demel, R. A., and Van Deenen, L. L. M. (1973), Biochim. Biophys. Acta 330, 269
70. Kimelberg, H. K., and Papahadjopoulos, D. (1974), J. Biol. Chem. 249, 1071
71. Grisham, C. M., and Barnett, R. E. (1973), Biochemistry 12, 2635
72. Wisnieski, B. J., Parkes, J. G., Huang, Y. O., and Fox, C. F. (1974), Proc. Nat. Acad. Sci. 71, 4381
73. Thilo, L., Träuble, H., and Overath, P. (1977), Biochemistry 16, 1283
74. Huang, L., Lorch, S. K., Smith, G. G., and Haug, A. (1974), FEBS Lett. 43, 1
75. McElhaney, R. N., and Souza, K. A. (1976), Biochim. Biophys. Acta 443, 348
76. Fukushima, H., Martin, C. E., Iida, H., Kitajima, Y., Thompson, G. A. Jr., and Nozawa, Y. (1976), Biochim. Biophys. Acta 431, 165
77. Arthur, H., and Watson, K. (1976), J. Bacteriol. 128, 56
78. McElhaney, R. N. (1974), J. Mol. Biol. 84, 145
79. Tsukagoshi, N., and Fox, C. F. (1973), Biochemistry 12, 2816
80. Jacobson, K., and Papahadjopoulos, D. (1975), Biochemistry 14, 152

81. Luna, E., and McConnell, H. M. (1977), *Biochim. Biophys. Acta* 470, 303
82. Bretscher, M. S. (1972), *J. Mol. Biol.* 71, 523
83. Hachimori, A., Muramatsu, N., and Nosoh, Y. (1970), *Biochim. Biophys. Acta* 206, 426
84. Spiro, R. G. (1973), *Advances in Protein Chemistry* 27, 349
85. Marshall, R. D. (1972), *Ann. Rev. Biochem.* 41, 673
86. Kornfeld, R., and Kornfeld, S. (1976), *Ann. Rev. Biochem.* 45, 217
87. Razin, S. (1975) *Prog. Surf. Membr. Sci.* 9, 257
88. Mescher, M. F., and Strominger, J. L. (1976), *J. Biol. Chem.* 251 2005
89. Kahane, I., and Brunner, H. (1977), *Infect. Immun.* 18, 273
90. Mescher, M. F., Strominger, J. L., and Watson, S. W. (1974), *J. Bacteriol.* 120, 945
91. Mescher, M. F., and Strominger, J. L. (1976), *Proc. Nat. Acad. Sci.* 73, 2687
92. Goldstein, I. J., (1976) in *Concanavalin A as a Tool*, Bittiger, H. and Schnebli, H. P., Eds., Wiley Publ., N. Y., N. Y.
93. Marks, G. L., Marshall, R. D., and Neuberger, A. (1963), *Biochem. J.* 87, 274
94. Tai, T., Yamashita, K., Ogata-Arakawa, M., Koide, N., Muramatsu, T., Iwashita, S., Inone, Y., and Kobata, A. (1975), *J. Biol. Chem.* 250, 8569
95. Storm, D. R., and Strominger, J. L. (1973), *J. Biol. Chem.* 248, 3940
96. Mayberry-Carson, K. H., Jewell, M. H., and Smith, P. F. (1978), *J. Bacteriol.* 133, 1510
97. Cook, G. M. W., and Stoddard, R. W. (1973), in *Surface Carbohydrates of Eucaryotic Cell*, Academic Press, N. Y., N. Y.
98. Carlson, D. M. (1968), *J. Biol. Chem.* 243, 616
99. Pamer, T., Glass, G. B. J., and Horowitz, M. I. (1968), *Biochemistry* 7, 3821
100. Lakshmi, T. S., and Nandi, P. K. (1976), *J. Phys. Chem.* 80, 249

101. Franks, F. and Reid, D. S. (1973), in *Water, A Comprehensive Treatise*, Vol. 2, Franks, F., Ed., Plenum Press, N. Y., N. Y.
102. Ball, C. D., Hardt, D. T., and Duddles, W. J. (1943), *J. Biol. Chem.* 151, 163
103. Oakenfull, D. G., and Fenwick, D. E. (1974), *J. Phys. Chem.* 78, 1759
104. Rees, D. A. (1972), *Biochem. J.* 126, 257
105. Rees, D. A. (1975), in *Biochemistry of Carbohydrates*, MTP International Review of Science, Vol. 5, Whelan, W. J., Ed., Univ. Park Press, Baltimore, Md., p. 1
106. Mort, A. J., and Lamport, D. T. A. (1977), *Anal. Biochem.* 82, 289